Stability of Wormholes with Singular Hypersurfaces in Einstein and Gauss-Bonnet theories of gravity

Department of Physics, Rikkyo University

Takafumi Kokubu

Stability of Wormholes with Singular Hypersurfaces in Einstein and Gauss-Bonnet theories of gravity

Takafumi Kokubu[a]

[a] Department of Physics, Rikkyo University, Tokyo 171-8501, Japan
takafumi-at-rikkyo.ac.jp

Abstract

We introduce a way to a spacetime short-cut that might be realized in theoretical physics. Such a short-cut provides us a very fast travel connecting the distant two points, namely, a faster-than-light travel. It is surprising that such science-fiction-like topics are put on the subject to theoretical physics. In classical theory of gravitational physics, one of these topics is a wormhole. Wormhole is a spacetime structure which connects two different universes or even two points of our universe. General relativity, the most successful and the simplest theory of classical gravitational theories, predicts a wormhole spacetime. Besides, quantum physics may support the possibility for existence of wormholes.

In this thesis, we pursue the possibility for eternal existence of such objects. First, we introduce properties of wormholes with its history of discoveries. Next, we review thin-shell wormholes that are categorized into a class of wormhole solutions. After that, we investigate negative tension branes as stable thin-shell wormholes in Reissner-Nordström-(anti) de Sitter spacetimes in d dimensional Einstein gravity. Imposing Z_2 symmetry, we construct and classify traversable static thin shell wormholes in spherical, planar (or cylindrical) and hyperbolic symmetries. In spherical geometry, we find the higher dimensional counterpart of Barceló and Visser's wormholes, which are stable against spherically symmetric perturbations. We also find the classes of thin shell wormholes in planar and hyperbolic symmetries with a negative cosmological constant, which are stable against perturbations preserving symmetries. In most cases, stable wormholes are found with the appropriate combination of an electric charge and a negative cosmological constant. However, as special cases, we find stable wormholes even with vanishing cosmological constant in spherical symmetry and with vanishing electric charge in hyperbolic symmetry.

Finally, the effect of the Gauss-Bonnet term on the existence and dynamical stability of thin-shell wormholes as negative tension branes is studied in the arbitrary dimensional spherically, planar, and hyperbolically symmetric spacetimes with a cosmological constant. We consider radial perturbations against the shell for the solutions, which have the Z_2 symmetry. The effect

of the Gauss-Bonnet term on the stability depends on the spacetime symmetry. For planar symmetric wormholes, the Gauss-Bonnet term does not affect their stability and they are at most marginally stable. If the coupling constant is positive and small, our setup proves that spherically symmetric wormholes are unstable against perturbations and the Gauss-Bonnet term tends to destabilize the wormholes. For hyperbolically symmetric wormholes, the Gauss-Bonnet term tends to stabilize them and there are stable wormholes.

Contents

Acknowledgement

I would like to give thanks to Tomohiro Harada, my supervisor, my symbol of theoretical physicists, for continuous support. He gave me a style how to pursue physics. I appreciate Hideki Maeda as my collaborator. He also gave me the style. I am happy to thank Sanjay Jhingan for sharing a priceless time. He taught me physics, positive perspective and lots of jokes. I thank Tsutomu Kobayashi for showing me his sharp sense to physics. I thank Shuichiro Yokoyama, Umpei Miyamoto, Tsuyoshi Houri, Hiroya Nemoto, Naoki Tsukamoto, Syo Kamata, Satoshi Okuda, Nami Uchikata, Tomo Tanaka, Mandar Patil, Takahisa Igata and Kentaro Tanabe. These intelligent physicists inspired me so much. As my colleague, I also appreciate Kohji Yajima. I thank Kumiko Inagawa and Remya Nair for their smile. I also wish to thank all of the present members of the theoretical physics laboratory. Finally, I wish to thank my family and Shizuka for continuous encouragement and support.

This thesis was supported in part by Rikkyo University Special Fund for Research.

Outline of Thesis

Section 1 is the introduction.

Section 2 describes preliminaries for studying the main purpose of the thesis. The preliminaries are based on [1] and [2].

In section 3, we show construction and linear stability against perturbations preserving symmetries of thin-shell wormholes.

In section 4, we mention there are many generalizations of the thin-shell wormhole by Poisson and Visser. In this section we review some of its generalizations.

In section 5, we concentrate on pure tension wormholes in Einstein gravity. This investigation is based on [4]. In this section we present a formalism for wormholes, which is more general than previous formalisms and also obtain a stability condition against perturbations preserving symmetries. Then, we introduce wormholes with a negative tension brane and we analyze the existence of static solutions, stability and horizon avoidance in spherical, planar and hyperbolic symmetries.

In section 6, we treat pure tension wormholes in Einstein-Gauss-Bonnet gravity. This investigation is based on [5]. At first, assuming that the shell is made of tension together with a perfect fluid, we derive the equation of motion for the shell and basic properties of the static shell are reviewed. After that, we show that the shell has negative energy density and hence the weak energy condition is violated. (However negative tension brane still satisfies the null energy condition). Next, we study the existence and stability of static thin-shell wormholes in the cases except for $k = -1$ with $m < 0$. Following subsection is devoted to performing the pictorial analysis to study the same problem in the case of $k = -1$ with $m < 0$. A detailed derivation of the equation of motion for a thin-shell is summarized in Appendix B. In Appendix C, a stability criterion with a perfect fluid is presented. Our basic notation is that: The convention for the Riemann curvature tensor is $[\nabla_\rho, \nabla_\sigma]V^\mu = R^\mu{}_{\nu\rho\sigma}V^\nu$ and $R_{\mu\nu} = R^\rho{}_{\mu\rho\nu}$. The signature of the Minkowski metric is taken as $\mathrm{diag}(-,+,+,\cdots,+,+)$, and Greek indices run over all spacetime indices. In this section the d-dimensional gravitational constant G_d is retained.

Section 7 is dedicated to discussions and conclusions.

1 Introduction

Wormholes are spacetime structures which connect two different Universes or even two points of our Universe. Wormholes have fascinated people for a long time and many sci-fi movies and novels are based on them. One may be surprised to know that wormholes are indeed a subject of theoretical physics. In a real world, unlike Blackholes, wormholes are hypothetical objects. Still, theoretical physicists have pursued such peculiar objects and revealed many properties of them because consequences of wormhole physics are appealing; they offer an instant travel between two distinct points and even realization of a time travel [6].

To understand what a wormhole is, it is better to follow the history of wormholes first. Interestingly, an insight into a wormhole shares the same year of discovery as the first black hole. In 1916 Karl Schwarzschild found his famous black hole solution of the Einstein equations, Schwarzschild black hole. In 1916, Ludwig Flamm found that Schwarzschild metric has hidden tunnel structure which connects two asymptotically flat spaces; he developed what is now called the embedding diagram [7]. Almost twenty years later after Flamm's work, Albert Einstein and Nathan Rosen published their famous paper about "the Einstein-Rosen bridge" which is the Schwarzschild spacetime that can be interpreted as a solution joining the two same Schwarzschild geometries at their horizons [8]. The bridge acts like a spacetime-tunnel since it connects two asymptotically flat regions.

1.1 The Einstein-Rosen bridge

The Einstein-Rosen bridge is unstable since the throat pinches off quickly. To understand this mechanism, let us see the dynamics of the bridge to understand the reason of the pinch off.

We will show here, how this tunnel structure is recognized. The Schwarzschild metric is written in the spherical coordinates (t, r, θ, ϕ) as

$$ds^2 = -\left(1 - \frac{2M}{r}\right) \mathrm{d}t^2 + \left(1 - \frac{2M}{r}\right)^{-1} \mathrm{d}r^2 + r^2(\mathrm{d}\theta^2 + \sin^2\theta \mathrm{d}\phi^2), \tag{1.1}$$

where M is a constant mass parameter. Suppose we take a constant time slice, $t = const$. Since the spacetime is spherically symmetric, we can take the equator slice, $\theta = \pi/2$, without loss of generality. Then the metric reduces to

$$ds^2|_{t=const,\theta=\pi/2} = \left(1 - \frac{2M}{r}\right)^{-1} \mathrm{d}r^2 + r^2 \mathrm{d}\phi^2. \tag{1.2}$$

Eq. (1.2) has a axial symmetry: $\phi \to \phi + const$. The metric (it is now a distance between the infinitesimal away two points) can be expressed as a two-dimensional surface in a three-dimensional flat space; ds^2 at t =const and $\theta = \pi/2$ is embeded into the three dimensional Euclidian space $\mathbb{R}^3$. In $\mathbb{R}^3$, the infinitesimal distance $\mathrm{d}\Sigma^2$ with the cylindrical coordinates (ρ, ψ, z) (ρ: distance from the z axis, ψ: angle around the z axis) is given by

$$\mathrm{d}\Sigma^2 = \mathrm{d}\rho^2 + \rho^2 \mathrm{d}\psi^2 + \mathrm{d}z^2. \tag{1.3}$$

A surface in a flat space can be described as $z = z(\rho, \psi)$ in the cylindrical coordinates. Since the coordinates r and ϕ are functions of ρ and ψ, we must have relation between (ρ, ψ, z) and (r, ϕ) to identify the equation of the surface, i.e.,

$$\rho = \rho(r, \phi), \quad \psi = \psi(r, \phi), \quad z = z(r, \phi). \tag{1.4}$$

Since the metric (1.2) is axially symmetric which means $\psi = \phi$ and $\rho = \rho(r)$, the surface function becomes the function of r, $z = z(r)$. Summarizing above,

$$\rho = \rho(r), \quad \psi = \phi, \quad z = z(r). \tag{1.5}$$

Substituting Eq. (1.5) into Eq. (1.3), then comparing this metric and Eq. (1.2), we get the relations

$$\left(\frac{\mathrm{d}z}{\mathrm{d}r}\right)^2 + \left(\frac{\mathrm{d}\rho}{\mathrm{d}r}\right)^2 = \left(1 - \frac{2M}{r}\right)^{-1}, \quad \rho^2 = r^2. \tag{1.6}$$

The simultaneous equations reduces to a single differential equation and is easy to integrate;

$$\left(\frac{\mathrm{d}z}{\mathrm{d}r}\right)^2 = \frac{2M}{r - 2M} \;\Rightarrow\; z = \pm 2\sqrt{2M(r - 2M)}. \tag{1.7}$$

A plot for Eq. (1.7) is shown in Fig. (1.1) below. One finds that two asymptotically flat regions ($\mathrm{d}z/\mathrm{d}r \to 0$ as $r \to \infty$) are connected by the neck $z = 0$. Due to the shape of a neck, we call it a *throat*.

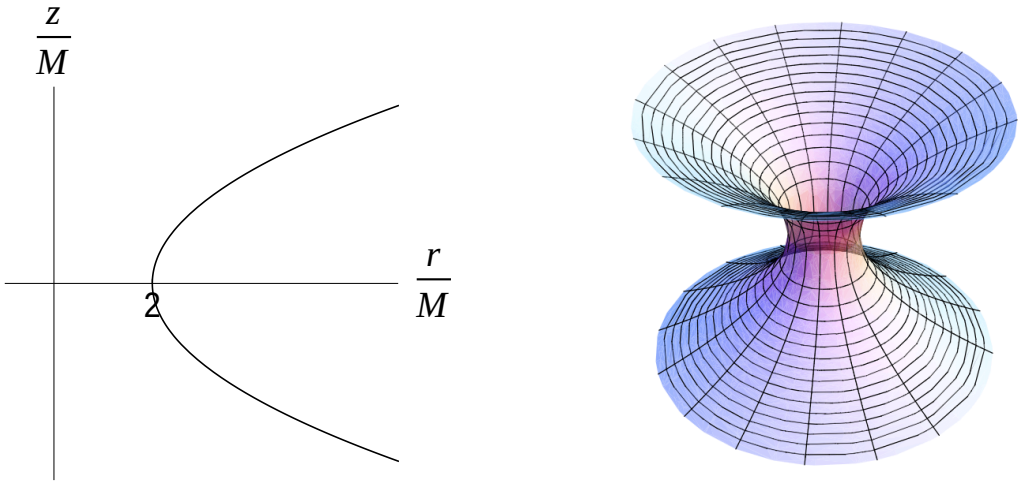

Figure 1.1: Left: The plot of Eq. (1.7). Right: The surface is obtained by rotating the function around z axis in the ϕ direction. The narrowest surface $z = 0$ corresponds to $r = 2M$.

At this stage, one may ask a question such as "if we live in an asymptotically flat region, namely, in the upper space of the Fig. (1.1), what does the other region correspond to? Can we pass though the throat and go to this other region?". A clear answer to this question, is produced in the paper by Fuller and Wheeler [9]. They revealed a dynamical property of the throat and also showed that no traveller can

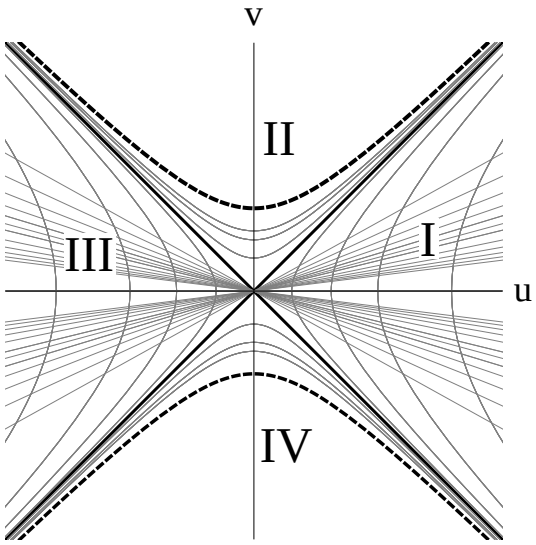

Figure 1.2: Kruskal diagram.

safely pass though the throat to go to the other region. We will show the dynamics of the throat by the following this argument.

The Kruskal diagram of the Schwarzschild spacetime is given by the Fig. (1.2). Here, v is a timelike coordinate while u is a spacelike coordinate. Region I and III represent outside of the black hole which corresponds to the region of $r > 2M$ in the Schwarzschild coordinates. Region II is inside of the black hole, $r < 2M$, while region IV is the white hole, that is considered as a time-reversal solution of the black hole. The straight lines $v = \pm u$ correspond to $r = 2M$, the event horizon of the spacetime. The dashed bold lines are the curvature singularity ($r = 0$). Straight lines between $v = +u$ and $v = -u$ are $t = const.$ while hyperbolas are $r = const.$ surfaces.

Here, we take a particular spacelike slice for the diagram as

$$\gamma = \frac{v}{\sqrt{4 + u^2}}, \quad \gamma = const. \tag{1.8}$$

which becomes $v = u$, as $u \to \pm\infty$. We draw $\gamma = const.$ surfaces of Eq. (1.8) in Fig. (1.3) as gray curves ((a) to (h)). As one can see, γ plays the role of time here; when γ increases, the surface Eq. (1.8) moves in the direction of increasing v. Since the surface Eq. (1.8) is spacelike, it moves in the time direction. In this figure, the red dotted straight line describes a null geodesic α released from the region IV, while the blue one is a null geodesic β released from region III. The throat cannot stay static and its dynamics is as described in Fig. (1.4). The process occurs in the order of (a) to (h);
(a) Photons α and β initially are in the lower sheet. They go to the center $r = 0$. Values $u = -2.67$ and $u = -2.08$ correspond to $r = 2M$ and $r = 0$, respectively. The vertical bold line is the curvature singularity $r = 0$. At this moment, the singularity is in between two quasi Euclidian spaces.
(b) Both photons go to the center. Throat is going to appear.
(c) Throat just opened. The circumference of the throat is smaller than $4\pi M$.
(d) The maximal throat, $2\pi r = 4\pi M$. The photon α has passed though the throat.
(e) Throat is shrinking. Both of photons have passed though the throat.

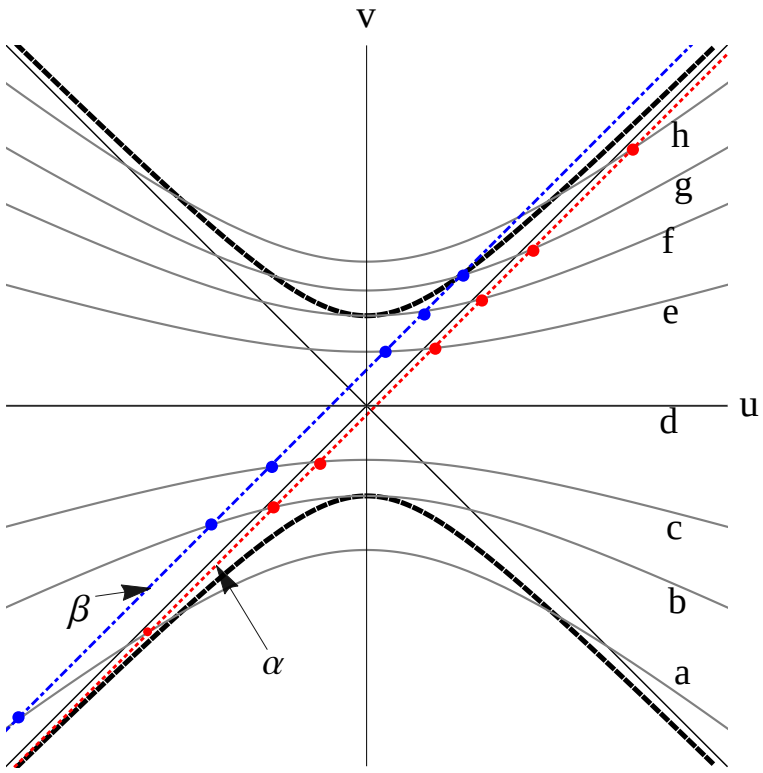

Figure 1.3: The red dotted line is the geodesics of photon α from the region IV while the blue one is of photon β from the region III. After passing through the anti horizon $v = -u$, the photon α goes to the region I and never across the event horizon $v = u$. the geodesics of the photon β must terminate at the singularity $r = 0$ in a finite time in the region II.

(f) The moment of throat closing. In this stage, both photons are still in the upper sheet, while the photon β approaches the central singularity.
(g) Photon β is just caught. Then, β disappears in the singularity and stops existing.
(h) Photon α keeps escaping to the null infinity of the upper sheet.

Although we have used a specific spacelike slice Eq. (1.8) to show the dynamical feature of the bridge, this dynamics does not change as long as the slice is spacelike.

From above, we conclude that although a timelike traveller might go to the upper space in just a finite time but cannot come back to the lower space. Hence, the Schwarzschild solution provides an one-way travel. To have a two-way travel, one can speculate that a two-way travel needs a Penrose diagram like Fig. (1.5). Apparently, this diagram shows that a timelike worldline can cross the throat again and again without hitting any singularities. Introduction of such a two-way tunnel spacetime is explained in the next subsection.

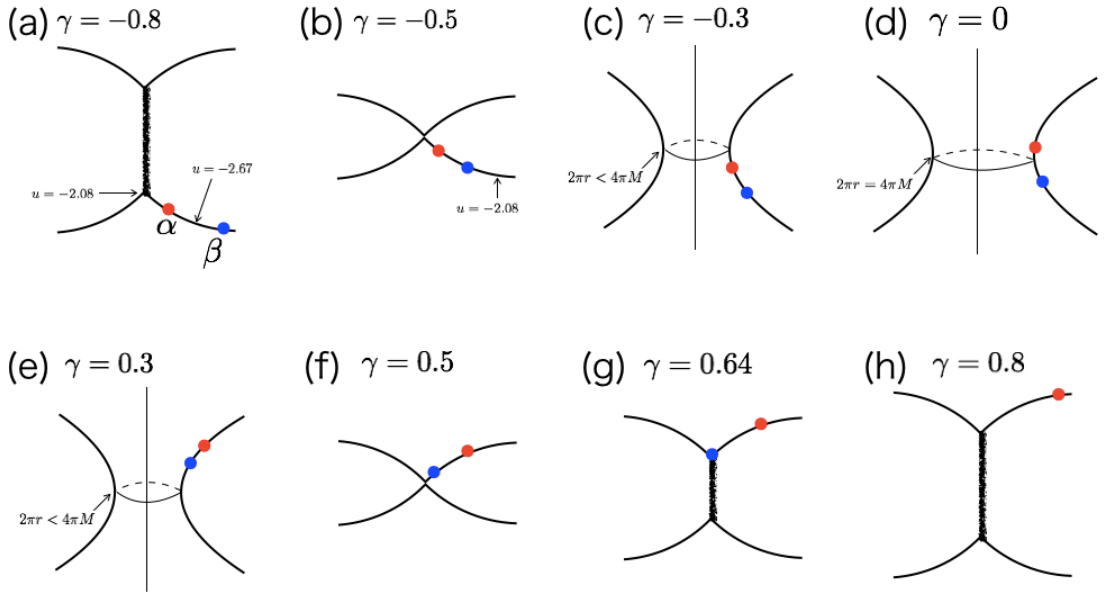

Figure 1.4: The dynamics of the throat and motion of photons. Throat emerges instantaneously and connects two asymptotically flat space-sheets. After that, it expands and then starts to contract. Finally it pinches off the connection between the two space-sheets. (a) Photons α and β are initially in the lower sheet. They go to the center $r = 0$. Here, $u = -2.67$ and $u = -2.08$ correspond to $r = 2M$ and $r = 0$, respectively. The vertical bold line is the curvature singularity $r = 0$. At this moment, the singularity is in between two quasi Euclidian spaces. (b) Both photons move towards center. Throat is going to emerge. (c) Throat just opened. The circumference of the throat is smaller than $4\pi M$. (d) The maximal throat. $2\pi r = 4\pi M$. The photon α has passed though the throat. (e) Throat is shrinking. Both of photons have passed though the throat. (f) The moment of throat shutdown. In this stage, both photons are still in the upper sheet, while the photon β approaches the central singularity. This photon β is eventually going to be eaten by the singularity. (g) Photon β is just caught. It disappears in the singularity and stop existing. (h) Photon α continues its journey to the null infinity of the upper sheet.

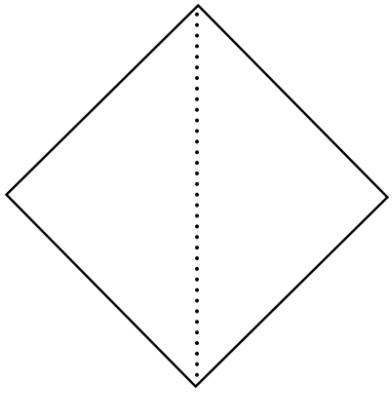

Figure 1.5: A Penrose diagram for a two-way traversable spacetime. The center vertical line describes a wormhole throat which connects the left and the right regions. From the above picture, a timelike traveller clearly can pass through the throat to go to the other region and also come back to the original region.

1.2 Wormhole properties in brief

Arguably, it was Michael Morris and Kip Thorne who established modern wormhole physics. In this subsection, we follow their approach to understand what properties wormholes should have. They have pioneered qualitative study for static and spherically symmetric spacetimes which have "two-way" *traversable* wormholes [10]. Since they knew what kinds of geometries describe tunnel structures, they deduced the metric which has such a geometry. Then substituting the metric into the Einstein equation they recovered the matter property and its distribution. Here we begin with a brief overview of their discussion.

A convenient choice of coordinates to describe static and spherically symmetric wormhole spacetimes is

$$\mathrm{d}s^2 = -e^{2\Phi(r)}\mathrm{d}t^2 + \left(1 - \frac{b(r)}{r}\right)^{-1}\mathrm{d}r^2 + r^2(\mathrm{d}\theta^2 + \sin^2\theta\mathrm{d}\phi^2), \tag{1.9}$$

where Φ and b are both functions of r. To simplify calculations, we introduce a orthonormal basis of reference frame of the static observers:

$$e^{\mu}_{\hat{t}}\partial_\mu = e^{-\Phi}\partial_t, \quad e^{\mu}_{\hat{r}}\partial_\mu = \sqrt{1-\frac{b}{r}}\partial_r, \quad e^{\mu}_{\hat{\theta}}\partial_\mu = \frac{1}{r}\partial_\theta, \quad e^{\mu}_{\hat{\phi}}\partial_\mu = \frac{1}{r\sin\theta}\partial_\phi. \tag{1.10}$$

In this basis, the metric takes the Minkowskian form : $g_{\hat{\mu}\hat{\nu}} = e_{\hat{\mu}}e_{\hat{\nu}} = \eta_{\mu\nu}$. Then the non-zero components of the Einstein tensor yields

$$G_{\hat{t}\hat{t}} = \frac{r'}{b^2}, \tag{1.11}$$

$$G_{\hat{r}\hat{r}} = 2\left(1-\frac{b}{r}\right)\frac{\Phi'}{b^2}, \tag{1.12}$$

$$G_{\hat{\theta}\hat{\theta}} = G_{\hat{\phi}\hat{\phi}} = \left(1-\frac{b}{r}\right)\left(\Phi'' - \Phi'\frac{b'r-b}{2r(r-b)} + (\Phi')^2 + \frac{\Phi'}{r} - \frac{b'r-b}{2r^2(r-b)}\right), \tag{1.13}$$

where $' := \mathrm{d}/\mathrm{d}r$. Since the geometry is both static and spherically symmetric, the vacuum equation must be the Schwarzschild black hole (Birkhoff's theorem), a non-traversable wormhole. Thus, if we want to build a wormhole spacetime we must handle spacetimes with specific form of stress-energy tensors. As the Einstein tensor takes diagonal form, the corresponding non-zero stress-energy tensor must also be diagonal. In the orthonormal basis we can then give each component of the stress-energy tensor the physical interpretation as

$$T_{\hat{t}\hat{t}} = \rho(r), \quad T_{\hat{r}\hat{r}} = -\tau(r), \quad T_{\hat{\theta}\hat{\theta}} = T_{\hat{\phi}\hat{\phi}} = p(r), \tag{1.14}$$

where ρ is the energy density, that static observers measure, τ is the radial tension that they measure in the radial direction (negative of the radial pressure), and p is the pressure that they measure in the lateral direction.

The Einstein equations

$$G_{\hat{\mu}\hat{\nu}} = 8\pi T_{\hat{\mu}\hat{\nu}} \tag{1.15}$$

give the following non-trivial equations for ρ, τ and p:

$$\rho = \frac{b'}{8\pi r^2}, \tag{1.16}$$

$$\tau = \frac{1}{8\pi r^2}\left(\frac{b}{r} - 2(r-b)\Phi'\right), \tag{1.17}$$

$$p = \frac{r}{2}\left((\rho-\tau)\Phi' - \tau'\right) - \tau. \tag{1.18}$$

One may solve the above equations to get the form of b and Φ by imposing specific component choice for $T_{\hat{\mu}\hat{\nu}}$, i.e., specific form of ρ, τ and p. An alternative way to solve them is that one imposes an equation of state as $\tau = \tau(\rho)$ and $p = p(\rho)$, and then one solves for Eq. (1.16) - Eq. (1.18).

1.2.1 Embedding wormholes and asymptotic flatness

The surface $b = r$ actually describes the throat. The reason for this is obvious from the embedding operation. We can play same game in Sec 1.1 to get the embedding of the metric Eq. (1.9). Going through the same process in Sec 1.1, we obtain a differential equation for z;

$$\frac{\mathrm{d}z}{\mathrm{d}r} = \pm\left(\frac{r}{b(r)} - 1\right)^{-\frac{1}{2}}. \tag{1.19}$$

This differential equation can now be integrated if $b(r)$ is determined. So b is called the shape function. Obviously, Eq. (1.19) diverges when $b = r =: r_0$. Since the schematic picture of Eq. (1.19) is similar to Fig. (1.1), one finds that the sphere with radius of r_0 describes the throat (Fig. (1.6)). We denote the throat, $b = r = r_0$, as the minimum surface. As mentioned, at the throat $\mathrm{d}z/\mathrm{d}r = \infty$.

Morris and Thorne further imposed the asymptotically flatness condition which means $\mathrm{d}z/\mathrm{d}r \to 0$ as $r \to \infty$.

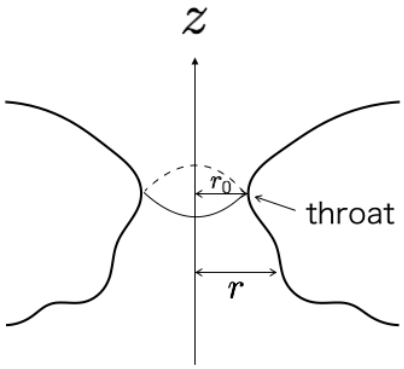

Figure 1.6: The embedding of the Morris-Thorne type metric. In general, wormholes do not have to have a mirror symmetry (like the Einstein-Rosen bridge) as long as the flaring out condition is satisfied.

1.2.2 The flaring-out condition

In Sec 1.2.1, we saw Eq. (1.19) diverges at the throat. In other words, the inverse function of $z = z(r)$, i.e., $r = r(z)$ satisfies

$$\left.\frac{\mathrm{d}r}{\mathrm{d}z}\right|_{r_0} = \pm\left(\frac{r_0}{b(r_0)} - 1\right)^{\frac{1}{2}} = 0. \tag{1.20}$$

For a spacetime to be a wormhole, there must be a throat that flares out. The flaring-out condition states

$$\frac{\mathrm{d}^2 r}{\mathrm{d}^2 z} = \frac{b - rb'}{2b^2} > 0 \tag{1.21}$$

- at or near the throat.

1.2.3 The absence of the horizon

For the wormhole to be traversable, there must be no horizons in a spacetime. By using the function Φ in the metric Eq. (1.9), it states

$$\Phi(r) \text{ is finite everywhere.} \tag{1.22}$$

1.2.4 Magnitude of the tension at the throat

The shape function b gives restrictions on ρ, τ and p through Eqs. (1.16)-(1.18). A critical restriction is at the throat, $b = r = r_0$. Then $(r - b)\Phi' \to 0$. Reviving c and G, this yields the huge tension;

$$\tau(r_0) = \frac{c^4}{8\pi G r_0^2} \sim 5 \times 10^{41} \frac{\mathrm{dyn}}{\mathrm{cm}^2} \left(\frac{10\mathrm{m}}{r_0}\right)^2. \tag{1.23}$$

1.2.5 Exotic matter

Besides some of the peculiar features about wormholes noted above, however, the most difficult thing to digest in wormhole physics is the necessity of exotic matters that can violate energy conditions. In general relativity, Morris-Thorne's static spherically symmetric traversable wormholes need stress-energy tensors that violate energy conditions at or near the throat. To see what happens to the relation between the tension τ and energy density ρ near the throat, we introduce a dimensionless function ξ as

$$\xi := \frac{\tau - \rho}{|\rho|} = \frac{1}{|b'|}\left(\frac{b}{r} - 2(r-b)\Phi' - b'\right). \tag{1.24}$$

Since Eq. (1.21) and $(r-b)\Phi' \to 0$ is satisfied around the throat, ξ reduces to

$$\xi|_{r\sim r_0} \simeq \frac{2b^2}{r|b'|}\frac{\mathrm{d}^2 r}{\mathrm{d}^2 z} > 0 \quad \Leftrightarrow \quad \tau > \rho \tag{1.25}$$

at or around the throat. We call the matter which has property $\tau > \rho$ as an *exotic matter* because the conventional matter satisfies the null energy condition, $T_{\mu\nu}k^\mu k^\nu \geq 0 \Leftrightarrow \tau \leq \rho$.

1.2.6 Another properties

Morris and Thorne required some additional conditions on traversable wormholes, tidal forces and a time to pass through wormholes. We do not explain these conditions here since we consider conditions that mentioned above (from Sec. 1.2.2 to 1.2.5) are the primary problems for wormholes. We refer the reader to [10] for details of tidal forces and a time to pass through wormholes.

1.3 Simple exact solutions and Stability

If we somehow solved the all difficulties about wormhole properties discussed above, there is still an important problem, i.e., the stability of wormhole spacetimes. Once one have a spacetime, its stability analysis against gravitational/matter perturbations is a problem with critical importance in the sense that only stable spacetimes may exist in "real world".

During few decades, after the paper by Einstein and Rosen, several exact solutions to the Einstein equations have been found and they have tunnel structures as described above [11]. These types of spacetimes are assumed to have a massless scalar field with the opposite sign of its kinetic term to the sign of the Einstein-Hilbert term in the Lagrangian. We often call such a scalar field a *ghost*, or (*phantom*) scalar field. We shall refer to the simplest exact wormhole solution as the Ellis solution (or the Ellis-Bronnikov solution).

Although wormhole solutions have been known for decades, their stability has not been conducted until quite recently. The first stability analysis is by C. Armendariz-Picon in 2002 [12]. Picon showed that the Ellis wormhole is stable against gravitational perturbations in a restricted class which do not change the throat radius. Subsequently, Shinkai and Hayward showed that the Ellis wormhole is unstable against either a normal and a phantom gaussian pulse of massless scalar field [13]. When a normal (ghost) pulse is injected into the throat, the throat must shrink (inflate). Gonzalez *et al.* have also proved that the Ellis wormhole is unstable against linear and non-linear spherically symmetric perturbations in which the throat is not fixed [14, 15]. They showed that a charged generalization of the wormhole is also unstable [16]. This unstable feature is invariant in the higher dimensional generalization of the Ellis spacetime [17].

2 Preliminaries

Soon after the publication of the paper by Morris and Thorne, M. Visser constructed another type of wormhole, *thin-shell wormholes*. Here, we first introduce mathematical preliminaries for construction of thin-shell wormholes. Sec 2.1 is based on a Poisson's book [1].

2.1 Hypersurfaces

2.1.1 Definition of hypersurface

Hypersurfaces Σ are defined as $(d-1)$ dimensional submanifold in d dimensional manifold. Σ is obtained by imposing the condition that

$$\Phi(x^\alpha) = 0 \tag{2.1}$$

to coordinates x^α. Or equivalently, we obtain Σ by describing

$$x^\alpha = x^\alpha(y^a), \tag{2.2}$$

where $y^a (a = 1, 2, \cdots, d-1)$ are coordinates intrinsic to a hypersurface. Let us take an example. Consider a two dimensional sphere with radius R in the three dimensional Euclid space. The surface of the sphere is given by $\Phi(x, y, z) = x^2 + y^2 + z^2 - R^2 = 0$ which agrees with Eq. (2.1). The other representation is $x^\alpha(\theta, \phi) = (R\sin\theta\cos\phi, R\sin\theta\sin\phi, R\cos\theta)$ which agrees with Eq. (2.2).

2.1.2 Normal vector

A vector $\Phi_{,\alpha}$ is normal to Σ (example: sphere in $\mathbb{R}^3$ is described by $\Phi = x^2 + y^2 + z^2 - R^2 \Rightarrow \Phi_{,\alpha} = 2(x, y, z) = 2\mathbf{r}/|\mathbf{r}|$).

For non-null hypersurfaces, we define the normal vector n_α as

$$n_\alpha := \varepsilon \frac{\Phi_{,\alpha}}{|\Phi^{,\beta}\Phi_{,\beta}|^{1/2}}, \tag{2.3}$$

where

$$n_\alpha n^\alpha = \varepsilon = \begin{cases} -1 : \Sigma \text{ is spacelike} \\ +1 : \Sigma \text{ is timelike} \end{cases} . \tag{2.4}$$

n_α towards the direction of increasing Φ : $n^\alpha \Phi_{,\alpha} > 0$. The definition Eq. (2.3) is useless if a hypersurface is null because the denominator becomes zero value. For null hypersurfaces, we define the normal vector k_α as

$$k_\alpha := -\Phi_{,\alpha}. \tag{2.5}$$

The sign of Eq. (2.5) is chosen so as to that the direction of k^α equals to the direction of increasing Φ (example: consider a surface of an expanding light in Minkowski spacetime. Then $\Phi = t - (x^2 + y^2 + z^2)^{1/2}$ describes the surface. The corresponding normal vector is $k^\alpha = (1, \mathbf{r}/|\mathbf{r}|)$).

Since k_α is null ($k^\alpha k_\alpha = 0$), this vector is perpendicular to itself. Moreover, it is also tangent to null hypersurface Σ because of

$$k_{\alpha;\beta}k^\beta = \Phi_{;\alpha\beta}\Phi^{,\beta} = \Phi_{;\beta\alpha}\Phi^{,\beta} = \frac{1}{2}(\Phi_{,\beta}\Phi^{,\beta})_{;\alpha} = \kappa k_\alpha, \tag{2.6}$$

where κ is a constant. In the last equality we used the fact that because $\Phi_{,\beta}\Phi^{,\beta} = 0$ on Σ, its gradient $(\Phi_{,\beta}\Phi^{,\beta})_{;\alpha}$ must be directed to k_α. Hence we have the equation

$$k_{\alpha;\beta}k^\beta = \kappa k_\alpha \tag{2.7}$$

which is general form of geodesic equations. In other words, null hypersurfaces are generated from null geodesics. In this sense, we call these null geodesics the generators.

Let λ be the parameter of null geodesics: a displacement along each generator is described as $\mathrm{d}x^\alpha = k^\alpha \mathrm{d}\lambda$. In general, λ is not an affine parameter. However, if surfaces Φ =constant cover a whole family of null hypersurface, $\kappa = 0$ and then λ is an affine parameter.

It is convenient to introduce new coordinates where behaviors of the generators are well described: We adopt the affine parameter λ as one of the coordinates, and also adopt two coordinates θ^A ($A = 2, 3, \cdots, d-1$) to label the generators (Fig. (2.1)). Thus, we set

$$y^a = (\lambda, \theta^A) \tag{2.8}$$

for the generators.

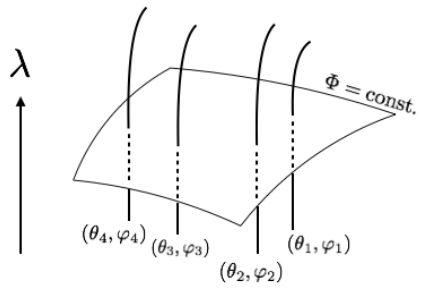

Figure 2.1: θ^A labels each generator.

2.1.3 Induced metric

The metric on any hypersurface is obtained by imposing a condition to the metric of y^a. From $x^\alpha = x^\alpha(y^a)$, we define

$$e^\alpha_a := \frac{\partial x^\alpha}{\partial y^a}. \tag{2.9}$$

e^α_a is tangent to curves on a hypersurface, that is $e^\alpha_a n_\alpha = 0$ for non-null Σ and $e^\alpha_a k_\alpha = 0$ for null Σ.

Rewriting the metric on Σ, $x^\alpha \to y^a$, yields

$$\mathrm{d}s^2_\Sigma = g_{\alpha\beta}\mathrm{d}x^\alpha \mathrm{d}x^\beta = g_{\alpha\beta}\left(\frac{\partial x^\alpha}{\partial y^a}\mathrm{d}y^a\right)\left(\frac{\partial x^\beta}{\partial y^b}\mathrm{d}y^b\right) = h_{ab}\mathrm{d}y^a\mathrm{d}y^b, \tag{2.10}$$

where

$$h_{ab} := g_{\alpha\beta}e^\alpha_a e^\beta_b. \tag{2.11}$$

h_{ab} is called *the induced metric* or the first fundamental form on Σ. The induced metric is actually a scalar under the transformation $x^\alpha \to x^{\alpha'}$, not tensor. However, it acts like a tensor under the transformation $y^a \to y^{a'}$. In this sense, h_{ab} is also called $(d-1)$-tensors. h_{ab} becomes simpler form when Σ is a null hypersurface. Due to Eq. (2.8), $e^\alpha_1 = (\partial x^\alpha/\partial\lambda)_{\theta^A} =: k^\alpha$. Then, $h_{11} = g_{\alpha\beta}e^\alpha_1 e^\beta_1 = g_{\alpha\beta}k^\alpha k^\beta = 0$ and $h_{11} = g_{\alpha 1}k^\alpha e^\beta_A = 0$. Hence

$$\mathrm{d}s^2_{\text{null }\Sigma} = h_{ab}\mathrm{d}y^a\mathrm{d}y^b = h_{1b}\mathrm{d}y^1\mathrm{d}y^b + h_{Ab}\mathrm{d}y^A\mathrm{d}y^b = h_{AB}\mathrm{d}y^A\mathrm{d}y^B = \sigma_{AB}\mathrm{d}\theta^A\mathrm{d}\theta^B, \tag{2.12}$$

where

$$\sigma_{AB} := h_{AB} = g_{\alpha\beta}e^\alpha_A e^\beta_B. \tag{2.13}$$

σ_{AB} is also called the induced metric and $(d-2)$-tensors.

$g^{\alpha\beta}$ can be decomposed into normal and tangential parts. For non-null case, the metric is decomposed into

$$g^{\alpha\beta} = \varepsilon n^\alpha n^\beta + h^{ab}e^\alpha_a e^\beta_b. \tag{2.14}$$

One can confirm that the above decomposition is adequate by operating inner product of n_β and e^a_α to Eq. (2.14). For null case, we must introduce an auxiliary null vector field N^α which satisfies the property $N_\alpha k^\alpha = -1$, $N_\alpha e^\alpha_A = 0$. Using this auxiliary null field, we decompose the metric into

$$g^{\alpha\beta} = -k^\alpha N^\beta - N^\alpha k^\beta + \sigma^{AB}e^\alpha_A e^\beta_B. \tag{2.15}$$

One can confirm that the above decomposition is adequate by operating inner product of k_α, N_α and e^a_α to Eq. (2.15).

2.1.4 Extrinsic curvature

In the rest of this thesis, we shall consider non-null hypersurfaces formalism of extrinsic curvature, junction conditions and thin-shell. The corresponding formalisms for null hypersurfaces need special treatments [1, 2, 3] . Thus the formalisms developed below are limited in a sense, however, goal of our thesis does not require null hypersurface analysis.

Consider a non-null hypersurface Σ, with a vector field A_α which is tangent to Σ. In this subsection we consider decomposition of this vector field into tangential and normal part. It is well known that exterinsic curvature is the normal component of vector field in this decomposition. The tangential component of the quantity $A^\alpha{}_{;\beta}e^\beta_b$ is the vector $A_{a|b} := A_{\alpha;\beta}e^\alpha_a e^\beta_b$. We now look for normal component of the vector $A^\alpha{}_{;\beta}e^\beta_b$.

To this end, we rewrite $A^{\alpha}_{\ ;\beta}e^{\beta}_{b}$ as $g^{\alpha}_{\mu}A^{\mu}_{\ ;\beta}e^{\beta}_{b}$ and substitute, tangential and the normal decomposition of metric derived above, Eq. (2.14) into $g^{\alpha}_{\mu}A^{\mu}_{\ ;\beta}e^{\beta}_{b}$:

$$A^{\alpha}_{\ ;\beta}e^{\beta}_{b} = A^{a}_{\ |b}e^{\alpha}_{a} - \varepsilon A^{a}(n_{\mu;\beta}e^{\mu}_{a}e^{\beta}_{b})n^{\alpha}. \tag{2.16}$$

Now, we introduce a new $(d-1)$-tensor, specific to the hypersurface,

$$K_{ab} := n_{\mu;\beta}e^{\mu}_{a}e^{\beta}_{b} \tag{2.17}$$

which is called *the extrinsic curvatures* or *the second fundamental form*. With this definition we can rewrite the previous equation as,

$$A^{\alpha}_{\ ;\beta}e^{\beta}_{b} = A^{a}_{\ |b}e^{\alpha}_{a} - \varepsilon A^{a}K_{ab}n^{\alpha}. \tag{2.18}$$

From Eq. (2.18) we can see that the answer to the question we asked is "yes": The vector $A^{\alpha}_{\ ;\beta}e^{\beta}_{b}$, indeed, has normal components. It is evident that the normal part vanishes when $K_{ab} = 0$. Let us consider now an important property for K_{ab}. The extrinsic curvature is a symmetric tensor, i.e., $K_{ab} = K_{ba}$ because

$$K_{ab} = n_{\alpha;\beta}e^{\alpha}_{a}e^{\beta}_{b} = -n_{\alpha}e^{\alpha}_{a;\beta}e^{\beta}_{b} = -n_{\alpha}e^{\alpha}_{b;\beta}e^{\beta}_{a} = n_{\alpha;\beta}e^{\alpha}_{b}e^{\beta}_{a} = K_{ba}. \tag{2.19}$$

Here we have used $n_{\alpha}e^{\alpha}_{a} = 0$ in the second and forth equality, and also used $e^{\alpha}_{a;\beta}e^{\beta}_{b} = e^{\alpha}_{b;\beta}e^{\beta}_{a}$ (i.e., the Lie transportation of the basis) in the third equality. Due to this symmetry, we can see extrinsic curvature as Lie derivative along the normal n_{α},

$$K_{ab} = n_{(\alpha;\beta)}e^{\alpha}_{a}e^{\beta}_{b} = \frac{1}{2}(\pounds_{n}g_{\alpha\beta})e^{\alpha}_{a}e^{\beta}_{b}. \tag{2.20}$$

The Trace of K_{ab} reads as

$$K = h^{ab}K_{ab} = n_{\alpha;\beta}h^{ab}e^{\alpha}_{a}e^{\beta}_{b} = n_{\alpha;\beta}g^{\alpha\beta} = n^{\beta}_{\ ;\beta}. \tag{2.21}$$

Hence, K equals to the expansion of the congruence of n^{α} that intersect Σ orthogonally. Therefore, we have a natural interpretion for extrinsic-curvature-scalar K, i.e., it is convex if $K > 0$, and concave if $K < 0$. A pictorial interpretation of K is given below Fig. (2.2).

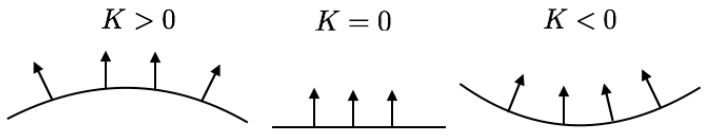

Figure 2.2: Pictorial interpretation of K. The congruence is diverging if $K > 0$ and converging if $K < 0$.

2.2 Junction conditions

Σ divides a spacetime into two parts, the one side is $\mathcal{M}^+$ with coordinates x^α_+ and the metric $g^{\alpha\beta}_+$ while the other side is $\mathcal{M}^-$ with coordinates x^α_- and the metric $g^{\alpha\beta}_-$. Then we ask: What conditions do we need to join $\mathcal{M}^+$ and $\mathcal{M}^-$ at Σ smoothly, so that $g^{\alpha\beta}_\pm$ respect the Einstein equations? To answer this question we formalize *junction conditions*. Junction conditions consist of two conditions: the first and the second junction condition.

This section 2.2 is based on a paper by Barrabes and Bressange [2].

2.2.1 Setup

We summarize the above setup and introduce some notations (from (I) to (VI)):
(I). $\mathcal{M}^+$ ($\mathcal{M}^-$) is a manifold which has the metric $g^+_{\mu\nu}$ ($g^-_{\mu\nu}$) and the coordinates x^μ_+ (x^μ_-).
(II). A manifold $\mathcal{M}$ results from gluing $\mathcal{M}^+$ and $\mathcal{M}^-$ at their boundaries $\partial\mathcal{M}^+ = \partial\mathcal{M}^- =: \Sigma$, i.e., $\mathcal{M} = \mathcal{M}^+ \cup \mathcal{M}^-$.
(III). The hypersurface Σ separates $\mathcal{M}$ into $\mathcal{M}^+$ and $\mathcal{M}^-$, i.e., $\Sigma = \mathcal{M}^+ \cap \mathcal{M}^-$.
(IV). We introduce a common coordinate system x^μ on $\mathcal{M}$.
(V). We define the deviation of an arbitrary tensorial function on the both sides of the hypersurface as

$$[F] := (F^+ - F^-)|_\Sigma, \tag{2.22}$$

where F^+ and F^- are functions in $\mathcal{M}^+$ and $\mathcal{M}^-$, respectively. So it is interpreted as the *jump* of an arbitrary tensorial function F on the both sides of the hypersurface. Clearly we have the relations

$$[n^\alpha] = [e^\alpha_a] = 0. \tag{2.23}$$

(VI). Let $\Phi(x) = 0$ be the surface function for Σ. We demand $\Phi(x)$ to have positive (negative) value in $\mathcal{M}^+$ ($\mathcal{M}^-$). Let n^α, defined in Eq. (2.3), be the normal vector for Σ pointing towards the + side. We draw the picture for the above setup and notations in Fig. (2.3). Since we want to identify the distributional description of the Einstein equations, we must calculate the distributional version of the Christoffel symbols, the Riemann tensor, the Ricci tensor and the Ricci scalar. Let us define the distributional function $\tilde{F}$ (F is a tensorial function) as

$$\tilde{F} := F^+\Theta(\Phi) + F^-\Theta(-\Phi), \tag{2.24}$$

where $\Theta(\Phi)$ is the Heaviside's step function:

$$\Theta(\Phi) = \begin{cases} 1 & : \Phi > 0 \\ 0 & : \Phi < 0 \\ 1/2 & : \Phi = 0 \end{cases} \tag{2.25}$$

and

$$\frac{\mathrm{d}}{\mathrm{d}\Phi}\Theta(\Phi) = \delta(\Phi), \tag{2.26}$$

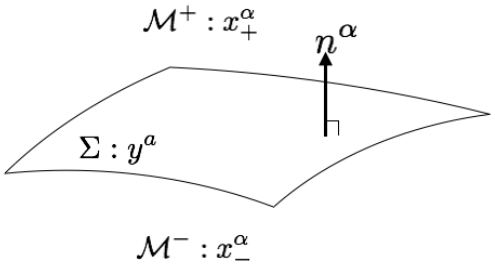

Figure 2.3: Σ partitions a single manifold into two regions, or equivlently, two manifolds are joined at Σ.

where $\delta(\Phi)$ is the Dirac distriution. Eq. (2.25) ensures the identity $\Theta(\Phi)+\Theta(-\Phi)=1$. A simple calculation shows that a derivative of $\tilde{F}$ is given by

$$\partial_\mu \tilde{F} = \widetilde{\partial_\mu F} + \chi n_\mu [F]\delta(\Phi). \tag{2.27}$$

We denote $n_\alpha = \nabla_\alpha \Phi/\chi$ with $\chi^{-1} = \varepsilon/|\nabla\Phi|$. Further we get a product of the two distributional functions:

$$\tilde{F}\tilde{G} = \widetilde{FG} - [F][G]\Theta(\Phi)\Theta(-\Phi), \tag{2.28}$$

where we used $\Theta(\Phi)+\Theta(-\Phi)=1 \Rightarrow \Theta^2(\Phi)+\Theta(\Phi)\Theta(-\Phi)=\Theta(\Phi)$. The last term $\Theta(\Phi)\Theta(-\Phi)$ in Eq. (2.28) vanishes for $\Phi \neq 0$, but does not vanish for $\Phi = 0$. Thus, in general Eq. (2.28) is not distributional.

2.2.2 First junction condition

We introduce the "distributional" metric (denoted with the tilde symbol) written by

$$\tilde{g}_{\mu\nu} = g^+_{\mu\nu}\Theta(\Phi) + g^-_{\mu\nu}\Theta(-\Phi). \tag{2.29}$$

Then its derivative is calculated as

$$\partial_\alpha \tilde{g}_{\mu\nu} = \widetilde{\partial_\alpha g_{\mu\nu}} + \chi n_\alpha [g_{\mu\nu}]\delta(\Phi). \tag{2.30}$$

Evidently, Eq. (2.30) has the delta term. It causes unfavorable property when we evaluate the Riemann tensor because the Riemann tensor includes the derivative of Eq. (2.30), $\mathrm{d}\delta(\Phi)/\mathrm{d}\Phi$, which is not defined. The presence of $\mathrm{d}\delta(\Phi)/\mathrm{d}\Phi$ forces the Christoffel symbols, the Riemann, the Ricci and the Einstein tensor to be non-distributional. We want the unfavored term to vanish. We want to have the distributional Einstein equations. To do so, we demand the co-efficient of $\delta(\Phi)$ in Eq. (2.30) vanishes, i.e.,

$$[g_{\mu\nu}] = 0. \tag{2.31}$$

This statement is written by the coordinate system x^α, but, we transform this statement into a coordinate-invariant form. Multiplying $e^\mu_a e^\nu_b$ to Eq. (2.31) means $[g_{\mu\nu}]e^\mu_a e^\nu_b = [g_{\mu\nu}e^\mu_a e^\nu_b] = 0$ which is

$$[h_{ab}] = 0. \tag{2.32}$$

Eq. (2.32) states that the induced metric must be same on the both sides of hypersurface. This is required to get distributional tensors. Eq. (2.32) is our first junction condition.

Note that when either F or G in Eq. (2.28) is the metric function $g^{\alpha\beta}$, one has

$$\tilde{g}^{\alpha\beta}\tilde{A} = \widetilde{g^{\alpha\beta}A} - [g^{\alpha\beta}][A]\Theta(\Phi)\Theta(-\Phi) = \widetilde{g^{\alpha\beta}A}. \tag{2.33}$$

Hence, the contraction of any distributional function $\tilde{A}$ with $\tilde{g}^{\alpha\beta}$ becomes distributional.

2.2.3 Second junction condition

Here, we start calculations for distributional tensors. The Christoffel symbols composed of the distributional metric are calculated as

$$\tilde{\Gamma}^{\alpha}_{\beta\gamma} = \Gamma^{+\alpha}_{\beta\gamma}\Theta(\Phi) + \Gamma^{-\alpha}_{\beta\gamma}\Theta(-\Phi) \tag{2.34}$$

and, from (2.27), their derivative is

$$\partial_\mu\tilde{\Gamma}^{\alpha}_{\beta\gamma} = \widetilde{\partial_\mu\Gamma^{\alpha}_{\beta\gamma}} + \chi n_\mu[\Gamma^{\alpha}_{\beta\gamma}]\delta(\Phi), \tag{2.35}$$

where

$$[\Gamma^{\alpha}_{\beta\gamma}] = (\Gamma^{+\alpha}_{\beta\gamma} - \Gamma^{-\alpha}_{\beta\gamma})|_\Sigma = \frac{1}{2}g^{\alpha\sigma}([g_{\sigma\beta,\gamma}] + [g_{\sigma\gamma,\beta}] - [g_{\beta\gamma,\sigma}]). \tag{2.36}$$

We used $[g_{\mu\nu}] = 0 \Leftrightarrow g^{+}_{\mu\nu}|_\Sigma = g^{-}_{\mu\nu}|_\Sigma =: g_{\mu\nu}|_\Sigma$.

If the derivative of the metric is *discontinuous* on Σ, we define $\gamma_{\alpha\beta}$ through the jump of the metric-differentiation:

$$[\partial_\mu g_{\alpha\beta}] =: \varepsilon^{-1}n_\mu\gamma_{\alpha\beta}. \tag{2.37}$$

Evidently $\gamma_{\alpha\beta}$ is symmetric. Contracting n^μ for Eq. (2.37), we find

$$\gamma_{\alpha\beta} = n^\mu[\partial_\mu g_{\alpha\beta}]. \tag{2.38}$$

Substituting Eq. (2.37) into the expression for $[\Gamma^{\alpha}_{\beta\gamma}]$, we have

$$[\Gamma^{\alpha}_{\beta\gamma}] = \varepsilon^{-1}(\gamma^{\alpha}{}_{(\beta}n_{\gamma)} - \frac{1}{2}n^\alpha\gamma_{\beta\gamma}). \tag{2.39}$$

Now, we have all tools for deriving the Einstein equations. From above quantities, the Riemann tensor is given by

$$\begin{aligned} R^{\mu}{}_{\nu\alpha\beta} =& \widetilde{R^{\mu}{}_{\nu\alpha\beta}} + \chi([\Gamma^{\mu}{}_{\nu\beta}]n_\alpha - [\Gamma^{\mu}{}_{\nu\alpha}]n_\beta)\delta(\Phi) + ([\Gamma^{\mu}{}_{\rho\beta}][\Gamma^{\rho}{}_{\nu\alpha}] - [\Gamma^{\mu}{}_{\rho\alpha}][\Gamma^{\rho}{}_{\nu\beta}])\Theta(\Phi)\Theta(-\Phi) \\ =& \widetilde{R^{\mu}{}_{\nu\alpha\beta}} + \chi\varepsilon^{-1}\left(\frac{1}{2}\gamma^{\mu}{}_{\beta}n_\nu n_\alpha - \frac{1}{2}n^\mu\gamma_{\nu\beta}n_\alpha - \frac{1}{2}\gamma^{\mu}{}_{\alpha}n_\nu n_\beta + \frac{1}{2}n^\mu\gamma_{\nu\alpha}n_\beta\right)\delta(\Phi) \\ &+ ([\Gamma^{\mu}{}_{\rho\beta}][\Gamma^{\rho}{}_{\nu\alpha}] - [\Gamma^{\mu}{}_{\rho\alpha}][\Gamma^{\rho}{}_{\nu\beta}])\Theta(\Phi)\Theta(-\Phi). \end{aligned} \tag{2.40}$$

The Ricci tensor is given by

$$R_{\nu\beta} = \widetilde{R_{\nu\beta}} + \chi\varepsilon^{-1}\left(\gamma_{(\nu}n_{\beta)} - \frac{\varepsilon}{2}\gamma_{\nu\beta} - \frac{1}{2}\gamma n_\nu n_\beta\right)\delta(\Phi) + \{\Theta(\Phi)\Theta(-\Phi)\text{term}\}, \tag{2.41}$$

where we defined

$$\gamma_\mu := \gamma_{\mu\alpha}n^\alpha, \quad \gamma := \gamma^\alpha{}_\alpha. \tag{2.42}$$

The Ricci scalar is

$$R = g^{\nu\beta}R_{\nu\beta} = \widetilde{g^{\nu\beta}R_{\nu\beta}} + \chi\varepsilon^{-1}\left(\gamma^\beta n_\beta - \varepsilon\gamma\right)\delta(\Phi) + \Theta(\Phi)\Theta(-\Phi)\text{term} \ . \tag{2.43}$$

$[g^{\nu\beta}] = 0$ and $\tilde{g}^{\nu\beta}|_\Sigma = (g^{+\nu\beta} + g^{-\nu\beta})/2 = g^{\nu\beta}|_\Sigma$ was used. Hence, the Einstein tensor takes the form

$$\begin{aligned} G_{\nu\beta} =& \tilde{R}_{\nu\beta} - \frac{\tilde{g}_{\nu\beta}}{2}\tilde{R} \\ =& \widetilde{G_{\nu\beta}} + \chi\varepsilon^{-1}\left(\gamma_{(\nu}n_{\beta)} - \frac{\varepsilon}{2}\gamma_{\nu\beta} - \frac{1}{2}\gamma n_\nu n_\beta - \frac{1}{2}g_{\nu\beta}(\gamma^\alpha n_\alpha - \varepsilon\gamma)\right)\delta(\Phi) + \Theta(\Phi)\Theta(-\Phi)\text{term} \ . \end{aligned} \tag{2.44}$$

Since the Einstein tensor includes the delta term, we set the distributional total stress-energy tensor as

$$T_{\mu\nu} = \widetilde{T_{\mu\nu}} + \chi S_{\mu\nu}\delta(\Phi). \tag{2.45}$$

Equating Eq. (2.44) with Eq. (2.45) yields the Einstein equations. This Einstein equations are distributional: $G^+_{\mu\nu} = 8\pi T^+_{\mu\nu}$ for $\Phi > 0$, $G^-_{\mu\nu} = 8\pi T^-_{\mu\nu}$ for $\Phi < 0$ and the delta term contributes for $\Phi = 0$. Since $\Phi = 0$ describes a hypersurface, the Einstein equations on $\Phi = 0$ yields equations of motion for Σ:

$$\gamma_{(\mu}n_{\nu)} - \frac{\varepsilon}{2}\gamma_{\mu\nu} - \frac{1}{2}\gamma n_\mu n_\nu - \frac{1}{2}g_{\mu\nu}(\gamma^\alpha n_\alpha - \varepsilon\gamma) = 8\pi\varepsilon S_{\mu\nu}. \tag{2.46}$$

Eq. (2.46) is our second junction condition. One can verify $S_{\mu\nu}$ lives on the hypersurface, $S_{\mu\nu}n^\nu = 0$, by straight forward calculation. After taking the contraction with respect to $g^{\mu\nu}$, Eq. (2.46) takes the form

$$8\pi\varepsilon S = -\gamma_\mu n^\mu + \varepsilon\gamma. \tag{2.47}$$

Note that $-\gamma_\mu n^\mu + \varepsilon\gamma$ is invariant under the gauge transformation:

$$\gamma_{\alpha\beta} \to \gamma_{\alpha\beta} + 2\lambda_{(\alpha}n_{\beta)}, \tag{2.48}$$

where λ_α is an arbitrarily vector field. Since a vector field λ^α has 4 degrees of freedom, we can set $\gamma^\alpha = 0$ by fixing the gauge. In this gauge our second junction condition Eq. (2.46) reduces to

$$-\varepsilon\gamma_{\mu\nu} + \gamma(g_{\mu\nu}\varepsilon - n_\mu n_\nu) = 16\pi\varepsilon S_{\mu\nu}, . \tag{2.49}$$

2.2.4 The intrinsic description

Since we have established the Einstein equations on a hypersurface as tensorial equations of $g_{\alpha\beta}$, we can re-express the equations in the intrinsic language as tensorial equations of h_{ab}.

We multiply $e^\mu_a e^\nu_b$ to both sides of Eq. (2.49). Then,

$$16\pi S_{ab} = -\gamma_{ab} + \gamma h_{ab}. \tag{2.50}$$

We used the relation

$$S_{ab} = S_{\mu\nu} e^\mu_a e^\nu_b, \tag{2.51}$$

since $S^{\mu\nu}$ lives on Σ. By the way, we calculate

$$\begin{aligned}[n_{\beta;\gamma}] =& -[\Gamma^\alpha_{\ \beta\gamma}] n_\alpha \\ =& -\frac{\varepsilon^{-1}}{2}(n_\gamma \gamma^\alpha_\beta n_\alpha + n_\beta \gamma^\alpha_\gamma n_\alpha - \varepsilon \gamma_{\beta\gamma}).\end{aligned} \tag{2.52}$$

Then we have the relation between the extrinsic curvature and γ_{ab} as follows

$$[K_{ab}] = [n_{\beta;\gamma}] e^\beta_a e^\gamma_b = \frac{1}{2}\gamma_{ab}. \tag{2.53}$$

We used $[e^\alpha_a] = 0$ and $e^\alpha_a n_\alpha = 0$. Using Eq. (2.53), we arrive

$$8\pi S_{ab} = -[K_{ab}] + [K] h_{ab}. \tag{2.54}$$

Eq. (2.54) shows us that the stress-energy tensor on the hypersurface S_{ab} vanishes if the extrinsic curvature is same at the both sides of the hypersurface, $[K_{ab}] = 0$. This means that a smooth joining of two manifolds $\mathcal{M}^+$ and $\mathcal{M}^-$ is possible if $[h_{ab}] = 0$ and $[K_{ab}] = 0$ are satisfied.

On the other hand, there is a stress-energy tensor which satisfies Eq. (2.54) on Σ if $[K_{ab}] \neq 0$, i.e., the extrinsic curvature is discontinuous at Σ. The matter with non-zero S_{ab} is confined to the infinitesimally thin surface Σ, so we call the surface *thin-shell*. For a timelike or spacelike Σ, Eq. (2.54) describes the motion for the thin-shell.

2.2.5 Constraints

As known, d-dimensional Einstein tensor is related with $(d-1)$-dimensional extrinsic curvature by the Codazzi equation,

$$(G_{\alpha\beta} e^\alpha_a n^\beta)_\pm = K_a^{\ b\pm}_{\ \ |b} - K^\pm_{,a}, \tag{2.55}$$

where $|$ is the covariant derivative defined on Σ. Substituting the gravitational field equations for the Codazzi equation Eq. (2.55) and taking their jump, we get

$$[K_a^{\ b}_{\ \ |b}] - [K_{,a}] = 8\pi [T_{\alpha\beta} e^\alpha_a n^\beta]. \tag{2.56}$$

Due to the above equations, a covariant derivative of Eq. (2.54) with respect to h_{ab} reads the constrains (the momentum constraints) expressed as below:

$$S_a^{\ b}_{\ \ |b} = -[T_{\alpha\beta} e^\alpha_a n^\beta]. \tag{2.57}$$

Another constraint is obtained by the the Gauss equation

$$-2\varepsilon (G_{\alpha\beta} n^\alpha n^\beta)_\pm = {}^{(d-1)}R + \varepsilon (K^{ab\pm} K_{ab\pm} - K^2_\pm), \tag{2.58}$$

where ${}^{(d-1)}R$ is the Ricci scalar which consists of the induced metric. Substituting Einstein equations into the Gauss equation and taking their jump, we obtain

$$-16\pi[T_{\alpha\beta}n^\alpha n^\beta] = [K^{ab}K_{ab} - K^2]. \tag{2.59}$$

We note that $[K^{ab}K_{ab}] = 2\bar{K}^{ab}[K_{ab}]$ and $[K^2] = 2\bar{K}[K]$, where $\bar{X} := (X_+ + X_-)|_\Sigma/2$. Contracting Eq. (2.54) with $2\bar{K}^{ab}$, we find $16\pi\bar{K}^{ab}S_{ab} = -[K^{ab}K_{ab}] + [K^2]$. Finally we obtain the another constraint (the Hamiltonian constraint),

$$\bar{K}^{ab}S_{ab} = [T_{\alpha\beta}n^\alpha n^\beta]. \tag{2.60}$$

2.2.6 Summary of junction conditions

We summarize the results of this subsection. For smooth joining of spacetimes at their boundaries,

$$[h_{ab}] = 0 \quad \text{and} \quad [K_{ab}] = 0 \tag{2.61}$$

are required.

On the other hand, if $[K_{ab}] \neq 0$, in addition to $[h_{ab}] = 0$, there is a stress-energy tensor which satisfies

$$8\pi S_{ab} = -[K_{ab}] + [K]h_{ab}. \tag{2.62}$$

S_{ab} is confined on Σ. The corresponding constraints are given by

$$S_a{}^b{}_{|b} = -[T_{\alpha\beta}e_a^\alpha n^\beta] \tag{2.63}$$

and

$$\bar{K}^{ab}S_{ab} = [T_{\alpha\beta}n^\alpha n^\beta], \tag{2.64}$$

where $\bar{K}^{ab} := (K_+^{ab} + K_-^{ab})|_\Sigma/2$.

2.3 Higher dimensional gravitational theories

Though general relativity is most successful simple gravitational theory, many alternative theories have also been theoretically investigated. Particularly, gravity models with four or higher dimension have been investigated in many aspects:

The notion of higher dimensional spacetimes was first introduced by Kaluza and Klein [18]. They found that the gravitational field and the electromagnetic field can be unified in five dimensional spacetimes. In their work, the length of the fifth dimension is confined to a very small scale.

The gauge/gravity correspondence conjectured by Maldacena [19] generally sheds light on structures in the anti de-Sitter spacetime in higher dimensions.

In the end of the twentieth century, Randall and Sundrum proposed an idea that we perhaps live in a (3+1) dimensional brane in the (4+1) dimensional spacetime whose extra dimension spreads widely with a negative cosmological constant, which is called a brane-world model [20]. In this model, the bulk five dimensional spacetime is the anti de-Sitter spacetime.

In a broader context, candidate theories for quantum gravity, such as superstring theory and M-theory, entail higher dimensional spacetimes.

In the rest of the thesis, we want to focus on our attention to Einstein and Einstein-Gauss-Bonnet theory of gravity.

2.3.1 Einstein gravity

The most natural and the simplest generalization into higher dimension is the higher dimensional generalization of general relativity. This generalization is taken place by writing the gravitational action in vacuum as

$$S_{\mathrm{E}} = \frac{1}{2\kappa_d^2}\int \mathrm{d}^d x\sqrt{-g}R \quad (d \geq 3), \tag{2.65}$$

where $\kappa_d := \sqrt{8\pi G_d}$ and G_d is a d-dimensional gravitational constant. The Ricci scalar R consists of d-dimensional metric. Variation of the action with respect to the metric gives the same form of general relativity, $G_{\mu\nu} = 0$. This Einstein gravity will be adopted later in this thesis.

2.3.2 Einstein-Gauss-Bonnet gravity

$d(\geq 5)$-dimensional Einstein-Gauss-Bonnet gravity in vacuum, of which action is given by

$$S = \frac{1}{2\kappa_d^2}\int \mathrm{d}^d x\sqrt{-g}\Big(R - 2\Lambda + \alpha L_{\mathrm{GB}}\Big), \tag{2.66}$$

where Λ is the cosmological constant. The Gauss-Bonnet term L_{GB} is defined by the following special combination of the Ricci scalar R, the Ricci tensor $R_{\mu\nu}$ and the Riemann tensor $R^{\mu}{}_{\nu\rho\sigma}$:

$$L_{\mathrm{GB}} := R^2 - 4R_{\mu\nu}R^{\mu\nu} + R_{\mu\nu\rho\sigma}R^{\mu\nu\rho\sigma}. \tag{2.67}$$

The Gauss-Bonnet term appears in the action as the ghost-free quadratic curvature correction term in the low-energy limit of heterotic superstring theory in ten dimensions

(together with a dilaton) [21]. In this context, the coupling constant α is regarded as the inverse string tension and positive definite.

For this reason, we assume $\alpha > 0$ throughout this thesis. In addition, we put another conservative assumption $1 + 4\tilde{\alpha}\tilde{\Lambda} > 0$, where

$$\tilde{\Lambda} := \frac{2\Lambda}{(d-1)(d-2)}, \qquad \tilde{\alpha} := (d-3)(d-4)\alpha, \tag{2.68}$$

so that the theory admits maximally symmetric vacua, namely Minkowski, de Sitter (dS), or anti-de Sitter (AdS) vacuum solutions. Although there exists a maximally symmetric vacuum for $1 + 4\tilde{\alpha}\tilde{\Lambda} = 0$, we don't consider this case for simplicity.

Variation of the action (2.66) with respect to the metric $g^{\mu\nu}$ gives the following vacuum Einstein-Gauss-Bonnet equations:

$$G^{\mu}{}_{\nu} + \alpha H^{\mu}{}_{\nu} + \Lambda \delta^{\mu}{}_{\nu} = 0, \tag{2.69}$$

where

$$G_{\mu\nu} := R_{\mu\nu} - \frac{1}{2} g_{\mu\nu} R, \tag{2.70}$$

$$H_{\mu\nu} := 2\Big(R R_{\mu\nu} - 2 R_{\mu\alpha} R^{\alpha}{}_{\nu} - 2 R^{\alpha\beta} R_{\mu\alpha\nu\beta} + R_{\mu}{}^{\alpha\beta\gamma} R_{\nu\alpha\beta\gamma} \Big) - \frac{1}{2} g_{\mu\nu} L_{\mathrm{GB}}. \tag{2.71}$$

The tensor $H_{\mu\nu}$ obtained from the Gauss-Bonnet term does not give any higher-derivative term and $H_{\mu\nu} \equiv 0$ holds for $d \leq 4$. As a result, Einstein-Gauss-Bonnet gravity is a second-order quasi-linear theory as Einstein gravity is.

3 Thin-shell wormhole

As mentioned in section (1.2), Morris and Thorne have pioneered qualitative study for static spherically symmetric wormholes.

An another class of traversable wormholes has been found by M. Visser. This class of wormholes can be obtained by a "cut-and-paste" procedure [22] and such structures are called *thin-shell* wormholes. E. Poisson and M. Visser first presented stability analysis for spherical perturbations around such thin-shell wormhole, and found that there are stable configurations according to the equation of state of an exotic matter residing on the throat [23]. The work of Poisson and Visser has been extended in different directions; charged thin-shell wormhole [24], thin-shell wormhole constructed by a couple of Schwarzschild spacetimes of different masses [25] and thin-shell wormhole with a cosmological constant [26]. Thin-shell wormhole in cylindrically symmetric spacetimes have also been studied [27, 28]. Garcia *et al.* published a paper about stability for generic static and spherically symmetric thin-shell wormhole [29]. Dias and Lemos studied stability in higher dimensional Einstein gravity [30].

This wormhole models are easy to construct, which certainly have a wormhole structure. Thin-shell spacetimes have no differentiability for its metric at their throat, i.e. they are only C^0, contrary to smooth wormhole models such as the Ellis wormhole, which are smooth (C^∞) at their throat. Though thin-shell wormholes are not smooth, they indeed have qualitatively common features with smooth wormholes. Hence, investigating of properties of thin-shell wormholes may prompt deeper understanding for properties of generic wormholes.

In this section, we show construction and linear stability against perturbations preserving symmetries of thin-shell wormholes.

3.1 Construction

In order to investigate wormhole stability, one must construct thin-shell wormholes. Here, we show how to build them.

First of all, we would like to note that the construction will be operated in spherically, planarly (or cylindrically) and hyperbolically symmetric spacetimes in d-dimensional ($d \geq 3$) Einstein gravity with an electromagnetic field and a cosmological constant in bulk spacetimes. Such rich setup is required for later analysis in Sec.4 and 5.

The formalism for maximally symmetric d-dimensional thin shell wormholes has been developed first by Dias and Lemos [30]. We extend their formalism to more general situations. We obtain wormholes by operating three steps invoking junction conditions [1].

Firstly, consider a couple of d dimensional manifolds, $\mathcal{M}_\pm$. We assume $d \geq 3$. The d dimensional Einstein equations are given by

$$G_{\mu\nu\pm} + \frac{(d-1)(d-2)}{6}\Lambda_\pm g_{\mu\nu\pm} = 8\pi T_{\mu\nu\pm}, \tag{3.1}$$

where $G_{\mu\nu\pm}$, $T_{\mu\nu\pm}$ and $\Lambda_\pm$ are Einstein tensors, stress-energy tensors and cosmological constants in the manifolds $\mathcal{M}_\pm$, respectively. The metrics on $\mathcal{M}_\pm$ are given by $g^\pm_{\mu\nu}(x^\pm)$. The metrics for static and spherically, planar and hyperbolically symmetric spacetimes

on $\mathcal{M}_\pm$ are written as

$$ds_\pm^2 = -f_\pm(r_\pm)dt_\pm^2 + f_\pm(r_\pm)^{-1}dr_\pm^2 + r_\pm^2(d\Omega_{d-2}^k)_\pm^2, \tag{3.2}$$

$$f_\pm(r_\pm) = k - \frac{\Lambda_\pm r_\pm^2}{3} - \frac{M_\pm}{r_\pm^{d-3}} + \frac{Q_\pm^2}{r_\pm^{2(d-3)}}, \tag{3.3}$$

respectively. $M_\pm$ and $Q_\pm$ correspond to the mass and charge parameters in $\mathcal{M}_\pm$, respectively. k is a constant that determines the geometry of the $(d-2)$ dimensional space and takes ± 1 or 0. $k = +1$, 0 and -1 correspond to a sphere, plane (or cylinder) and a hyperboloid, respectively. $(d\Omega_{d-2}^k)^2$ is given by

$$\begin{aligned}
(d\Omega_{d-2}^1)^2 =& d\theta_1^2 + \sin^2\theta_1 d\theta_2^2 + \ldots + \prod_{i=2}^{d-3}\sin^2\theta_i d\theta_{d-2}^2 \\
(d\Omega_{d-2}^0)^2 =& d\theta_1^2 + d\theta_2^2 + \ldots + d\theta_{d-2}^2 \\
(d\Omega_{d-2}^{-1})^2 =& d\theta_1^2 + \sinh^2\theta_1 d\theta_2^2 + \ldots + \sinh^2\theta_1 \prod_{i=2}^{d-3}\sin^2\theta_i d\theta_{d-2}^2.
\end{aligned} \tag{3.4}$$

We should note that by generalized Birkhoff's theorem [31], the metric (3.2) is the unique solution of Einstein equations of electrovacuum for $k = \pm 1$. However, this is *not* unique for $k = 0$. Therefore, we should regard Eq. (3.2) as a special electrovacuum spacetime for $k = 0$.

Secondly, we construct a manifold $\mathcal{M}$ by gluing $\mathcal{M}_\pm$ at their boundaries. We choose the boundary hypersurfaces $\partial\mathcal{M}_\pm$ as follows:

$$\partial\mathcal{M}_\pm := \{r_\pm = a \mid f_\pm(a) > 0\}, \tag{3.5}$$

where a is called the thin shell radius. Then, by gluing the two regions $\tilde{\mathcal{M}}_\pm$ which are defined as

$$\tilde{\mathcal{M}}_\pm := \{r_\pm \geq a \mid f_\pm(a) > 0\} \tag{3.6}$$

with matching their boundaries, $\partial\mathcal{M}_+ = \partial\mathcal{M}_- := \Sigma$, we can construct a new manifold $\mathcal{M}$ which has a wormhole throat at Σ. Σ should be a timelike hypersurface, on which the line element is given by

$$ds_\Sigma^2 = -d\tau^2 + a(\tau)^2(d\Omega_{d-2}^k)^2. \tag{3.7}$$

The surface function for Σ is given by $\Phi = r - a(\tau) = 0$. τ stand for proper time on the junction surface Σ whose position is described by the coordinates $x^\mu(y^a) = x^\mu(\tau, \theta_1, \theta_2, \ldots, \theta_{d-2}) = (t(\tau), a(\tau), \theta_1, \theta_2, \ldots, \theta_{d-2})$, where Greek indices run over $1, 2, \ldots, d$ and Latin indices run over $1, 2, \ldots, d-1$. $\{y^a\}$ is the intrinsic coordinates on Σ.

Thirdly, by using the junction conditions, we derive the Einstein equations for the submanifold Σ. To achieve this, we define unit normals to hypersurfaces $\partial\mathcal{M}_\pm$. The unit normals are defined by Eq. (2.3) and in this case it is

$$n_{\alpha\pm} := \pm\frac{\Phi_{,\alpha}}{\left|\Phi^{,\mu}\Phi_{,\mu}\right|^{\frac{1}{2}}}. \tag{3.8}$$

To construct thin shell wormholes, we make the unit normals on $\partial\mathcal{M}_\pm$ take different signs, while to construct normal thin shell models, the unit normals are chosen to be of same signs. Tangent vector e^α_a is defined in Eq. (2.9). We also define the four-velocity $u^\alpha_\pm$ of the boundary as

$$\begin{aligned} u^\alpha_\pm =& e^\alpha_{\tau\pm} = (\dot{t}_\pm, \dot{a}, 0, \ldots, 0) \\ =& \left(\frac{1}{f_\pm(a)} \sqrt{f_\pm(a) + \dot{a}^2}, \dot{a}, 0, \ldots, 0 \right), \end{aligned} \tag{3.9}$$

where $\dot{} := \partial/\partial\tau$ and $u^\alpha u_\alpha = -1$ is satisfied. The explicit form of Eq. (3.8) is

$$n_{\alpha\pm} = \pm \left(-\dot{a}, \frac{\sqrt{f_\pm + \dot{a}^2}}{f_\pm}, 0, \ldots, 0 \right) \tag{3.10}$$

and the unit normal satisfies $n_\alpha n^\alpha = 1$ and $u^\alpha n_\alpha = 0$.

3.2 Equation of motion for the shell

The equations for the shell Σ are given by Eq. (2.62). The non zero components of the extrinsic curvature are the following:

$$K^{\tau\pm}_\tau = \pm(f_\pm + \dot{a}^2)^{-\frac{1}{2}}(\ddot{a} + \frac{1}{2} f'_\pm), \tag{3.11}$$

$$K^{\theta_1\pm}_{\theta_1} = K^{\theta_2\pm}_{\theta_2} = \ldots = K^{\theta_{d-2}\pm}_{\theta_{d-2}} = \pm \frac{1}{a} \sqrt{f_\pm + \dot{a}^2}, \tag{3.12}$$

where $' := \mathrm{d}/\mathrm{d}a$. Consequently, the non zero components of $[K^i_j]$ are

$$[K^\tau_\tau] = \frac{B_+(a)}{A_+(a)} + \frac{B_-(a)}{A_-(a)}, \tag{3.13}$$

$$[K^{\theta_1}_{\theta_1}] = \ldots = [K^{\theta_{d-2}}_{\theta_{d-2}}] = \frac{A_+(a) + A_-(a)}{a}, \tag{3.14}$$

where

$$A_\pm(a) := \sqrt{f_\pm + \dot{a}^2} \ , \ B_\pm(a) := \ddot{a} + \frac{1}{2} f'_\pm. \tag{3.15}$$

Since our metrics Eq. (3.2) are diagonal, S^i_j is also diagonal and written as

$$S^i_j = \mathrm{diag}(-\sigma, p, p, \ldots, p), \tag{3.16}$$

where p is the surface pressure (of opposite sign to surface tension) and σ is the surface energy density living on the thin-shell. Hence, we obtain the explicit form of Eq. (2.62):

$$\sigma = -\frac{d-2}{8\pi a}(A_+ + A_-), \tag{3.17}$$

$$p = \frac{1}{8\pi} \left\{ \frac{B_+}{A_+} + \frac{B_-}{A_-} + \frac{d-3}{a}(A_+ + A_-) \right\}. \tag{3.18}$$

Note that we deduced a critical property of wormholes that *σ must be negative*.

The conservation law for the surface stress-energy tensor S^i_j is given by Eq. (2.63). Since the stress-energy tensor T^α_β in the bulk spacetime only contains the electromagnetic field,

$$T^\alpha_\beta = \frac{Q^2}{8\pi r^{2(d-2)}}\mathrm{diag}(-1,-1,1,\cdots,1), \tag{3.19}$$

one can find $T^\alpha_\beta e^a_\alpha n^\beta = 0$. Hence Eq. (2.63) yields $S_a{}^b{}_{|b} = 0$ that is

$$\frac{d}{d\tau}(\sigma a^{d-2}) + p\frac{d}{d\tau}(a^{d-2}) = 0. \tag{3.20}$$

Eq. (3.20) corresponds to the conservation law. For later convenience for calculations, we recast Eq. (3.20) as

$$\sigma' = -\frac{d-2}{a}(\sigma + p). \tag{3.21}$$

We can get the master equation for the thin-shell throat by recasting Eq. (3.17) as follows:

$$\dot{a}^2 + V(a) = 0, \tag{3.22}$$

where

$$V(a) = -\left(\frac{4\pi a\sigma}{d-2}\right)^2 - \left(\frac{f_+ - f_-}{2}\right)^2\left(\frac{d-2}{8\pi a\sigma}\right)^2 + \frac{1}{2}\left(f_+ + f_-\right). \tag{3.23}$$

From Eq. (3.22), the range of a which satisfies $V(a) \leq 0$ is the movable range for the shell. Since we obtained Eq. (3.22) by twice squaring of Eq. (3.17), there is possibility that we take wrong solutions which satisfy Eq. (3.22) but do not satisfy Eq. (3.17). See Appendix for the condition of right solutions. By differentiating Eq. (3.22) with respect to τ, we get the equation of motion for the shell as

$$\ddot{a} = -\frac{1}{2}V'(a). \tag{3.24}$$

Suppose a thin-shell throat be static at $a = a_0$ and its throat radius *must* satisfy the relation

$$f(a_0) > 0. \tag{3.25}$$

This condition is called the horizon-avoidance condition in Ref [32].

We analyze stability against small perturbations preserving symmetries. To determine whether the shell is stable or not against the perturbation, we use Taylor expansion of the potential $V(a)$ around the static radius a_0 as

$$V(a) = V(a_0) + V'(a_0)(a-a_0) + \frac{1}{2}V''(a_0)(a-a_0)^2 + \mathcal{O}((a-a_0)^3). \tag{3.26}$$

From Eqs. (3.22) and (3.24), $\dot{a}_0 = 0, \ddot{a}_0 = 0 \Leftrightarrow V(a_0) = 0, V'(a_0) = 0$ so the potential given by Eq. (3.26) reduces to

$$V(a) = \frac{1}{2}V''(a_0)(a-a_0)^2 + \mathcal{O}((a-a_0)^3). \tag{3.27}$$

The leading term is quadratic as to a and has the co-efficient $V''(a_0)$. The sign of the co-efficient makes the form of the potential near static solutions. Therefore, the stability condition against radial perturbations for the static shell is given by

$$V''(a_0) > 0. \tag{3.28}$$

3.3 The simplest thin-shell wormhole

As mentioned before, due to Eq. (3.17), wormholes must have a negative surface energy density, namely, an exotic matter. Hence, the stability of such wormholes depend not only on their geometries but on exotic matters on Σ. Here, in the following, we see the simplest thin-shell wormhole made from gluing two Schwarzschild spacetimes and its stability with various kinds of exotic matter.

3.3.1 The simplest wormhole (Schwarzschild surgery)

The simplest wormhole was first proposed by Visser. As mentioned above, the simplest thin-shell wormhole is constructed from cutting and pasting the couple of identical Schwarzschild spacetimes in the four dimensions, that is, in Eq. (3.3) we take $d = 4$, $k = 1$, $M_\pm = 2M$, $Q_\pm = 0$ and $\Lambda_\pm = 0$ and hence $f(r)_\pm = f(r) = 1 - 2M/r$. Then Eq. (3.23) reduces to

$$V(a) = f(a) - (2\pi a\sigma)^2, \tag{3.29}$$

where σ is not specified yet.

3.4 Stability with various kinds of exotic matter

In the simplest setup of thin-shell wormholes, the potential takes the form of Eq. (3.29). In this setup, we want to study a stability analysis with various kinds of exotic matter, i.e., general fluid, barotropic fluid and a pure tension matter field.

3.4.1 General fluid

First we learn a stability analysis with general fluid, i.e., we do not specify an equation of state for the exotic matter residing on the shell. This case is in the book by Visser [22]. To begin with, we investigate asymptotic form of the potential Eq. (3.29). The explicit form of Eq. (3.29) is

$$V(a) = 1 - \frac{2M}{a} - (2\pi a\sigma)^2. \tag{3.30}$$

In the potential we see that the contribution of M is dominant for $a \to 0$ while the contribution of σ^2 is dominant for $a \to \infty$. Typical forms of the potential is in Fig. (3.1). If fortunately we have $V(\infty) = 0$, the wormhole is prevented from an eternal throat expansion. This condition is explicitly written as

$$V(a \to \infty) = 0 \Leftrightarrow (2\pi\sigma)^2 < a^{-2}. \tag{3.31}$$

Hene we can say that $\sigma \simeq 0$ as $a \to \infty$. Let us carry out Taylor's expansion of p around $\sigma \simeq 0$:

$$\begin{aligned} p &= p|_{\sigma=0} + \left.\frac{\partial p}{\partial \sigma}\right|_{\sigma=0} \sigma + \mathcal{O}(\sigma^2) \\ &=: p_{\sigma 0} + \beta_{\sigma 0}^2 \sigma + \mathcal{O}(\sigma^2). \end{aligned} \tag{3.32}$$

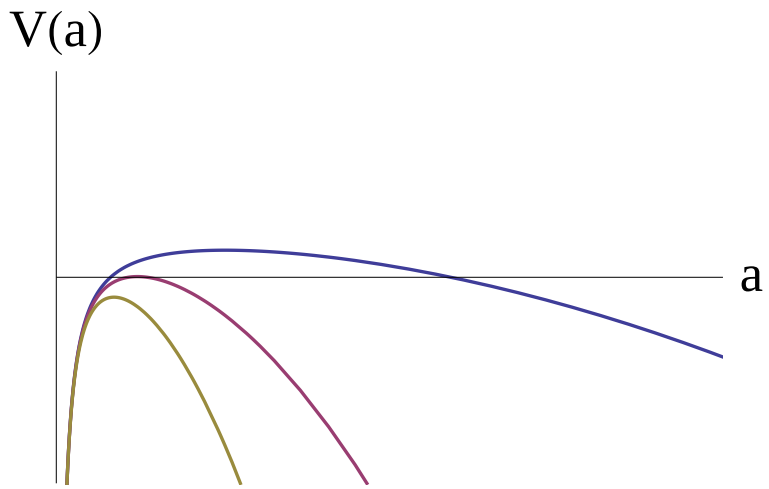

Figure 3.1: Typical figures of the potential. M (assumed to have a positive value in the figure) is dominant for $a \to 0$ while σ^2 is dominant for $a \to \infty$. Movable range for the shell is confined below the axis a.

On the other hand, the conservation law Eq. (3.20) is solved for p:

$$p = -\sigma - \frac{1}{2}\frac{\mathrm{d}\sigma}{\mathrm{d}a}a. \tag{3.33}$$

From Eq. (3.32) and Eq. (3.33), we get

$$(\beta_{\sigma 0}^2 + 1)\sigma = -p_{\sigma 0} - \frac{1}{2}\frac{\mathrm{d}\sigma}{\mathrm{d}a}a. \tag{3.34}$$

For $\beta_{\sigma 0}^2 \neq -1$, this can be integrated as

$$\sigma = Ca^{-2(\beta_{\sigma 0}^2+1)} - (\beta_{\sigma 0}^2 + 1)p_{\sigma 0} \tag{3.35}$$

with a constant C. Actually, $p_{\sigma 0}$ must vanish because of the asymptotic behavior of σ. Hence one obtain

$$\sigma = Ca^{-2(\beta_{\sigma 0}^2+1)}. \tag{3.36}$$

Due to Eq. (3.31) and Eq. (3.36), we see the condition that wormhole is stable against explosion is

$$1 + 2\beta_{\sigma 0}^2 > 0. \tag{3.37}$$

We emphasize that this linear equation of state is valid only for large a. As a throat moves inward from infinity, $\mathcal{O}(\sigma^2)$ term in Eq. (3.32) becomes significant gradually.

Though we have just shown that Eq. (3.37) is no-explosion condition, we also want to have a no-collapse condition. As mentioned above, we see the contribution of M is dominant for $a \to 0$. Since there is no hope for $M > 0$, we assume $M < 0$ for getting no-collapse condition. We also assume that σ becomes zero around $a = 0$: $\sigma \to 0$ as

$a \to 0$. Then we can use Eq. (3.36) also for small a. The two assumptions allow us to write the potential near $a = 0$ as

$$V(a) \simeq 1 + \frac{2|M|}{a} - (2\pi C)^2 a^{-2(2\beta_{\sigma 0}^2+1)}. \tag{3.38}$$

If $a^{-2(2\beta_{\sigma 0}^2+1)} > a^{-1}$, namely, if

$$\beta_{\sigma 0}^2 < -\frac{1}{4} \tag{3.39}$$

is satisfied (and parameters M and C are chosen appropriately), this condition prevents the wormhole from its throat collapsing. Therefore, the overlap of Eq. (3.37) and Eq. (3.39) is fully stable condition:

$$-\frac{1}{2} < \beta_{\sigma 0}^2 < -\frac{1}{4}. \tag{3.40}$$

We summarize the above discussion: It is shown that an equation of state, with an appropriate parameter, protects a wormhole from infinite throat-explosion. Moreover, the two following assumptions can protect the wormhole from collapsing: (1) negative Schwarzschild mass $M < 0$. (2) $\sigma \to 0$ as $a \to 0$. Under the assumptions, one can realize a wormhole which is dynamically and non-linearly stable against collapse and explosion.

3.4.2 Barotropic fluid

This is the case in the paper by Poisson and Visser [23]. They assumed barotropic equation of state, $p = p(\sigma)$. Then Eq. (3.21) can be integrated as

$$\log(a) = -\frac{1}{2}\int \frac{d\sigma}{\sigma + p(\sigma)}. \tag{3.41}$$

Since Eq. (3.41) is a equation for σ, the solution is given by $\sigma = \sigma(a)$. Substituting $\sigma(a)$ into the master equation Eq. (3.29) reads

$$V(a) = f(a) - \left(2\pi a \sigma(a)\right)^2. \tag{3.42}$$

Static solutions $a = a_0$ satisfy

$$\sigma(a_0) := \sigma_0 = -\frac{1}{2\pi a_0}\sqrt{1 - \frac{2M}{a_0}}, \tag{3.43}$$

$$p(a_0) := p_0 = \frac{1}{4\pi a_0}\frac{1 - M/a_0}{\sqrt{1 - 2M/a_0}}. \tag{3.44}$$

The wormhole is stable if the potential satisfies Eq. (3.28). To evaluate $V''(a_0)$ we calculate V' and V'' which include σ' and σ''. We re-write Eq. (3.21) as

$$(\sigma a)' = -(\sigma + 2p) \tag{3.45}$$

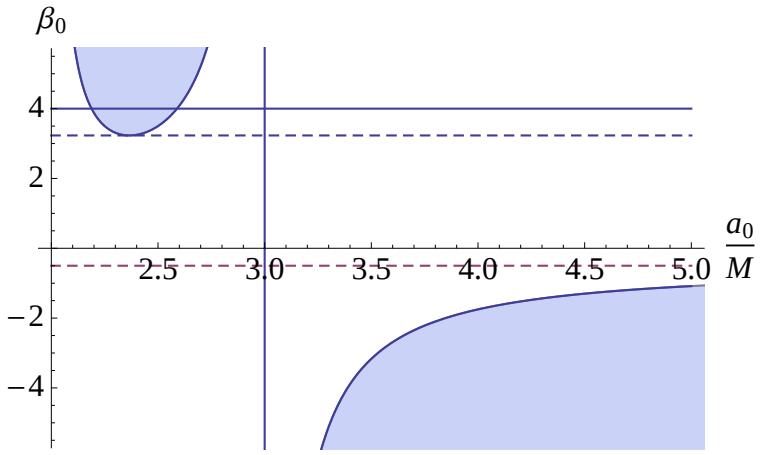

Figure 3.2: If β_0 is given one knows the range of a_0, the stable static throat solution. Region $a_0 < 2M$ is meaningless since such region does not exist in the wormhole. The upper broken line is $\beta_0 = \frac{3+\sqrt{3}}{2}$ while lower is $\beta_0 = -\frac{1}{2}$. Shaded region corresponds to stable region. We drawn the horizontal line with $\beta_0 = 4$ for an example. In this case, wormhole can be stable if $2.19M < a_0 < 2.59M$.

Differentiation of Eq. (3.45) reads

$$(\sigma a)'' = \frac{2}{a}(\sigma + p)(1 + 2\beta(\sigma)), \tag{3.46}$$

where

$$\beta(\sigma) := \left.\frac{dp}{d\sigma}\right|_{\sigma}. \tag{3.47}$$

From Eq. (3.46) and Eq. (3.46), $V'(a)$ and $V''(a)$ becomes

$$V'(a) = \frac{2M}{a^2} + 8\pi\sigma a(\sigma + 2p), \tag{3.48}$$

$$V''(a) = -\frac{4M}{a^3} - 8\pi^2((\sigma + p)^2 + 2\sigma(1 + 2\beta)(\sigma + p)). \tag{3.49}$$

Substituting the explicit descriptions of σ_0 and p_0, we finally arrive

$$V''(a_0) = -\frac{2}{a_0^2}\left(\frac{2M}{a_0} + \frac{\frac{M^2}{a_0^2}}{1 - \frac{2M}{a_0}} + (1 + 2\beta_0)(1 - \frac{3M}{a_0})\right). \tag{3.50}$$

Hence the stability condition is

$$\beta_0(1 - \frac{3M}{a_0}) < -\frac{1 - \frac{3M}{a_0} + \frac{3M^2}{a_0^2}}{2(1 - \frac{2M}{a_0})}. \tag{3.51}$$

Since values of a_0 change the sign of $(1 - \frac{3M}{a_0})$, this condition is split into two parts:

$$\begin{aligned} &\beta_0 > F(a_0) : 2M < a_0 < 3M, \\ &\beta_0 < F(a_0) : 3M < a_0, \end{aligned} \tag{3.52}$$

where

$$F(a) \equiv -\frac{1-\frac{3M}{a}+\frac{3M^2}{a^2}}{2(1-\frac{2M}{a})(1-\frac{3M}{a})}. \tag{3.53}$$

When $a_0 = 3M$ it is unstable regardless of the value β_0 because $V''(a_0 = 3M) = -2/(9M^2) < 0$. Due to Eq. (3.52), one can identify the stable range of a_0 if β_0 is given. Stable regions are depicted as shaded regions in Fig. (3.2).

Although there are two values a_0 that stand for two extremums of $F(a_0)$, namely, $a_0/M = (3 \pm \sqrt{3})/2$, the smaller solution $(3-\sqrt{3})/2$ is a meaningless value because we consider the range $a_0 > 2M$.

From the above analysis, we can state that if we take a particular value of β_0, stability range a_0 is determined. Since particular β_0 relates to particular equation of state of exotic matters, this statement is equivalent to that types of exotic matter determine the range of radius a_0 which is stable static throat radius.

We summarize the stability analysis in the assumption of barotropic equation of state:
1) There are stable solutions in $\beta_0 \geq \frac{3+\sqrt{3}}{2}$ or $\beta_0 < -\frac{1}{2}$.
2) No solution in $\frac{3+\sqrt{3}}{2} > \beta_0 > -\frac{1}{2}$ is stable.
3) The solution at $a_0 = 3M$ is unstable regardless of the value of β_0.

In the work of Poisson and Visser, they took the barotropic equation of state $p = p(\sigma)$ and the stability analysis does not need to specify the form of the equation of state. As one can see in Fig. (3.2), there is no stable wormhole between $0 < \beta_0^2 < 1$. β_0^2 can be interpreted as the square of the magnitude of the speed of sound for the exotic matter. Poisson and Visser pointed out that since we don't know about microphysics for exotic matter there is no guarantee that β_0^2 actually is the speed of sound. Therefore region with $\beta_0^2 \leq 0$ and $\beta_0^2 \geq 1$ is not a priori ruled out.

3.4.3 Pure tension

We will see that what happens if we adopt a pure tension as the exotic matter. Pure tension is an equation of state that is written by

$$p = -\sigma \quad (\sigma : \text{const.}). \tag{3.54}$$

In our wormhole situation, σ must be negative-definite because of Eq. (3.17). In this setup, due to Eq. (3.43), Eq. (3.44) and Eq. (3.54) we identify the position of the static solution as $a_0 = 3M$. Then we have $V''(3M) = -4/(27M^2) - 4(2\pi\sigma)^2 < 0$, that is, the wormhole is unstable.

4 Generalized Thin-shell wormholes

In Sec.3 we mentioned there are many generalizations of the thin-shell wormhole introduced by Visser. In this section we review some of its generalizations done by several authors.

4.1 Charged generalization

A charged generalization is a theoretically natural extension of the simplest thin-shell wormhole. This is done by Eiroa and Romero [24]. A charged wormhole is constructed from cutting and pasting the couple of identical Reisnner-Nordström spacetimes in the four dimensions. This situation is reproduced in our formura by putting

$$d = 4, k = 1, M_\pm = 2M, Q_\pm = Q, \Lambda_\pm = 0$$

into Eq. (3.3). In this case, stability condition reduces to

$$-(1 - \frac{3M}{a_0} + \frac{2Q^2}{a_0^2})\beta_0^2 > \frac{1}{2(1 - \frac{2M}{a_0} + \frac{Q^2}{a_0^2})}\big(1 - \frac{3M}{a_0} + \frac{3M^2}{a_0^2} - \frac{Q^2}{a_0 M}\big). \tag{4.1}$$

Stable regions are drawn with each value of charge $|Q|$ in Fig. (4.1). The outer horizon r_+ corresponds to

$$\frac{r_+}{M} = 1 + \sqrt{1 - \frac{|Q|^2}{M^2}}, \tag{4.2}$$

Therefore regions inside of the outer horizons (vertical lines in the figure) have no physical meaning. One finds stable region appears in $0 < \beta_0^2 < 1$, the sound-speed condition that is supposed to be satisfied for conventional matters. After the charge reaches the extremal value, $|Q| = M$, there is no longer horizon. So any static solution a_0 can be stable for corresponding β_0^2. We should emphasize that there are *always* stable solutions when $1 < \frac{|Q|}{M} \leq \frac{3}{\sqrt{8}} \sim 1.06$ *regardless of values of* β_0^2.

4.2 Presence of a cosmological constant

Another generalization have operated in a cosmological sense. Lobo and Crawford developed the construction by putting cosmological constant to the simplest wormhole [26]. In our notation, such situation is recovered by taking

$$d = 4, k = 1, M_\pm = 2M, Q_\pm = 0, \Lambda_\pm = \Lambda$$

in Eq. (3.3). Stability condition reduces to

$$\beta_0^2 \left(1 - \frac{3M}{a_0}\right) < -\frac{1 - 3M/a_0 + 3M^2/a_0^2 - \Lambda M a_0}{2\,(1 - 2M/a_0 - \Lambda a_0^2/3)}. \tag{4.3}$$

Since ingredient spacetime is Schwarzschild-(anti) de-Sitter, for any Λ the event horizon r_H (and also the cosmological horizon for $\Lambda > 0$) exists where the equation

$$1 - \frac{2M}{r} - \frac{\Lambda r^2}{3} = 0 \tag{4.4}$$

holds. Evidently, $\Lambda = 0$ corresponds to the Schwarzschild shell wormhole. Fig. (4.2) and Fig. (4.3) show Schwarzschild-de Sitter and Schwarzschild-anti de Sitter thin-shell wormhole, respectively.

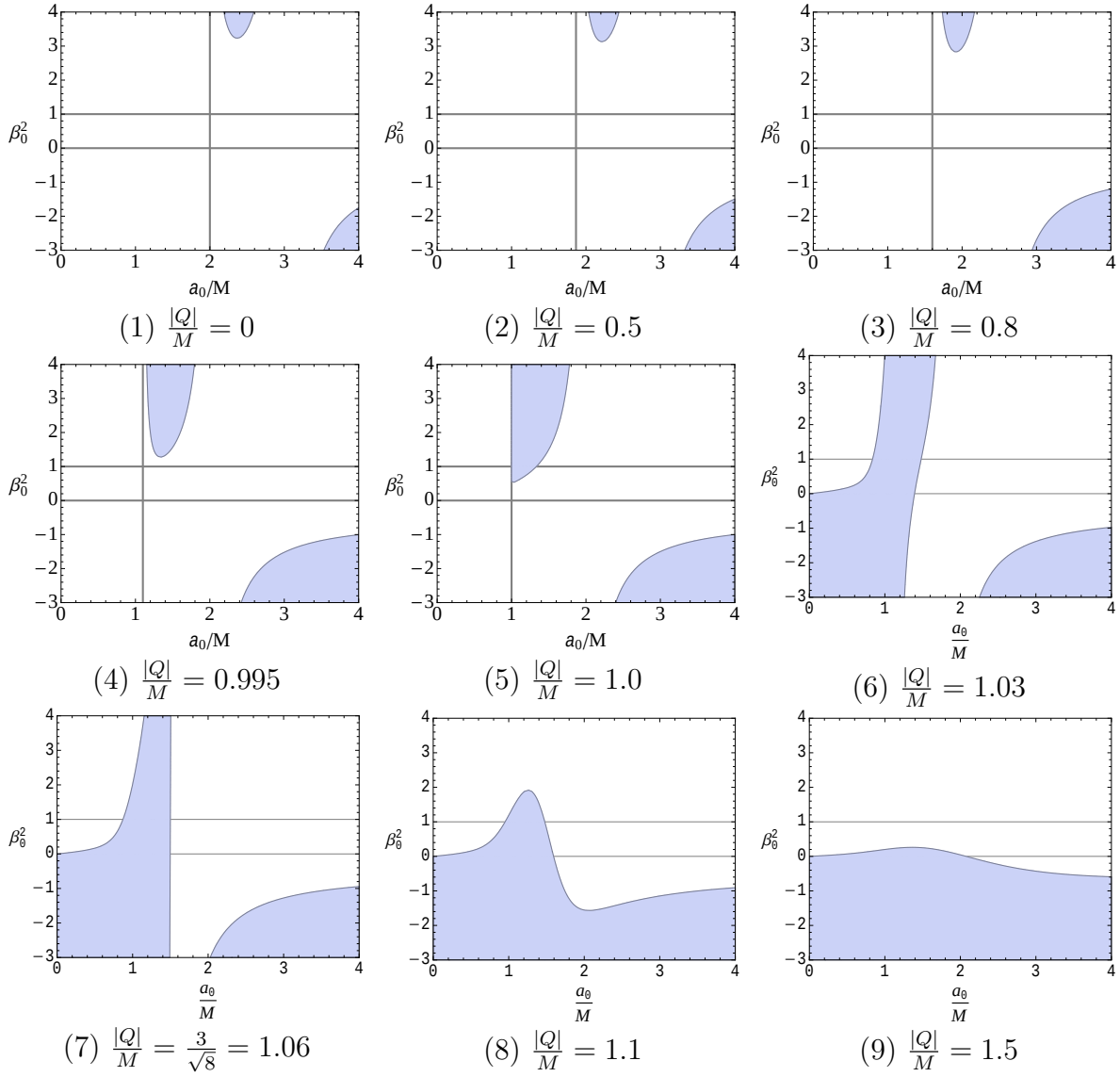

(1) $\frac{|Q|}{M} = 0$ (2) $\frac{|Q|}{M} = 0.5$ (3) $\frac{|Q|}{M} = 0.8$

(4) $\frac{|Q|}{M} = 0.995$ (5) $\frac{|Q|}{M} = 1.0$ (6) $\frac{|Q|}{M} = 1.03$

(7) $\frac{|Q|}{M} = \frac{3}{\sqrt{8}} = 1.06$ (8) $\frac{|Q|}{M} = 1.1$ (9) $\frac{|Q|}{M} = 1.5$

Figure 4.1: Charged thin shell wormhole. Shaded regions correspond to stable regions. The outer horizon r_+ corresponds to $\frac{r_+}{M} = 1 + \sqrt{1 - \frac{|Q|^2}{M^2}}$, therefore regions inside of the outer horizons(vertical lines) have no physical meaning in these figures when $0 \leq \frac{|Q|}{M} \leq 1$.

4.2.1 Schwarzschild-de Sitter thin-shell wormhole: $\Lambda > 0$

For each value of ΛM^2, there are two vertical lines where the denominator diverges in Eq. (4.3). These lines correspond to the event horizon and the cosmological horizon, respectively. Hence the left (right) side of the event (cosmological) horizon is the meaningless region. For any curves, "the region above curves lying in $a_0 < 3M$" and "the region below curves lying in $a_0 > 3M$" are stable regions. One finds that in the case of the Schwarzschild-de Sitter thin-shell wormhole, *stability region decreases with increasing* Λ relative to the Schwarzschild thin-shell wormhole ($\Lambda = 0$).

4.2.2 Schwarzschild-anti de Sitter thin-shell wormhole: $\Lambda < 0$

For each value of ΛM^2, there a vertical line where the denominator diverges in Eq. (4.3). This vertical line corresponds to the event horizon. Hence the left side of the event horizon is the meaningless region. Stable regions are similar manner to the case of the Schwarzschild-de Sitter thin-shell wormhole. One finds that in the case of the Schwarzschild-anti de Sitter thin-shell wormhole, *stability region increases with decreasing* Λ relative to the Schwarzschild thin-shell wormhole ($\Lambda = 0$).

4.2.3 (anti) de-Sitter thin-shell wormhole

We can also construct (anti-) de-Sitter wormhole just by putting $M \to 0$ in Eq. (4.3):

$$\beta_0^2 < -\frac{1}{2(1 - \Lambda a_0^2/3)}. \tag{4.5}$$

See Fig. (4.4) and Fig. (4.5) for stable equilibrium.

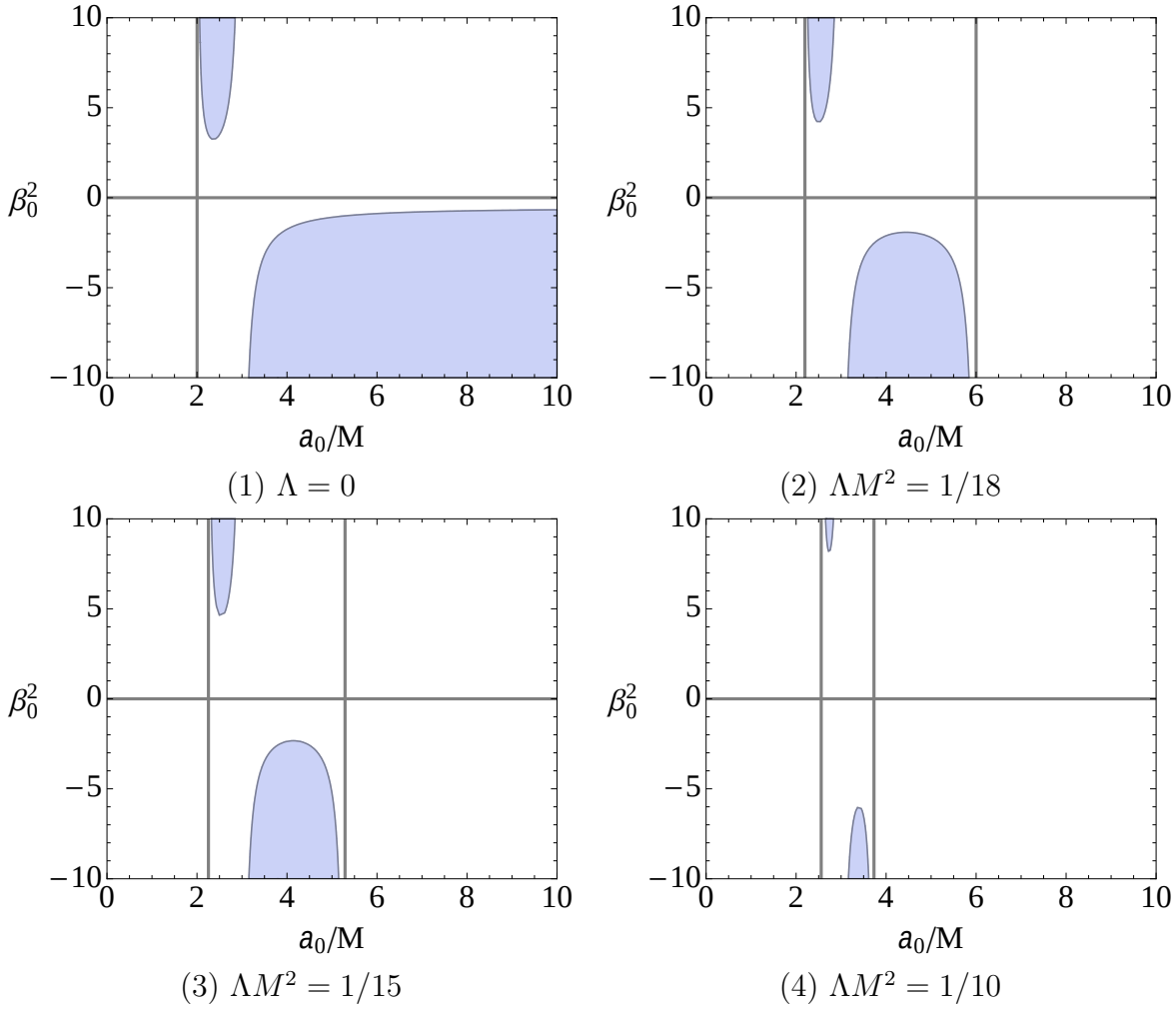

(1) $\Lambda = 0$ (2) $\Lambda M^2 = 1/18$

(3) $\Lambda M^2 = 1/15$ (4) $\Lambda M^2 = 1/10$

Figure 4.2: Schwarzschild-de Sitter thin-shell wormhole. The shaded regions indicate the stability. In figure (2), (3) and (4), the right side vertical lines correspond to the cosmological horizons. Stability region decreases with increasing ΛM^2 relative to the Schwarzschild thin-shell wormhole ($\Lambda = 0$).

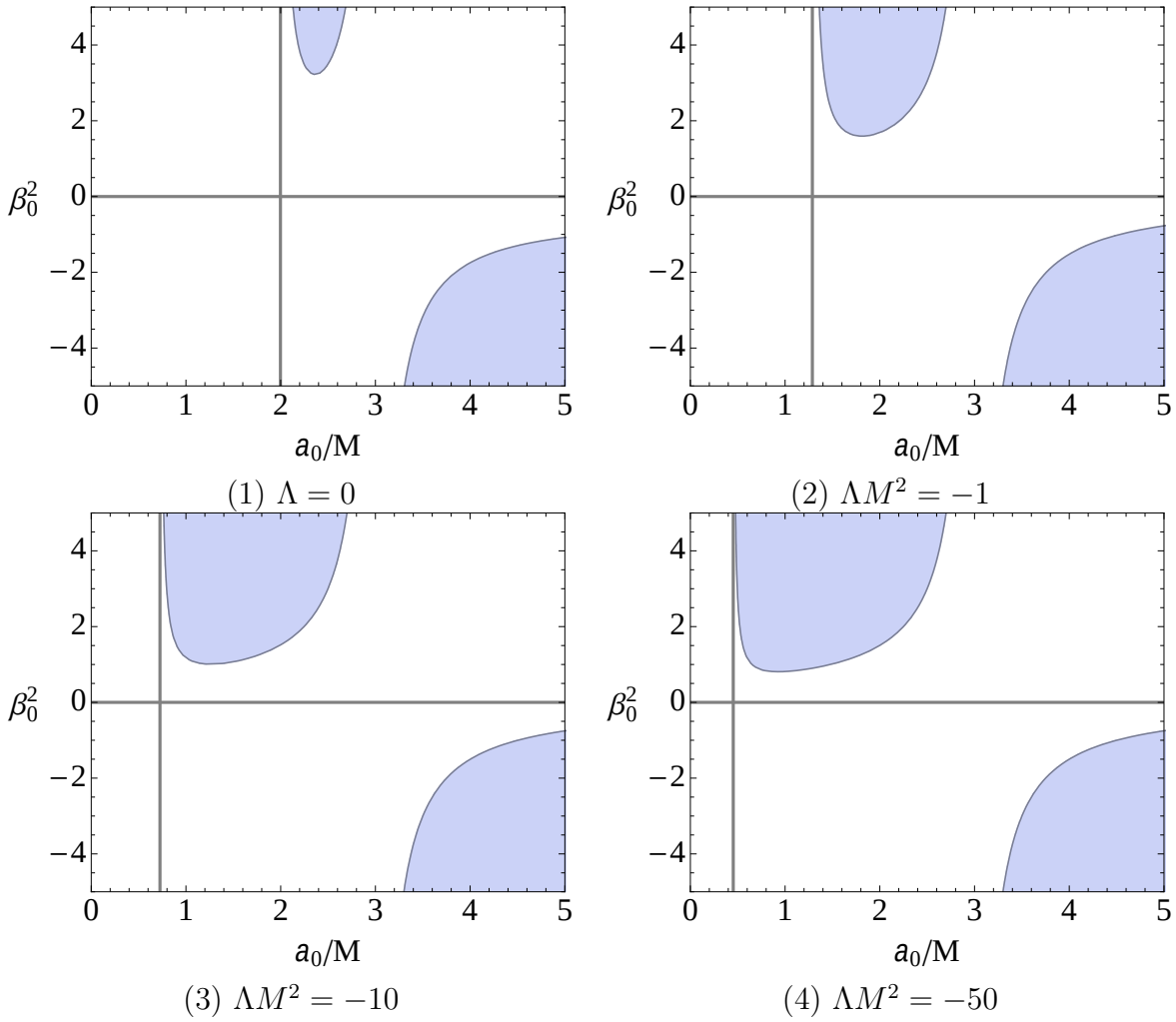

(1) $\Lambda = 0$ (2) $\Lambda M^2 = -1$

(3) $\Lambda M^2 = -10$ (4) $\Lambda M^2 = -50$

Figure 4.3: Schwarzschild-anti de Sitter thin-shell wormhole. The shaded regions indicate the stability. Stability region increases with decreasing ΛM^2 relative to the Schwarzschild thin-shell wormhole ($\Lambda = 0$).

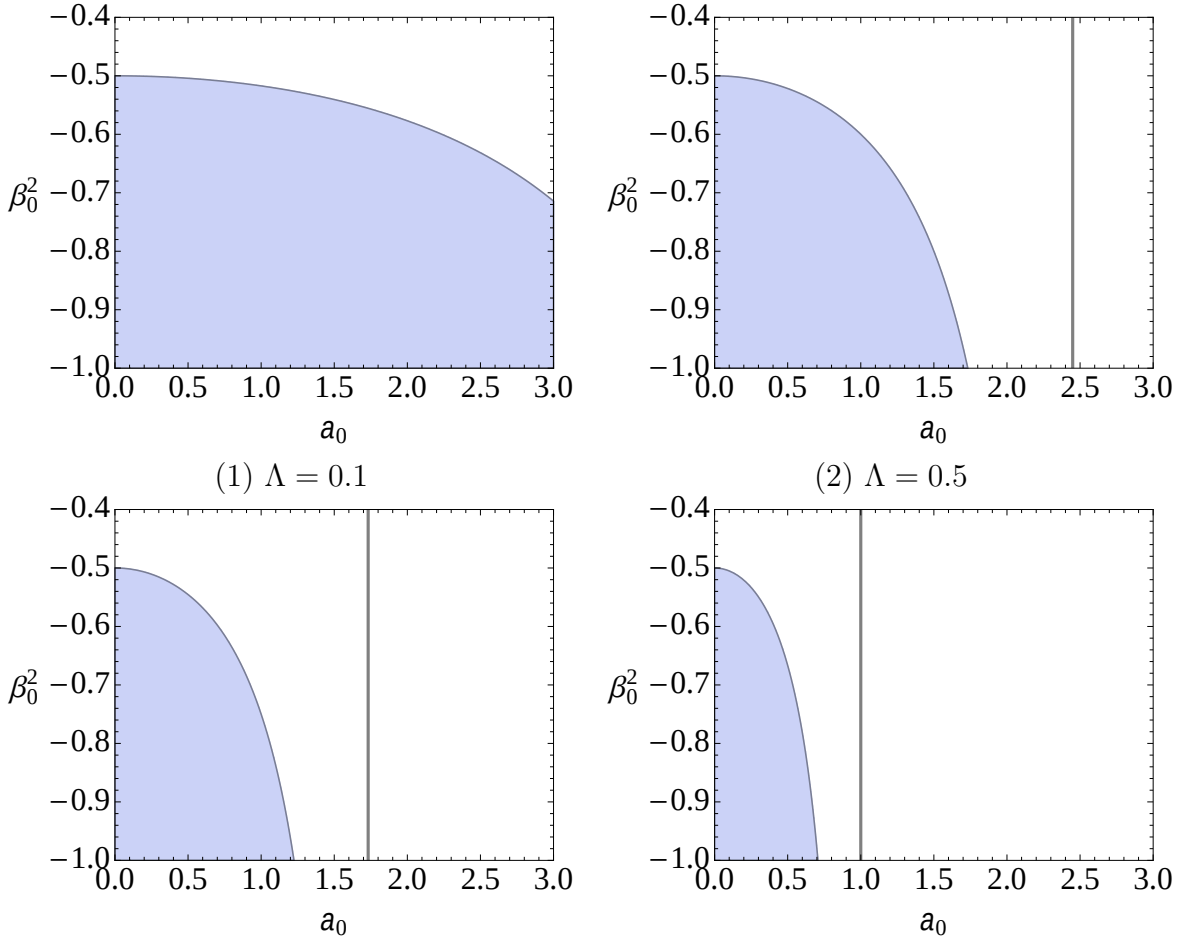

(1) $\Lambda = 0.1$ (2) $\Lambda = 0.5$

(3) $\Lambda = 1$ (4) $\Lambda = 3$

Figure 4.4: de-Sitter wormhole. Stable region is below the curve. Each vertical line represents the cosmological horizon. Hence, the right side of the vertical line is meaningless region.

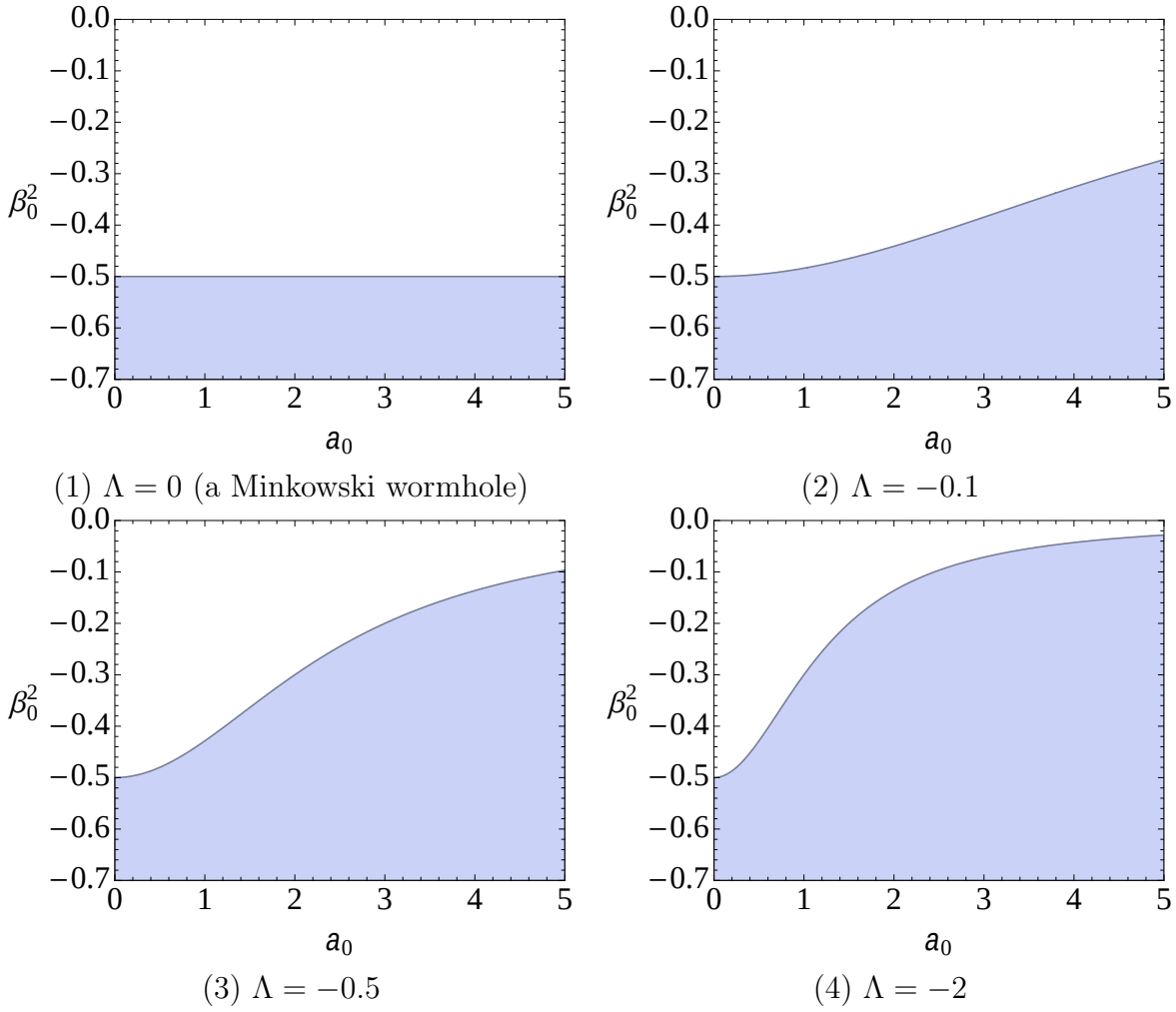

(1) $\Lambda = 0$ (a Minkowski wormhole)

(2) $\Lambda = -0.1$

(3) $\Lambda = -0.5$

(4) $\Lambda = -2$

Figure 4.5: Anti de-Sitter wormhole. Stable region is below the curve.

4.3 Non-Z_2 symmetric case

The simplest thin-shell wormhole is made by gluing couple of Schwarzschild spacetimes with $M_+ = M_- =: M$. Ishak and Lake expanded this analysis into the different mass case, i.e, M is not continuous at Σ. See [25] for detail. This situation corresponds to

$$d = 4, k = 1, M_\pm \to 2M_\pm, Q_\pm = \Lambda_\pm = 0 \tag{4.6}$$

in Eq. (3.3). In this situation, $V''(a_0)$ reduce to the following form:

$$V''(a_0) = -\mathcal{A} - \frac{2}{(d-2)^2}\left(\mathcal{C}^2 + \mathcal{B}\mathcal{D}\right) - \frac{(d-2)^2}{2}\left(\mathcal{F}^2 + \mathcal{E}\mathcal{G}\right), \tag{4.7}$$

where

$$\mathcal{A} :=(d-2)(d-3)\frac{\bar{M}}{a_0^{d-1}}, \tag{4.8}$$

$$\mathcal{B} := -\frac{d-2}{2}\delta_1, \tag{4.9}$$

$$\mathcal{C} := -\frac{d-2}{2}\frac{\delta_2}{a_0}, \tag{4.10}$$

$$\mathcal{D} :=\frac{(d-2)(d-3)}{2a_0^2}(\delta_2 - \delta_1) + \frac{(d-2)^2}{2a_0^2}(\delta_2 - \delta_1)\beta_0^2, \tag{4.11}$$

$$\mathcal{E} := -\frac{2}{(d-2)}\frac{m(a_0)}{a_0\delta_1}, \tag{4.12}$$

$$\mathcal{F} := -\frac{2}{(d-2)}\frac{m'(a_0)}{a_0\delta_1} + \frac{2}{(d-2)}\frac{m(a_0)}{a_0^2}\frac{\delta_1+\delta_2}{\delta_1^2}, \tag{4.13}$$

$$\begin{aligned}\mathcal{G} :=& -\frac{2}{(d-2)}\frac{m''(a_0)}{a_0\delta_1} + \frac{4}{d-2}\frac{m'(a_0)}{(a_0\delta_1)^2}(\delta_1+\delta_2) \\ &+2\frac{d-3}{d-2}\frac{m(a_0)}{a_0^3\delta_1} - 2\frac{d-5}{d-2}\frac{m(a_0)\delta_2}{a_0^3\delta_1^2} - \frac{2m(a_0)}{(a_0\delta_1)^2}\frac{1}{a_0}(\delta_2-\delta_1)\beta_0^2 - \frac{4}{(d-2)}\frac{m(a_0)}{(a_0\delta_1)^3}(\delta_1+\delta_2)^2.\end{aligned} \tag{4.14}$$

We have defined $m, \bar{x}$ and $\hat{x}$ as

$$m(a) := \frac{\hat{M}}{a^{d-4}},\ \bar{x} := \frac{x_+ + x_-}{2},\ \hat{x} := \frac{x_+ - x_-}{2}. \tag{4.15}$$

$\delta_{1,2}$ was also defined through the equations:

$$\sigma(a_0) = -\frac{d-2}{8\pi a_0}(A_+(a_0) + A_-(a_0)) =: -\frac{d-2}{8\pi a_0}\delta_1, \tag{4.16}$$

$$\begin{aligned}p(a_0) &= \frac{1}{8\pi a_0}\left(\left(\frac{B_+(a_0)}{A_+(a_0)} + \frac{B_-(a_0)}{A_-(a_0)}\right)a_0 + (d-3)\{A_+(a_0) + A_-(a_0)\}\right) \\ &=: \frac{1}{8\pi a_0}(\delta_2 + (d-3)\delta_1).\end{aligned} \tag{4.17}$$

Putting $d = 4$ into Eq. (4.7) recovers the condition $V''(a_0) > 0$ by Ishak and Lake. Stable equilibrium is dipicted in Fig. (4.6). We found stable region decreases with increasing the difference between M_+ and M_-.

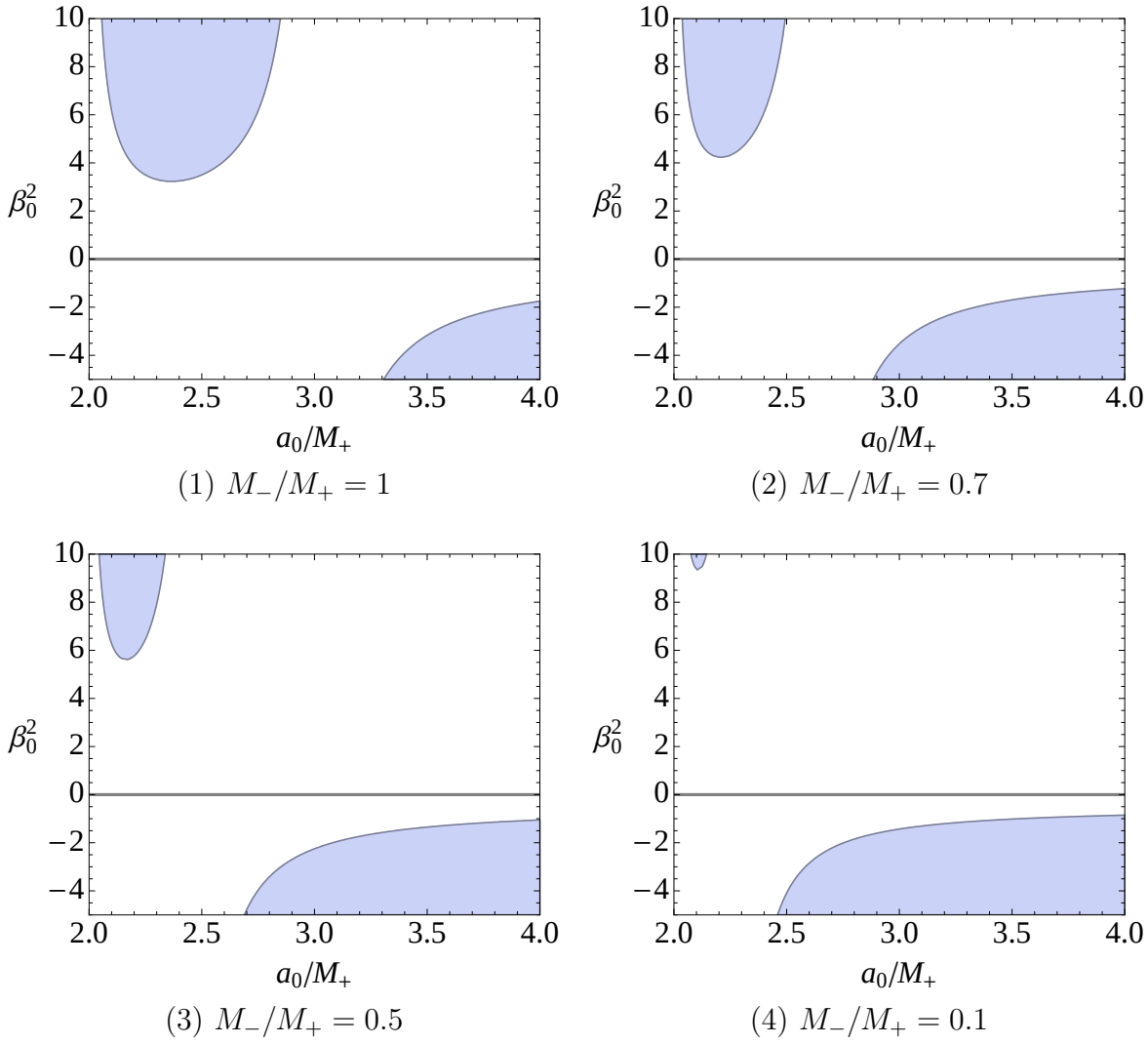

(1) $M_-/M_+ = 1$ (2) $M_-/M_+ = 0.7$

(3) $M_-/M_+ = 0.5$ (4) $M_-/M_+ = 0.1$

Figure 4.6: Non-Z_2 symmetry. The shaded regions represent the stability. Stable region decreases with increasing the difference between M_+ and M_-. The horizontal axis is normalized by M_+.

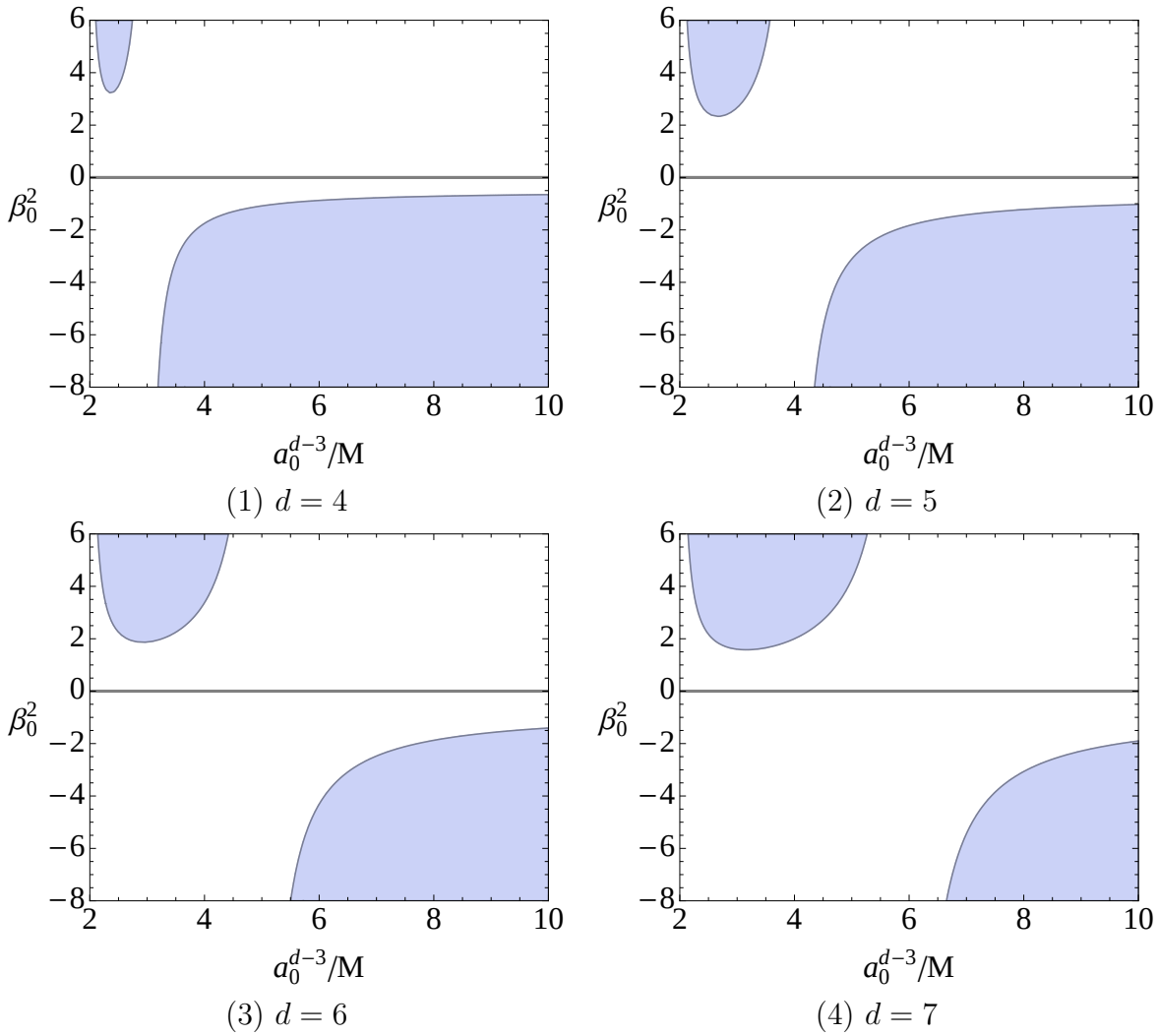

(1) $d = 4$ (2) $d = 5$

(3) $d = 6$ (4) $d = 7$

Figure 4.7: A higher dimensional generalization. The shaded regions represent the stability.

4.4 In higher dimensions

A higher dimensional generalization is introduced by Dias and Lemos in [30]. We show a spherically symmetric shell wormhole in arbitrary dimension, say, a Tangherlini shell wormhole. In Eq. (3.3), this situation corresponds to

$$d = d, k = 1, M_\pm = 2M, Q_\pm = \Lambda_\pm = 0. \tag{4.18}$$

Putting these values into Eq. (4.7) - Eq. (4.14), we have the stable condition. Fig. (4.7) shows the stable equilibrium. We find the stable region increases with d.

5 Pure tension wormholes in Einstein gravity

5.1 Advantage of use of pure tension

Though we introduced a wormhole with a pure tension brane in Sec. 3.4.3, we did not mention the reason why we considered such a matter field. Pure tension branes are more exceptional than other matter fields.

Pure tension branes, whether the tension is positive or negative, have particular interest because they have Lorentz invariance and have no intrinsic dynamical degrees of freedom. In the context of stability, pure negative tension branes have no intrinsic instability by their own, although they violate the weak energy condition. This is in contrast with the Ellis wormholes, for which a phantom scalar field is assumed as a matter content and it suffers the so-called ghost instability because of the kinetic term of a wrong sign [13, 14, 15].

The construction of traversable wormholes by using negative tension branes have first been proposed by C. Barceló and M. Visser [32]. We proved that a wormhole with a pure tension brane analyzed in Sec. 3.4.3 was unstable. Barceló and Visser investigated pure tension wormholes in more general construction: They analyzed dynamics of spherically symmetric traversable wormholes obtained by operating the cut-and-paste procedure for negative tension 2-branes (three dimensional timelike singular hypersurface) in four dimensional spacetimes. They found stable brane wormholes constructed by pasting a couple of Reissner-Nordström-(anti) de Sitter spacetimes. In their work [32], the both of the charge and a negative cosmological constant is important to sustain such wormholes. And in most cases, a negative cosmological constant tends to make the black hole horizons smaller. However, in exceptional cases, one can obtain wormholes with a vanishing cosmological constant, if the absolute value of the charge satisfies a certain condition.

5.2 Pure tension wormholes in Einstein gravity

In this thesis, we concentrate on stability of thin-shell wormholes (TSWs) against radial perturbations. The radial perturbation is important in the context of stability analysis in the following reasons: (i) Since the stability analysis against radial perturbations is much simpler than nonradial perturbations which entail gravitational radiation, it is a natural first step to investigate radial stability of wormhole models. For thin shell models, the stability analysis against radial perturbations is particularly simple. (ii) The previous study suggests that the radial perturbation of wormhole spacetimes is most dangerous: The paper by C. Armendariz-Picon [12] showed that the Ellis wormhole is stable against metric perturbations including nonradial perturbations which do not change the throat radius. Subsequently, the Ellis wormhole turned out to be unstable against radial perturbation which changes the radius of the throat. The throat must shrink or inflate [13]. From the above, we might say that for the Ellis wormhole, the radial perturbation which changes the radius of the throat is the most "dangerous" perturbation, as mentioned in Bronnikov's book [33]. One can expect that this property applies to not only the Ellis wormhole but also other wormhole solutions.

The effects caused by the electromagnetic field on the stability of a TSW are not well

known. One may wonder whether the existence of the electric charge of wormholes can stabilize the wormholes. Therefore, it is worth studying electrically charged TSWs. In spherically symmetric and hyperbolically symmetric spacetimes, the Reissner-Nordstöm (anti) de-Sitter spacetime is the unique solution to the higher dimensional Einstein-Maxwell equation. In cylindrically symmetric and planar symmetric spacetimes, the Reissner-Nordstöm (anti) de-Sitter spacetime is not unique but one of the possible static solutions.

In recent several years, the possibility of stable wormholes in various theories of modified gravity has gathered attention and has been extensively investigated by many authors [28, 34, 36]. However, the possibility of wormholes whose exotic matter is a pure tension brane has not yet fully been checked in those theories. To study such possibility, it is important and necessary to fully understand the existence and stability of all kinds of Z2 symmetric RN-(A)dS TSWs in higher dimensional pure Einstein-Maxwell theory.

In this section, we investigate negative tension branes as thin shell wormholes in spherical, planar (or cylindrical) and hyperbolic symmetries in d dimensional Einstein gravity with an electromagnetic field and a cosmological constant in bulk spacetimes. In spherical geometry, we find the higher dimensional counterpart of Barceló and Visser's wormholes which are stable against spherically symmetric perturbations. As the number of dimensions increases, larger charge is allowed to construct such stable wormholes without a cosmological constant. Not only in spherical geometry, but also in planar and hyperbolic geometries, we find static wormholes which are stable against perturbations preserving symmetries.

5.3 Effective potential

From now on, for simplicity, we assume Z2 symmetry, that is, we assume $M_+ = M_-$, $Q_+ = Q_-$ and $\Lambda_+ = \Lambda_-$ and hence $f_+(r) = f_-(r)$. We denote $M_+ = M_- = M$, $Q_+ = Q_- = Q$, $\Lambda_+ = \Lambda_- = \Lambda$ and $f(r) := f_+(r) = f_-(r)$. We investigate wormholes which consist of a negative tension brane. From Eqs. (3.17) and (3.18), the surface energy density and surface pressure for the negative tension brane are represented as

$$\sigma = -\frac{d-2}{4\pi a}A = \alpha, \tag{5.1}$$

$$p = \frac{1}{4\pi}\left(\frac{B}{A} + \frac{d-3}{a}A\right) = -\alpha, \tag{5.2}$$

where α is a constant with a negative value. The effective potential reduces to

$$V(a) = f(a) - \left(\frac{4\pi\alpha}{d-2}\right)^2 a^2. \tag{5.3}$$

5.4 Static solutions, stability criterion and horizon-avoidance condition

The present system may have static solutions $a = a_0$. We define $p_0 := p(a_0)$ and $\sigma_0 := \sigma(a_0)$, where a_0 satisfies Eq. (3.25) :

$$\sigma_0 = -\frac{d-2}{4\pi a_0} A_0 = \alpha, \tag{5.4}$$

$$p_0 = \frac{1}{4\pi}\left(\frac{B_0}{A_0} + \frac{d-3}{a_0} A_0\right) = -\alpha, \tag{5.5}$$

where

$$A_0 := \sqrt{f(a_0)}, B_0 := \frac{1}{2} f'(a_0). \tag{5.6}$$

Eliminating α from Eqs. (5.4) and (5.5), we can obtain the equation for the static solutions,

$$\frac{a_0}{2} f'(a_0) - f(a_0) = 0. \tag{5.7}$$

The explicit form of Eq. (5.7) is

$$2k a_0^{2(d-3)} - (d-1) M a_0^{d-3} + 2(d-2)Q^2 = 0. \tag{5.8}$$

The stability conditions for wormholes are shown before as $V''(a_0) > 0$. The corresponding stability conditions is

$$\begin{aligned} V''(a_0) =& f_0'' - 2\left(\frac{4\pi\alpha}{d-2}\right)^2 = f_0'' - 2\frac{f_0}{a_0^2} > 0 \\ \Leftrightarrow& (d-3)\left(4k - (d-1)\frac{M}{a_0^{d-3}}\right) < 0. \end{aligned} \tag{5.9}$$

We used Eq. (5.8) to derive Eq. (5.9). As one can see, since static solutions of Eq. (5.8) and stability conditions of Eq. (5.9) do not contain Λ, the cosmological constant only affects the horizon-avoidance condition of Eq. (3.25). By studying both the existence of static solutions and stability conditions, we can search static and stable wormholes.

5.5 $d = 3$

We first analyze static solutions and stability for $d = 3$. In this case, the stability analysis is simple. The metric becomes

$$f(a) = k - M + Q^2 - \frac{\Lambda}{3} a^2, \tag{5.10}$$

so the potential is

$$V(a) = k - M + Q^2 - \Lambda_{\text{eff}} a^2, \tag{5.11}$$

where

$$\Lambda_{\text{eff}} := \frac{\Lambda}{3} + \left(\frac{4\pi\alpha}{d-2}\right)^2. \tag{5.12}$$

Since the shell is static, $V'(a_0) = 0$, we obtain

$$\Lambda_{\text{eff}} = 0. \tag{5.13}$$

Therefore the potential is $V(a) = k - M + Q^2$. Besides, $V(a_0) = 0$ yields $k - M + Q^2 = 0$ so we obtain

$$f(a) = -\frac{\Lambda}{3}a^2, V(a) = 0. \tag{5.14}$$

Therefore any radius a_0 is static. We find $V''(a_0) = 0$, which means the wormholes is marginally stable. The horizon-avoidance condition $f(a_0) > 0 \Leftrightarrow \Lambda < 0$ is satisfied because of (5.12) and (5.13). This wormhole is constructed by pasting a couple of anti de-Sitter spacetimes.

5.6 $d \geq 4$

From now on, we assume $d \geq 4$. For $k \neq 0$ and $M \neq 0$, Eq. (5.8) is a quadratic equation. The static solutions are then given by

$$a_{0\pm}^{d-3} = \frac{d-1}{4k}M(1 \pm b), \tag{5.15}$$

where

$$b := \sqrt{1 - k\frac{q^2}{q_c^2}}, q := \frac{|Q|}{|M|}, q_c := \frac{(d-1)}{4\sqrt{d-2}}. \tag{5.16}$$

Combining Eqs. (5.15) and (5.9), we can see that for $b = 0$, the positive and negative sign solutions coincide and their stability depends on higher order terms. For $b > 0$ and $k = +1$, the negative sign solution is stable, while the positive sign solution is unstable. For $k = -1$, we can conclude $b \geq 1$ and stability depends on the sign of mass M. The horizon-avoidance condition (3.25) reduces to

$$\frac{1}{3}\Lambda a_{0\pm}^2 < -\frac{(d-3)k}{(d-1)(d-2)(1 \pm b)}\left[2 - (d-1)(1 \pm b)\right]. \tag{5.17}$$

We investigate $k = +1$ and $k = -1$ cases, separately.

5.6.1 $k = 1$ and $M \neq 0$

Though the original range for b is $0 \leq b \leq 1$, $b = 0 \Leftrightarrow q = q_c$ does not satisfy the stability condition: For $q = q_c$, there is the only one static solution,

$$a_0^{d-3} = \frac{d-1}{4}M. \tag{5.18}$$

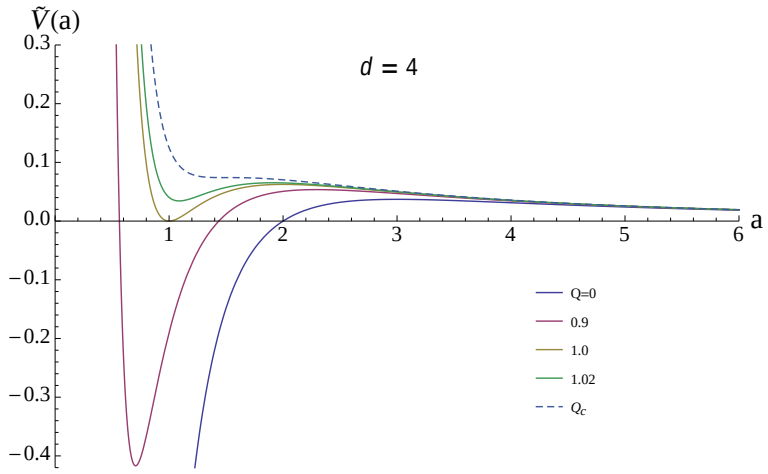

Figure 5.1: The potential $\tilde{V}(a)$ for $d = 4$, $k = +1$ and $M = 2$. The dashed line is the potential for the critical value defined in Eq. (5.16).

This double root solution is linearly marginally stable but nonlinearly unstable because $V'''(a_0) \neq 0$. From Eq. (5.18), we must have positive mass $M > 0$ to make sure a_0 to be positive. The horizon-avoidance condition reduces to

$$\lambda < R(d), \tag{5.19}$$

where λ is a dimensionless quantity corresponding to Λ and $R(d)$ is defined by

$$\lambda := \frac{\Lambda}{3}|M|^{\frac{2}{d-3}}, R(d) := \left(\frac{4}{d-1}\right)^{\frac{2}{d-3}} \frac{(d-3)^2}{(d-1)(d-2)}. \tag{5.20}$$

Since $R(d)$ is positive, we can have the wormhole even without Λ.

If $b = 1 \Leftrightarrow Q = 0$, the negative sign solution vanishes. The positive sign solution which does not satisfy the stability condition is

$$a_{0+}^{d-3} = \frac{d-1}{2}M. \tag{5.21}$$

From Eq. (5.21), M must be positive. One can verify that the horizon-avoidance condition is satisfied even without Λ.

When $0 < b < 1 \ \Leftrightarrow 0 < q < q_c$, there are two static solutions

$$a_{0\pm}^{d-3} = \frac{d-1}{4}M(1 \pm b). \tag{5.22}$$

The stability condition is satisfied if we take the negative sign solution of Eq. (5.22). The positive sign solution is unstable. Since the static solution must be positive, we must have $M > 0$. The following transformation helps us to understand the potentials:

$$\tilde{V}(a) := \frac{k}{a^2} - \frac{M}{a^{d-1}} + \frac{Q^2}{a^{2(d-2)}}$$

so that

$$\dot{a}^2 + V(a) = 0 \Leftrightarrow \left(\frac{d\ln a}{d\tau}\right)^2 + \tilde{V}(a) = \Lambda_{\text{eff}}.$$

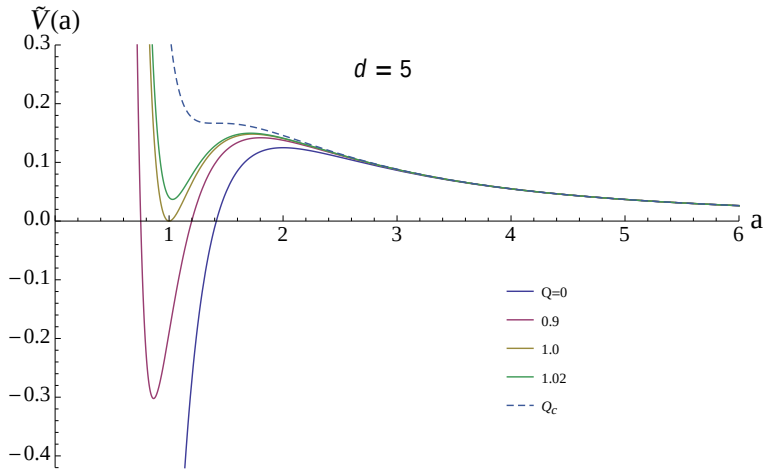

Figure 5.2: The potential for $d = 5$, $k = +1$ and $M = 2$.

The potentials $\tilde{V}(a)$ are plotted in Figs. 5.1 and 5.2 for $d = 4$ and $d = 5$, respectively. The horizon-avoidance condition (5.17) reduces to

$$\lambda < H_{\pm}(d, q), \tag{5.23}$$

where

$$H_{\pm}(d, q) := -\left\{\frac{4}{(d-1)(1 \pm b)}\right\}^{\frac{2}{d-3}} \frac{d-3}{(d-1)(d-2)(1 \pm b)} \left[2 - (d-1)(1 \pm b)\right]. \tag{5.24}$$

The positive and the negative sign corresponds with the sign of Eq. (5.22) in same order. When one take the positive sign, $H_+(d, q)$, one can find the inside of the square brackets of Eq. (5.24) is negative, then $H_+(d, q)$ is positive. Therefore Eq. (5.23) is satisfied even with $\Lambda = 0$ in the case of $H_+(d, q)$. Similarly, in the case of the negative sign, $H_-(d, q)$, if the inside of the square brackets of Eq. (5.24) can be negative, Eq. (5.23) is satisfied even with $\Lambda = 0$. In this stable case, one can achieve this situation if and only if

$$\frac{1}{2} < q < q_c \tag{5.25}$$

is satisfied. $H_{\pm}(d, q)$ are plotted in Fig. 5.3. Therefore, we can construct a stable TSW without Λ when the condition Eq. (5.25) is satisfied. So the extremal or subextremal charge $q \leq 1/2$ of the Reissner-Nordström spacetime cannot satisfy Eq. (5.25). We can reconfirm the previous result by taking $d = 4$ and $M = 2m$ for Eq. (5.25) as

$$1 < \left(\frac{|Q|}{m}\right)^2 < \frac{9}{8}. \tag{5.26}$$

This coincides with the previous result by Barceló and Visser [32]. From Eq. (5.25), as d increases, larger charge is allowed to construct a stable wormhole without Λ. This class of wormholes are constructed by pasting a couple of over-charged higher dimensional Reissner-Nordström spacetimes.

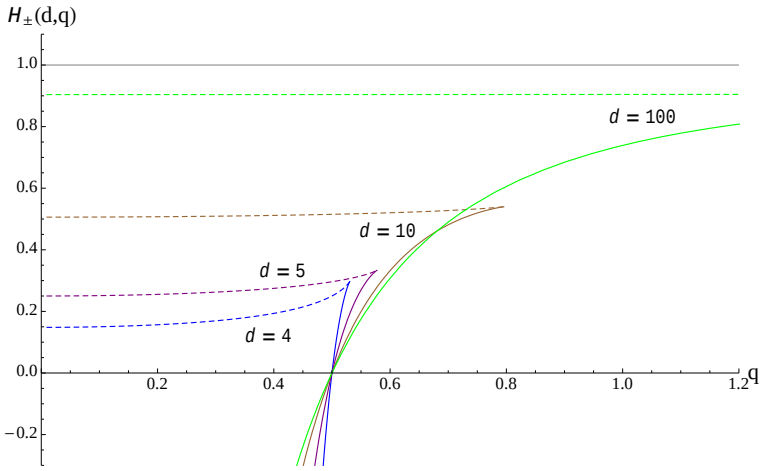

Figure 5.3: The functions $H_{\pm}(d,q)$ defined in Eq. (5.24) are plotted. The dashed lines are $H_{+}(d,q)$ and the solid lines are $H_{-}(d,q)$. The regions below these curves represent the regions of λ which satisfy Eq. (5.23). When $q < 1/2$, $H_{+}(d,q)$ is positive, while $H_{-}(d,q)$ is negative. When $1/2 < q < q_c$, both $H_{\pm}(d,q)$ are positive. As the number of dimensions and charge increase, it approaches 1.

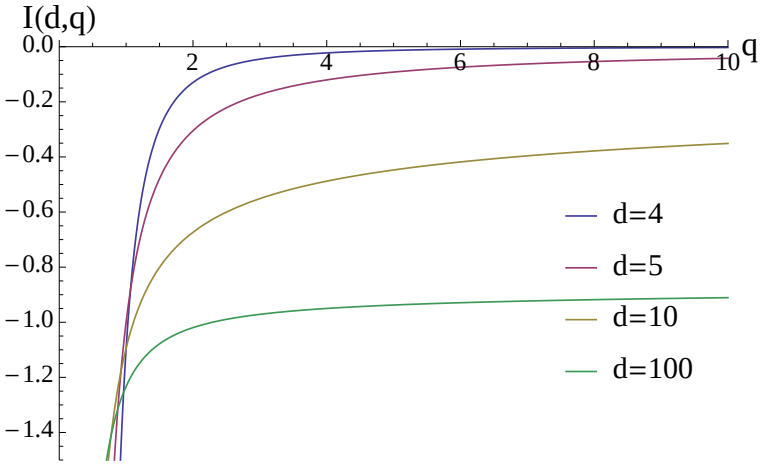

Figure 5.4: The function $I(d,q)$ defined in Eq. (5.30) is plotted. The regions below these curves represent the regions of λ which satisfy Eq. (5.29). $I(d,q)$ is negative. In $d = 4$, $I(4,q) \to 0$ as $q \to \infty$.

5.6.2 $k = -1$ and $M \neq 0$

The static solution is given by

$$a_{0\pm}^{d-3} = -\frac{d-1}{4} M(1 \pm b), \tag{5.27}$$

where

$$b = \sqrt{1 + \frac{q^2}{q_c^2}}. \tag{5.28}$$

b is more than than or equal to unity i.e. $b \geq 1$. If $M > 0$ and $Q \neq 0$, the stability condition Eq. (5.9) is satisfied, if we take the negative sign solution of Eq. (5.27). If $M > 0$ and $Q = 0$, since the negative sign solution vanishes and the positive sign solution is negative, there is no static solution. Therefore, if $M > 0$ and $Q \neq 0$, we can have stable wormholes. In this case the horizon-avoidance condition Eq. (5.17) reduces to

$$\lambda < I(d, q), \tag{5.29}$$

where

$$I(d, q) := -\frac{d-3}{(d-1)(d-2)} \left\{ \frac{4}{(d-1)(b-1)} \right\}^{-\frac{2}{d-3}} \left[\frac{2}{b-1} + d - 1 \right]. \tag{5.30}$$

Eq. (5.29) can be satisfied only if Λ is negative and $|\Lambda|$ is sufficiently large. One can find that the inside of the square brackets on the right hand side of Eq. (5.30) is positive, so the vanishing cosmological constant cannot satisfy Eq. (5.30) unlike for $k = +1$. The value of $I(d, q)$ determines the maximum value for λ which is needed to achieve the horizon-avoidance condition Eq. (5.29). $I(d, q)$ is plotted in Fig. 5.4. Since $I(d, q) < 0$, we need a negative cosmological constant for the horizon-avoidance condition to be satisfied.

If $M < 0$, the stability condition is satisfied if we take the positive sign solution Eq. (5.27) whether it is with or without charge. The negative sign solution contradicts $a_0 > 0$. The positive sign solution is

$$a_{0+}^{d-3} = \frac{d-1}{4} |M|(1 + b). \tag{5.31}$$

In this case, the horizon-avoidance condition Eq. (5.17) reduces to

$$\lambda < N(d, q), \tag{5.32}$$

where

$$N(d, q) := \left\{ \frac{4}{(d-1)(1+b)} \right\}^{\frac{2}{d-3}} \frac{d-3}{(d-1)(d-2)(1+b)} \left[2 - (d-1)(1+b) \right]. \tag{5.33}$$

$N(d, q)$ is plotted in Fig. 5.5. Since $N(d, q) < 0$, we find that a negative cosmological constant is needed to achieve the horizon avoidance.

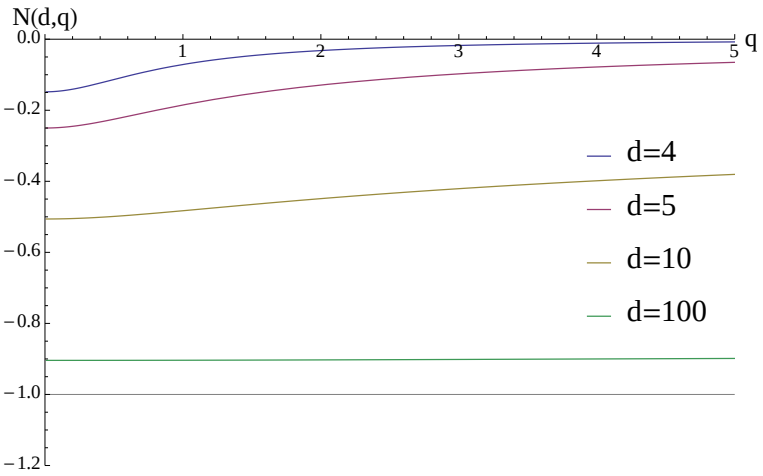

Figure 5.5: The function $N(d,q)$ defined in Eq. (5.33) is plotted. The regions below these curves represent the regions of λ which satisfy Eq. (5.32). $N(d,q)$ is negative. As the number of dimensions increases, it approaches -1.

5.6.3 $k \neq 0$ and $M = 0$

For $k = +1$, from Eq. (5.8), we find there is no static solution. For $k = -1$, Eq. (5.8) has a double root solution:

$$a_0^{d-3} = \sqrt{d-2}|Q|, \tag{5.34}$$

where $Q \neq 0$ must hold for the positivity of a_0. One can easily verify the stability condition is satisfied in this case. The horizon avoidance Eq. (3.25) reduces to

$$\frac{\Lambda}{3} < S(d,q), \tag{5.35}$$

where

$$S(d,q) := -|Q|^{-\frac{2}{d-3}}(d-3)(d-2)^{d-4} \tag{5.36}$$

Since the right hand side of Eq. (5.35) is negative, we need a negative cosmological constant for the stable wormhole in this case. However, even an arbitrarily small $|\Lambda|$ can satisfy Eq. (5.35), if $|Q|$ is sufficiently large.

5.6.4 $k = 0$ and $M \neq 0$

There is the only one static solution that is

$$a_0^{d-3} = 2\frac{d-2}{d-1}\frac{|Q|^2}{M}. \tag{5.37}$$

$M > 0$ and $Q \neq 0$ must hold since a_0 must be positive. The stability condition is satisfied in this case. The horizon-avoidance condition reduces to

$$\lambda < J(d,q), \tag{5.38}$$

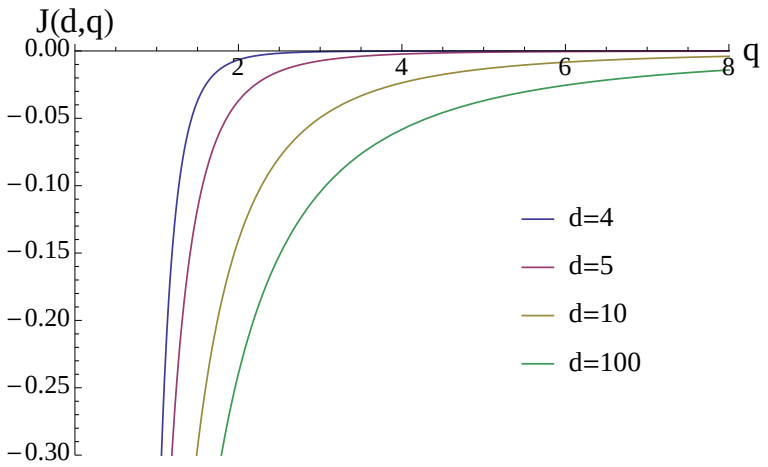

Figure 5.6: The function $J(d,q)$ defined in Eq. (5.39) is plotted. The regions below these curves represent the regions of λ which satisfy Eq. (5.38). $J(d,q)$ is negative. As the number of dimensions increases, it approaches $-1/4q^2$.

where

$$J(d,q) := -\frac{1}{4}\left(\frac{1}{q}\right)^{2\frac{d-1}{d-3}}\left(\frac{d-1}{2(d-2)}\right)^{\frac{2}{d-3}}\frac{(d-1)(d-3)}{(d-2)^2}. \tag{5.39}$$

Since $J(d,q)$ is negative, Λ should be negative. Taking a limit of $d\to\infty$ leads to

$$\lambda\left(\frac{|Q|}{M}\right)^2 < -\frac{1}{4} \quad \text{as} \quad d\to\infty. \tag{5.40}$$

The function $J(d,q)$ is plotted in Fig. 5.6. Since $J(d,q)$ is negative, we need a negative cosmological constant for the horizon avoidance.

5.6.5 $k=0$ and $M=0$

In this case, we must have $Q=0$ to satisfy Eq. (5.8). Then we get $V(a) = -\Lambda_{\text{eff}}a^2$, where Λ_{eff} is defined in Eq. (5.12). Since the shell is static, $V'(a_0)=0$, we find

$$\Lambda_{\text{eff}} = 0 \Leftrightarrow \frac{\Lambda}{3} = -\left(\frac{4\pi\alpha}{d-2}\right)^2. \tag{5.41}$$

Then, the potential vanishes, i.e., $V(a)=0$, which means the wormhole can be static at an arbitrarily radius and is marginally stable. Since the cosmological constant turned out to be negative from Eq. (5.41), we have $f(a) = (4\pi\alpha/d-2)^2a^2$, then the horizon avoidance $f(a_0)>0$ is automatically satisfied. This solution is what we can call an another side of Randall-Sundrum (RS) II brane world model [35]. In both cases, the ingredients are a couple of anti de-Sitter (AdS) spacetimes. The RS II model is a compactified spacetime by pasting the *interiors* of a couple of AdS spacetimes at the boundaries, while the wormhole solution is a non-compactified spacetime by pasting the *exteriors* of a couple of AdS spacetimes at the boundaries.

6 Pure tension wormholes in Einstein-Gauss-Bonnet gravity

In 2011, Kanti, Kleihaus, and Kunz numerically constructed four-dimensional spherically symmetric wormhole solutions in Einstein-Gauss-Bonnet-dilaton gravity and showed that they are dynamically stable against spherical perturbations [36]. The Gauss-Bonnet term non-minimally coupled to a dilaton scalar field appears in the Lagrangian as the ghost-free quadratic correction in the low-energy limit of heterotic string theories [21]. Although this Einstein-Gauss-Bonnet-dilaton theory is realized only in ten dimensions, their result gives courage and hope toward the construction of wormholes in our universe described by a well-motivated effective theory of gravity. Then a natural question arises: Which is the main ingredient stabilizing the wormhole, the Gauss-Bonnet term or its dilaton coupling?

The main purpose of the thesis is to clarify the effect of the Gauss-Bonnet term on the dynamical stability. For this purpose, we will study the simplest thin-shell wormhole which is made of its tension. While dynamical stability of thin-shell wormholes have been intensively investigated both in general relativity (Einstein gravity) [22, 23, 24, 25, 26, 27, 29, 30] and in various models of modified gravity [34], this is the best set-up to analyze stability as a pure gravitational effect because such a thin shell does not suffer from the matter instability.

In Einstein gravity, such thin-shell wormholes have been fully investigated in the previous section. In the vacuum case, such thin-shell wormholes are stable against radial perturbations only in the hyperbolically symmetric case with negative mass in the bulk spacetime [4].

In this section, we will study the same system with the Gauss-Bonnet term but without a dilaton in the Lagrangian. Since the Gauss-Bonnet term becomes total derivative and does not affect the field equations in four or lower dimensions in the absence of the non-minimal coupling to a dilaton, we will consider five or higher-dimensional spacetimes. In comparison with the general relativistic case, the equation of motion for the shell is much more complicated. For this reason, although thin-shell wormholes have been investigated in Einstein-Gauss-Bonnet gravity by many authors [37], the stability analysis has not been completed yet even against radial perturbations.

In Sec.6.8, for investigating stability of shell wormholes, we will develop a systematic method that is applied to any gravitational theories. This method can make stability analysis simpler.

6.1 Bulk solution

We will study the properties of thin-shell wormholes in Einstein-Gauss-Bonnet gravity. Such wormhole solutions are constructed by gluing two bulk solutions at a timelike hypersurface.

In the thesis , we consider the d-dimensional vacuum solution with a maximally symmetric base manifold [38] as the bulk solution, of which metric is given by

$$\mathrm{d}s_d^2 = g_{\mu\nu}\mathrm{d}x^\mu \mathrm{d}x^\nu = -f(r)\mathrm{d}t^2 + f(r)^{-1}\mathrm{d}r^2 + r^2\gamma_{AB}\mathrm{d}z^A\mathrm{d}z^B, \tag{6.1}$$

where z^A and γ_{AB} $(A, B = 2, 3, \cdots, d-1)$ are the coordinates and the unit metric on

the base manifold and

$$f(r) := k + \frac{r^2}{2\tilde{\alpha}}\left(1 \mp \sqrt{1 + \frac{4\tilde{\alpha}m}{r^{d-1}} + 4\tilde{\alpha}\tilde{\Lambda}}\right). \tag{6.2}$$

Here $k = 1, 0, -1$ is the curvature of the maximally symmetric base manifold corresponding to the spherical, planar, and hyperbolically symmetric spacetime, respectively. m is called the mass parameter.

The expression of the metric function (6.2) shows that there are two branches of solutions corresponding to the different signs in front of the square root. The branch with the minus sign, called the GR branch, allows the general relativistic limit $\alpha \to 0$ as

$$f(r) = k - \frac{m}{r^{d-3}} - \tilde{\Lambda} r^2. \tag{6.3}$$

On the other hand, the metric in the branch with the plus sign, called the non-GR branch, diverges in this limit. In the following section, we will consider the bulk solution only in the GR branch as a conservative choice.

The global structure of the spacetime (6.1) depending on the parameters has been completely classified [39]. There are two classes of curvature singularities in the spacetime. One is the central curvature singularity at $r = 0$. Since we assume $\tilde{\alpha} > 0$ and $1 + 4\tilde{\alpha}\tilde{\Lambda} > 0$, the interior of the square root becomes zero at some $r = r_{\rm b} (> 0)$ for negative m. This corresponds to another curvature singularity called the branch singularity and the metric becomes complex at $r < r_{\rm b}$. In this case, the domain of the coordinate r is $r \in (r_{\rm b}, \infty)$.

The spacetime has a Killing horizon at $r = r_{\rm h}$ satisfying $f(r_{\rm h}) = 0$ depending on the parameters. In order to construct static thin-shell wormholes, the bulk spacetime needs to be static. For this reason, we consider the bulk solution (6.1) in the domain $r \in (r_{\rm h}, \infty)$ if there is no branch singularity and $r \in (\max\{r_{\rm b}, r_{\rm h}\}, \infty)$ if there is a branch singularity. We define the future (past) direction by increasing (decreasing) direction of t.

6.2 Equation of motion for a thin-shell

A thin-shell wormhole spacetime is constructed by gluing two bulk spacetimes (6.1) at a timelike hypersurface $r = a$. Here the bulk spacetimes are defined in the domain $r \geq a (> r_{\rm h})$ and may have different parameters. Then the junction conditions, which are the field equations (2.69) in the distributional sense, tell us the matter content on the thin-shell at $r = a$. Finally, the equation of motion for the shell is obtained as a closed system when an equation of state for the matter is assumed.

The junction condition in Einstein-Gauss-Bonnet gravity is given by

$$[K^i{}_j] - \delta^i{}_j[K] + 2\alpha\Big(3[J^i{}_j] - \delta^i{}_j[J] - 2P^i{}_{kjl}[K^{kl}]\Big) = -\kappa_d^2 S^i{}_j, \tag{6.4}$$

$i, j = 1, 2, \cdots, (d-1)$ are indices for the coordinates on the timelike shell [40, 41, 42]. In the junction conditions (6.4), $K^i{}_j$ is the extrinsic curvature of the shell and $K := h^{ij}K_{ij}$,

where h_{ij} is the induced metric on the shell. Other geometrical quantities are defined by

$$J_{ij} := \frac{1}{3}\left(2KK_{ik}K^k{}_j + K_{kl}K^{kl}K_{ij} - 2K_{ik}K^{kl}K_{lj} - K^2K_{ij}\right), \tag{6.5}$$

$$P_{ikjl} := \mathcal{R}_{ikjl} + 2h_{i[l}\mathcal{R}_{j]k} + 2h_{k[j}\mathcal{R}_{l]i} + \mathcal{R}h_{i[j}h_{l]k}, \tag{6.6}$$

where $\mathcal{R}_{ijkl}$, $\mathcal{R}_{ij}$, and $\mathcal{R}$ are the Riemann tensor, Ricci tensor, and Ricci scalar on the shell. P_{ijkl} is the divergence-free part of the Riemann tensor $\mathcal{R}_{ijkl}$ satisfying $D_iP^i{}_{jkl} = 0$, where D_i is the covariant derivative on the shell. Lastly, $S^i{}_j$ is the energy-momentum tensor on the shell, which satisfies the conservation equations $D_iS^i{}_j = 0$.

A static thin-shell wormhole is realized as a static solution for the equation of motion. However in general, a is not constant but changes in time, representing a moving shell. In such a case, a may be written as a function of the proper time τ on the shell as $a = a(\tau)$.

Now let us derive the equation of motion for the shell. We describe the position of the thin-shell as $r = a(\tau)$ and $t = T(\tau)$ in the spacetime (6.1) and assume the form of $S^i{}_j$ as

$$S^i{}_j = \mathrm{diag}(-\rho, p, p, \cdots, p) + \mathrm{diag}(-\sigma, -\sigma, -\sigma, \cdots, -\sigma). \tag{6.7}$$

This assumption means that the matter on the shell consists of a perfect fluid and the constant tension σ of the shell, where ρ and p are the energy density and pressure of the perfect fluid. Assuming the Z_2 symmetry for the bulk spacetime, we write down the junction conditions (6.4) as

$$\frac{1}{2}\kappa_d^2(\rho+\sigma) = -\frac{(d-2)f\dot{T}}{a}\left\{1 + \frac{2\tilde{\alpha}}{3}\left(2\frac{\dot{a}^2}{a^2} + \frac{3k}{a^2} - \frac{f}{a^2}\right)\right\}, \tag{6.8}$$

$$\begin{aligned}-\frac{1}{2}\kappa_d^2(p-\sigma) = &-\frac{a}{f\dot{T}}\left\{\frac{\ddot{a}}{a} + \frac{f'}{2a} + (d-3)\left(\frac{\dot{a}^2}{a^2} + \frac{f}{a^2}\right)\right\} \\ &- \frac{2\tilde{\alpha}a}{f\dot{T}}\left\{\frac{d-5}{3}\left(\frac{\dot{a}^2}{a^2} + \frac{f}{a^2}\right)\left(2\frac{\dot{a}^2}{a^2} + \frac{3k}{a^2} - \frac{f}{a^2}\right)\right. \\ &\left. + \left(2\frac{\dot{a}^2}{a^2} + \frac{k}{a^2} + \frac{f}{a^2}\right)\frac{\ddot{a}}{a} + \frac{f'}{2a}\left(\frac{k}{a^2} - \frac{f}{a^2}\right)\right\},\end{aligned} \tag{6.9}$$

where $f = f(a)$. A dot and a prime denote the derivative with respect to τ and a, respectively. (See Appendix B for the details of derivation.) The above equations give the equation of motion for a thin-shell in Einstein-Gauss-Bonnet gravity.

In order to obtain the equation of motion in a closed system, an equation of state for the perfect fluid is required. One possibility is the following linear equation of state with a constant γ :

$$p = (\gamma - 1)\rho. \tag{6.10}$$

With this equation state, the energy-conservation equation on the shell $D_iS^i{}_j = 0$, written as

$$\dot{\rho} = -(d-2)(p+\rho)\frac{\dot{a}}{a}, \tag{6.11}$$

is integrated to give

$$\rho = \frac{\rho_0}{a^{(d-2)\gamma}}, \tag{6.12}$$

where ρ_0 is a constant.

6.3 Effective potential for the shell

The dynamics of the shell governed by Eqs. (6.8) and (6.9) with an equation of state (6.10) can be discussed as a one-dimensional potential problem. Then the shape of the effective potential $V(a)$ for the shell determines the stability of static configurations, namely the static wormholes.

Let us derive the effective potential $V(a)$. Squaring Eq. (6.8) and using Eq. (B.24), we obtain

$$\Omega(a)^2 = \left(\frac{f}{a^2} + \frac{\dot{a}^2}{a^2}\right)\left\{1 + \frac{2}{3}\tilde{\alpha}\left(2\frac{\dot{a}^2}{a^2} + \frac{3k}{a^2} - \frac{f}{a^2}\right)\right\}^2, \tag{6.13}$$

where

$$\Omega(a)^2 := \frac{\kappa_d^4(\rho(a)+\sigma)^2}{4(d-2)^2}. \tag{6.14}$$

This is a cubic equation for $\dot{a}^2$. The position of the throat $a = a_0$ for a static wormhole is obtained by solving the following algebraic equation for a_0:

$$\Omega_0^2 = \frac{f_0}{a_0^2}\left\{1 + \frac{2}{3}\tilde{\alpha}\left(\frac{3k}{a_0^2} - \frac{f_0}{a_0^2}\right)\right\}^2, \tag{6.15}$$

where $f_0 := f(a_0)$ and $\Omega_0^2 := \Omega(a_0)^2$.

For convenience, we define

$$A(r) := 1 + \frac{4\tilde{\alpha}m}{r^{d-1}} + 4\tilde{\alpha}\tilde{\Lambda} \tag{6.16}$$

with which the metric function (6.2) in the GR branch is written as

$$f(r) = k + \frac{r^2}{2\tilde{\alpha}}\left(1 - \sqrt{A(r)}\right). \tag{6.17}$$

$A > 0$ is required for the real metric and the absence of branch singularity. In the GR branch, because of the existence of the square root in Eq. (6.17), the following inequality holds:

$$r^2 + 2\tilde{\alpha}k - 2\tilde{\alpha}f(r) > 0, \tag{6.18}$$

which will be used later.

Actually, Eq. (6.13) admits only a single real solution for $\dot{a}^2$:

$$\dot{a}^2 = -V(a), \tag{6.19}$$

which has the form of the one-dimensional potential problem. The effective potential $V(a)$ is defined by

$$V(a) := f(a) - J(a)a^2, \tag{6.20}$$

where $J(a)$ is defined by

$$J(a) := \frac{\left(B(a) - A(a)^{1/2}\right)^2}{4\tilde{\alpha}B(a)}, \tag{6.21}$$

$$B(a) := \left\{ 18\tilde{\alpha}\Omega(a)^2 + A(a)^{3/2} + 6\sqrt{\tilde{\alpha}\Omega(a)^2(9\tilde{\alpha}\Omega(a)^2 + A(a)^{3/2})} \right\}^{1/3}. \tag{6.22}$$

One can see $B > A^{1/2}$. Ω^2 can be expressed in terms of A and B as

$$\Omega^2 = \frac{(B^3 - A^{3/2})^2}{36\tilde{\alpha}B^3}. \tag{6.23}$$

6.4 Existence conditions for static shell

Here we summarize the existence conditions for a static shell located at $a = a_0$. Equation (6.19) is interpreted as the conservation law of mechanical energy for the shell. By differentiating Eq. (6.19) with respect to τ, we obtain the equation of motion for the shell as

$$\ddot{a} = -\frac{1}{2}V'(a). \tag{6.24}$$

From Eqs. (6.19) and (6.24), a_0 is determined algebraically by $V(a_0) = 0$ and $V'(a_0) = 0$.

In addition, a_0 must satisfy $A(a_0) > 0$ and $f(a_0) > 0$. The latter condition $f(a_0) > 0$ is called the horizon-avoidance condition in the previous section and Ref. [32], which simply means that the position of the throat is located in the static region of the spacetime. Actually, this condition is always satisfied because we have $V(a_0) = 0$ and Eq. (6.20) implies $f(a) > V(a)$.

6.5 Negative energy density of the shell

In closing this section, we show that the energy density on the shell $\rho + \sigma$ must be negative for static wormholes. The condition $\rho + \sigma \geq 0$ and Eq. (6.8) with $a = a_0 (> 0)$ yields

$$a_0^2 \leq -\frac{4\tilde{\alpha}k}{2 + \sqrt{A_0}}, \tag{6.25}$$

where $A_0 := A(a_0)$. Clearly, this is not satisfied for $k = 1, 0$ under the assumption $\tilde{\alpha} > 0$. For $k = -1$. Eq. (6.25) gives

$$a_0^2 \leq \frac{4\tilde{\alpha}}{2 + \sqrt{A_0}} < 2\tilde{\alpha} \tag{6.26}$$

and this is not satisfied because there is a constraint $a_0^2 > 2\tilde{\alpha}$ for the throat radius in the GR branch, which can be shown from the combination of Eq. (6.18) and $f(a_0) > 0$. Now we have shown that the energy density on the shell is negative in the physical set up considered in the thesis. Hence the weak energy condition is violated in the GR-branch with $\alpha > 0$. However, negative-tension brane still satisfies the null energy condition.

Hereafter we will consider the case without a perfect fluid on the shell ($\rho = p = 0$) and assume $\sigma < 0$. The resulting static thin-shell wormholes are made of the pure (negative) tension σ and satisfy the null energy condition. This simplest set up is preferred by the minimal violation of the energy conditions. The energy-momentum tensor for negative tension is equivalent to a positive cosmological constant. Such a matter corresponds to an inverted harmonic oscillator in classical mechanics. A technical advantage in this set up is the constancy of Ω^2.

6.6 Existence conditions

The location of the static wormhole throat $a = a_0$ is determined by the following algebraic equation obtained by eliminating σ from Eqs. (6.8) and (6.9):

$$\left(\frac{f_0}{a_0} - \frac{f_0'}{2}\right)\left(1 + 2\tilde{\alpha}\frac{k - f_0}{a_0^2}\right) + \frac{8\tilde{\alpha}kf_0}{a_0^3} = 0, \tag{6.27}$$

where $f_0' := f'(a_0)$. In the limit of $\alpha \to 0$, Eq. (6.27) reduces to the corresponding equation in Einstein gravity [4]. The explicit form of Eq. (6.27) is

$$ka_0^2\sqrt{A_0} = 2ka_0^2 - \frac{(d-1)m}{2a_0^{d-5}} + 4\tilde{\alpha}k^2. \tag{6.28}$$

This equation shows that $m = 0$ is required for $k = 0$ and then a_0 is totally undetermined in the domain where both $A_0 > 0$ and $f_0 > 0$ hold. The metric function (6.2) with $m = k = 0$ shows that the horizon avoidance condition $f_0 > 0$ is satisfied only for $\Lambda < 0$. Stability of this wormhole will be investigated in Section 6.10.1.

On the other hand, for $k = 1$ (-1), the left-hand side of Eq. (6.28) is positive (negative) and hence the throat radius must satisfy

$$k\left\{2ka_0^2 - \frac{(d-1)m}{2a_0^{d-5}} + 4\tilde{\alpha}\right\} > 0. \tag{$\mathcal{A}$}$$

For $k \neq 0$, squaring Eq. (6.28) gives the following algebraic equation for a_0:

$$\begin{aligned}(3 - 4\tilde{\alpha}\tilde{\Lambda})a_0^{2(d-3)} + 16\tilde{\alpha}ka_0^{2(d-4)} + 16\tilde{\alpha}^2 a_0^{2(d-5)} \\ - 2(d-1)kma_0^{d-3} - 4d\tilde{\alpha}ma_0^{d-5} + \frac{1}{4}(d-1)^2m^2 = 0.\end{aligned} \tag{6.29}$$

Static wormhole solutions with the throat radius a_0 must satisfy Eq. (6.29) and also several constraints.

The first constraint is the inequality ($\mathcal{A}$). Another constraint comes from Eqs. (6.58) and (6.59). Eliminating f_0^2, we obtain

$$f_0 = \frac{1}{4k\tilde{\alpha}}\left\{\frac{(d-1)m}{a_0^{d-5}} - 2(ka_0^2 + 2\tilde{\alpha})\right\}. \tag{6.30}$$

Since the right-hand side of Eq. (6.30) must be positive, we have a necessary condition for physical solutions:

$$k\left\{\frac{(d-1)m}{a_0^{d-5}} - 2(ka_0^2 + 2\tilde{\alpha})\right\} > 0. \tag{$\mathcal{B}$}$$

We do not have to impose the condition $A_0 > 0$ to avoid the complex metric in the bulk spacetime because any real solution of Eq. (6.29) satisfies it. This is shown as follows. Eq. (6.29) is solved for m/a_0^{d-5} as

$$\frac{m}{a_0^{d-5}} = \frac{2\left(2k(d-1)a_0^2 + 4d\tilde{\alpha} \pm \sqrt{(d-1)^2(1+4\tilde{\alpha}\tilde{\Lambda})a_0^4 + 16k(d-1)\tilde{\alpha}a_0^2 + 16(2d-1)\tilde{\alpha}^2}\right)}{(d-1)^2}. \tag{6.31}$$

Substituting this into $A_0 = 1 + 4\tilde{\alpha}\tilde{\Lambda} + 4\tilde{\alpha}m/a_0^{d-1}$, we obtain

$$A_0 = \frac{U \pm 8\tilde{\alpha}\sqrt{U - 16\tilde{\alpha}^2}}{(d-1)^2 a_0^4}, \tag{6.32}$$

where

$$U := (d-1)^2(1+4\tilde{\alpha}\tilde{\Lambda})a_0^4 + 16\tilde{\alpha}\left\{k(d-1)a_0^2 + 2d\tilde{\alpha}\right\}. \tag{6.33}$$

For any real solution of Eq. (6.29), the interior of the square root in Eq. (6.31) is non-negative, which gives the following lower bound of $\tilde{\Lambda}$:

$$\tilde{\Lambda} \geq -\frac{(d-1)^2 a_0^4 + 16(d-1)\tilde{\alpha}ka_0^2 + 16(2d-1)\tilde{\alpha}^2}{4(d-1)^2\tilde{\alpha}a_0^4}. \tag{6.34}$$

This inequality implies $U \geq 16\tilde{\alpha}^2$ and hence U is positive. Therefore A_0 with the plus sign in Eq. (6.32) is positive. Positivity of A_0 with the minus sign is shown by direct computations without using the inequality (6.34).

6.7 Non-existence for $k = 1$ with $m \leq 0$ and $k = -1$ with $m \geq 0$

It is shown that there is no static thin-shell wormhole for $k = 1$ with $m \leq 0$ and $k = -1$ with $m \geq 0$. For the proof, we use Eq. (6.19) in the following form:

$$\left(\frac{\mathrm{d}\ln a}{\mathrm{d}\tau}\right)^2 + \bar{V}(a) = 0, \tag{6.35}$$

where

$$\bar{V}(a) := \frac{f(a)}{a^2} - J(a). \tag{6.36}$$

There is no static solution if $\bar{V}(a)$ is monotonic. $\bar{V}'$ is computed to give

$$\bar{V}' = -\frac{1}{4\tilde{\alpha}B^2}\left\{\frac{8k\tilde{\alpha}B^2}{a^3} + (B^2 - A)B' + BA'\right\}. \tag{6.37}$$

The following expressions;

$$A'(a) = -\frac{4(d-1)\tilde{\alpha}m}{a^d}, \tag{6.38}$$

$$B'(a) = \frac{A(a)^{1/2}A'(a)}{2B^2}\left(1 + \frac{3\tilde{\alpha}\Omega^2}{\sqrt{\tilde{\alpha}\Omega^2(9\tilde{\alpha}\Omega^2 + A(a)^{3/2})}}\right) \tag{6.39}$$

imply $B' \leq 0$ (≥ 0) and $A' \leq 0$ (≥ 0) for $m \geq 0$ $(m \leq 0)$ with equality holding for $m = 0$. Together with the facts $A, B > 0$ and $B > A^{1/2}$, it is shown that $\bar{V}'$ is negative definite for $k = 1$ with $m \leq 0$ and positive definite for $k = -1$ with $m \geq 0$.

6.8 Stability criterion

As explained at the beginning of this section, the sign of $V''(a_0)$ determines stability of a static thin-shell wormhole. In this subsection, we will derive $V''(a_0)$ in a convenient form to prove the (in)stability.

6.8.1 Einstein gravity

First let us consider Einstein gravity as a simple lesson. In the general relativistic limit $\alpha \to 0$, Eq. (6.13) reduces to

$$\Omega^2 = \frac{f(a)}{a^2} + \frac{\dot{a}^2}{a^2}. \tag{6.40}$$

By solving Eq. (6.40) for $\dot{a}^2$, we define a potential $V(a)$ of the conservation law of the one-dimensional potential problem. Then we directly calculate the second derivative of $V(a)$. However, without such direct calculations, in principle we can derive the form of $V''(a_0)$ by operating a systematic method below, which can be applied also in more general theories of gravity.

Suppose we get a master equation as $\dot{a}^2 + V(a) = 0$. By this master equation, $\dot{a}^2$ in Eq. (6.40) is replaced by $-V(a)$ to give

$$\Omega^2 = \frac{f(a) - V(a)}{a^2}. \tag{6.41}$$

Differentiating this equation twice, we obtain

$$0 = a(f' - V') - 2(f - V), \tag{6.42}$$
$$0 = a(f'' - V'') - (f' - V'). \tag{6.43}$$

In Einstein gravity, the metric function is

$$f(a) = k - \frac{m}{a^{d-3}} - \tilde{\Lambda} a^2, \tag{6.44}$$

which satisfies

$$f'(a) = \frac{(d-3)(k-f) - \tilde{\Lambda}(d-1)a^2}{a}, \tag{6.45}$$
$$f''(a) = \frac{\tilde{\Lambda}(d-1)(d-4)a^2 - (k-f)(d-2)(d-3)}{a^2}. \tag{6.46}$$

Substituting Eq. (6.45) into Eq. (6.42) and evaluating it at $a = a_0$ satisfying $V(a_0) = V'(a_0) = 0$, we obtain

$$f_0 (:= f(a_0)) = \frac{d-3}{d-1} k - \tilde{\Lambda} a_0^2. \tag{6.47}$$

Combining this with Eq. (6.44), we obtain the algebraic equation to determine a_0:

$$\frac{2k}{d-1} = \frac{m}{a_0^{d-3}}. \tag{6.48}$$

For $k = 0$, Eq. (6.48) requires $m = 0$ and a_0 is totally undetermined. For $k = 1(-1)$, Eq. (6.48) requires $m > (<)0$ and the throat radius a_0 is given by

$$a_0 = \left(\frac{(d-1)m}{2k}\right)^{1/(d-3)}. \tag{6.49}$$

As seen in Eq. (6.49), Λ does not contribute to the size of the wormhole throat. However, it appears in the horizon-avoidance condition $f_0 > 0$. Equation (6.47) shows that $f_0 > 0$ requires $\Lambda < 0$ in the case of $k = 0, -1$. In the case of $\Lambda = 0$, $f_0 > 0$ is satisfied only for $k = 1$. In the case of $\Lambda > 0$ and $k = 1$, $f_0 > 0$ gives a constraint $a_0 < a_{\rm c}^{(\rm GR)}$ on the size of the wormhole throat, where

$$a_{\rm c}^{(\rm GR)} := \left(\frac{(d-3)k}{(d-1)\tilde{\Lambda}}\right)^{1/2}. \tag{6.50}$$

On the other hand, in the case of $\Lambda < 0$ and $k = -1$, $f_0 > 0$ gives $a_0 > a_{\rm c}^{(\rm GR)}$. Combining this inequality with Eq. (6.49), we obtain the range of the mass parameter admitting static wormhole solutions; $0 < m < m_{\rm c}^{(\rm GR)}$ for $k = 1$ with $\Lambda > 0$ and $m < m_{\rm c}^{(\rm GR)} (< 0)$ for $k = -1$ with $\Lambda < 0$, where

$$m_{\rm c}^{(\rm GR)} := \frac{2k}{d-1}\left(\frac{(d-3)k}{(d-1)\tilde{\Lambda}}\right)^{(d-3)/2}. \tag{6.51}$$

In Einstein gravity, a simple criterion for the stability of static solutions is available. Substituting Eqs. (6.45) and (6.46) into Eq. (6.43), evaluating them at $a = a_0$, we obtain

$$\begin{aligned} V''(a_0) =& -\frac{(d-1)(d-3)m}{a_0^{d-1}} \\ =& -\frac{2(d-3)k}{a_0^2}, \end{aligned} \tag{6.52}$$

where we used Eqs. (6.44) and (6.48). This simple expression clearly shows that the wormhole is stable only for $k = -1$ with $m < 0$ [4]. Existence and stability of static thin-shell wormholes in Einstein gravity are summarized in Table 6.1.

6.8.2 Einstein-Gauss-Bonnet gravity

Although it is more complicated, we can play this game in Einstein-Gauss-Bonnet gravity in a similar manner. Replacing $\dot{a}^2$ by $-V(a)$ in the master equation (6.13), we obtain

$$\Omega^2 = \frac{f(a) - V(a)}{a^2}\left\{1 + \frac{2\tilde{\alpha}(-2V(a) + 3k - f(a))}{3a^2}\right\}^2. \tag{6.53}$$

In Einstein-Gauss-Bonnet gravity, the metric function is

$$f(a) = k + \frac{a^2}{2\tilde{\alpha}}\left(1 - \sqrt{1 + 4\tilde{\alpha}\tilde{\Lambda} + \frac{4\tilde{\alpha}m}{a^{d-1}}}\right), \tag{6.54}$$

Table 6.1: The existence and stability of Z_2 symmetric static thin-shell wormholes made of pure negative tension in Einstein gravity, where $a_c^{(GR)}$ and $m_c^{(GR)}$ are defined by Eqs. (6.50) and (6.51), respectively.

		Existence	Possible range of a_0	Stability
$k=1$	$\Lambda>0$	$0<m<m_c^{(GR)}$	$0<a_0<a_c^{(GR)}$	Unstable
	$\Lambda\leq 0$	$m>0$	$a_0>0$	Unstable
$k=0$	$\Lambda\geq 0$	None	–	–
	$\Lambda<0$	$m=0$	$a_0>0$	Marginally stable
$k=-1$	$\Lambda\geq 0$	None	–	–
	$\Lambda<0$	$m<m_c^{(GR)}(<0)$	$a_0>a_c^{(GR)}$	Stable

which satisfies

$$f'(a) = \frac{(d-5)\tilde{\alpha}(k-f)^2+(d-3)a^2(k-f)-\tilde{\Lambda}(d-1)a^4}{a\{a^2+2\tilde{\alpha}(k-f)\}}, \tag{6.55}$$

$$f''(a) = \frac{L(a)}{a^2\{a^2+2\tilde{\alpha}(k-f)\}^3}, \tag{6.56}$$

where

$$\begin{aligned} L(a) :=& 2(d-1)^2\tilde{\alpha}\tilde{\Lambda}^2a^8-\tilde{\Lambda}a^4(d-1)\Big\{12\tilde{\alpha}^2(k-f)^2+12\tilde{\alpha}a^2(k-f)-(d-4)a^4\Big\} \\ &-(k-f)\Big\{2(d-3)(d-5)\tilde{\alpha}^3(k-f)^3+4(d^2-8d+13)\tilde{\alpha}^2a^2(k-f)^2 \\ &+3(d-2)(d-5)\tilde{\alpha}a^4(k-f)+(d-2)(d-3)a^6\Big\}. \end{aligned} \tag{6.57}$$

Equation (6.54) gives

$$m = a^{d-3}\Big\{-\tilde{\Lambda}a^2+(k-f(a))+\tilde{\alpha}a^{-2}(k-f(a))^2\Big\}. \tag{6.58}$$

Differentiating (6.53) and evaluating at $a=a_0$, we obtain

$$f_0^2 = \frac{\{(d-1)a_0^2+2k(d+1)\tilde{\alpha}\}f_0+(d-1)\tilde{\Lambda}a_0^4-k\{(d-3)a_0^2+(d-5)\tilde{\alpha}k\}}{(d-1)\tilde{\alpha}}. \tag{6.59}$$

where we used Eq. (6.55). This equation reduces to Eq. (6.47) for $\alpha\to 0$. Equation (6.59) will be used to replace f_0^p $(p=2,3,4,\cdots)$ by f_0.

Differentiating Eq. (6.53) twice and using Eqs. (6.55) and (6.56), we finally obtain $V''(a_0)$ in a rather compact form:

$$V''(a_0) = -\frac{2kP(a_0)}{a_0^2(a_0^2+2k\tilde{\alpha}+2\tilde{\alpha}f_0)(a_0^2+2k\tilde{\alpha}-2\tilde{\alpha}f_0)}, \tag{6.60}$$

$$P(a_0) := 4\tilde{\alpha}^2f_0\Big\{6k-(d-3)f_0\Big\}+(a_0^2+2k\tilde{\alpha})\Big\{(d-3)a_0^2+2(d-5)k\tilde{\alpha}\Big\}, \tag{6.61}$$

where we have eliminated $\tilde{\Lambda}$ by using Eq. (6.59). This expression reduces to Eq. (6.52) for $\alpha \to 0$. Because of Eq. (6.18), the denominator in the expression of $V''(a_0)$ is positive and therefore the sign of the function $P(a_0)$ determines the stability of the shell.

6.9 Effect of the Gauss-Bonnet term on the stability for $\tilde{\alpha}/a_E^2 \ll 1$

Before moving onto the full-order analysis, let us clarify how the Gauss-Bonnet term affects the stability of thin-shell wormholes in the situation where $\tilde{\alpha}$ is small.

In the general relativistic limit $\tilde{\alpha} \to 0$ with $k = \pm 1$, Eq. (6.28) gives

$$a_0^{d-3} = \frac{(d-1)mk}{2} =: a_{\rm E}^{d-3}. \tag{6.62}$$

This is the static solution in Einstein gravity which requires $mk > 0$ [4]. Now we obtain the static solution for $\epsilon := \tilde{\alpha}/a_E^2 \ll 1$ in a perturbative method. We expand a_0 in a power series of ϵ :

$$a_0 = a_{\rm E} + a_{(1)}\epsilon + a_{(2)}\epsilon^2 + \dots. \tag{6.63}$$

Substituting this expression into Eq. (6.28) and expanding it in a series of ϵ, we obtain

$$a_{(1)} = \frac{2\tilde{\Lambda}(d-1)a_{\rm E}^2 - 4(d-2)k}{(d-1)(d-3)} a_{\rm E}. \tag{6.64}$$

This allows us to derive the expansion of Eq. (6.60):

$$\begin{aligned} V''(a_0) \simeq & -\frac{2(d-3)k}{a_{\rm E}^2} + \frac{4(d-3)ka_{(1)}\epsilon}{a_{\rm E}^3} + \frac{8k^2\epsilon}{a_{\rm E}^2} \\ = & -\frac{2(d-3)k}{a_{\rm E}^2} - \frac{8k\epsilon}{a_{\rm E}^2}\left(\frac{d-3}{d-1}k - \tilde{\Lambda}a_{\rm E}^2\right). \end{aligned} \tag{6.65}$$

The first term of Eq. (6.65) coincides with Eq. (6.52) and inside the bracket of the second term is positive because of Eq. (6.47). Hence we arrive a simple conclusion about the effect of the Gauss-Bonnet term for small $\tilde{\alpha}$; it destabilizes wormholes in the spherically symmetric case ($k = 1$), while it stabilizes in the hyperbolically symmetric case ($k = -1$).

6.10 Stability for $k = 0, 1$

In this subsection, we will prove (in)stability of the static thin-shell wormhole in the framework of Einstein-Gauss-Bonnet gravity. We are going to study the sign of $V''(a_0)$ given by Eq. (6.60) for $k = 0$ and $k = 1$. Because the analysis is much more complicated in the case of $k = -1$, it will be treated in the next section.

6.10.1 $k = 0$ with $m = 0$: Marginally stable

The analysis for $k = 0$ is very simple. For $k = 0$, Eq. (6.28) gives $m = 0$ and a_0 is totally undetermined. Therefore, any size of the static wormhole throat is allowed for $k = 0$. This is consistent with the fact that Eq. (6.60) gives $V''(a_0) = 0$, namely the wormhole is marginally stable.

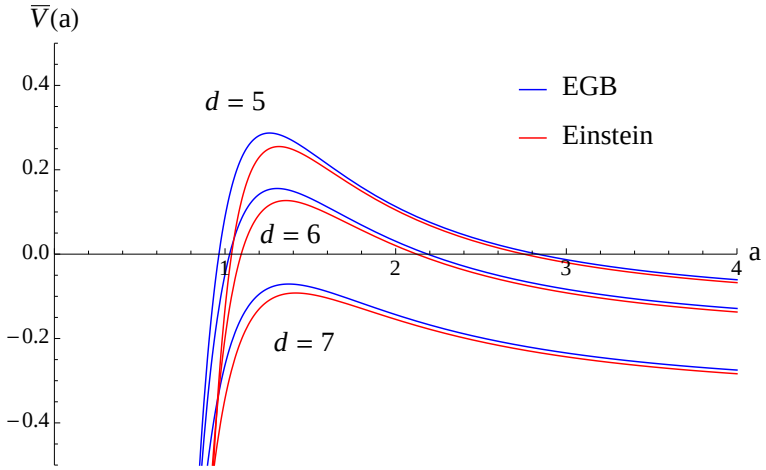

Figure 6.1: The potential $\bar{V}(a)$ for $d = 5, 6, 7$ in Einstein and Einstein-Gauss-Bonnet (EGB) gravity with $k = 1$, $\alpha = 0.02$, $m = 1$, $\Lambda = 1$ and $\sigma = -0.1$.

6.10.2 $k = 1$ with $m > 0$: Unstable

In Section 6.7, we have shown that there is no static wormhole for $k = 1$ with $m \leq 0$. In the thesis, we don't clarify the parameter region with positive m admitting static wormhole solutions because they are all dynamically unstable in any case. In Fig. 6.1, we plot the profile of $\bar{V}(a)$ with $k = 1$ and $m > 0$, in which there is a local maximum. This implies that the corresponding static solution is unstable. We will prove this analytically.

For $k = 1$, positivity of $P(a_0)$ in Eq. (6.60) means instability of the static wormhole. Using the inequality (6.18), we evaluate the lower bound of $P(a_0)$ as

$$\begin{aligned}
P(a_0) =& 4\tilde{\alpha}^2 f_0 \Big\{ 6 - (d-3) f_0 \Big\} + (a_0^2 + 2\tilde{\alpha}) \Big\{ (d-3) a_0^2 + 2(d-5)\tilde{\alpha} \Big\} \\
>& 4\tilde{\alpha}^2 f_0 \Big\{ 6 - (d-3) f_0 \Big\} + 2\tilde{\alpha} f_0 \Big\{ (d-3) a_0^2 + 2(d-5)\tilde{\alpha} \Big\} \\
=& 2\tilde{\alpha} f_0 \Big\{ 2(d-3)\tilde{\alpha} \Big(\frac{a_0^2}{2\tilde{\alpha}} - f_0 \Big) + 2(d+1)\tilde{\alpha} \Big\} \\
>& 2\tilde{\alpha} f_0 \Big\{ -2(d-3)\tilde{\alpha} + 2(d+1)\tilde{\alpha} \Big\} = 16\tilde{\alpha}^2 f_0 > 0.
\end{aligned} \tag{6.66}$$

Therefore, the wormhole is dynamically unstable. In closing this section, we note that a similar analysis for $k = 0, 1$ can reveal the instability of thin-shell wormholes which are made of a dust fluid. (See Appendix C.)

6.11 Stability for $k = -1$ with $m < 0$

In the follwing section, we will provide the stability analysis for $k = -1$. Since we have shown that there is no static wormhole for $k = -1$ with $m \geq 0$ in Section 6.7, we will discuss the case with $m < 0$.

6.11.1 Preliminaries for pictorial analysis

For our purpose, we introduce $x := a_0^2$ and $y := m/a_0^{d-5}$, with which Eq. (6.29) is written as $h(x, y) = 0$, where

$$h(x,y) :=(3-4\tilde{\alpha}\tilde{\Lambda})x^2 - 2(d-1)kxy + \frac{1}{4}(d-1)^2y^2 + 16\tilde{\alpha}kx - 4d\tilde{\alpha}y + 16\tilde{\alpha}^2. \quad (6.67)$$

We adopt a pictorial analysis in the (x, y) plane in the domain of $x > 0$ and $y < 0$.

For $3 - 4\tilde{\alpha}\tilde{\Lambda} \neq 0$, $h(x, y) = 0$ is solved to give $x = x_\pm(y)$, where

$$x_\pm(y) := \frac{2k\{(d-1)y - 8\tilde{\alpha}\} \pm \sqrt{Z(y)}}{2(3-4\tilde{\alpha}\tilde{\Lambda})}. \quad (6.68)$$

The function $Z(y)$ in the above expression is defined by

$$\begin{aligned} Z(y) :=& 4\left\{(d-1)y - 8\tilde{\alpha}\right\}^2 - (3-4\tilde{\alpha}\tilde{\Lambda})\left\{(d-1)^2y^2 - 16d\tilde{\alpha}y + 64\tilde{\alpha}^2\right\} \\ =& (d-1)^2(1+4\tilde{\alpha}\tilde{\Lambda})y^2 - 16\tilde{\alpha}(4d\tilde{\alpha}\tilde{\Lambda} + d - 4)y + 64\tilde{\alpha}^2(1+4\tilde{\alpha}\tilde{\Lambda}). \end{aligned} \quad (6.69)$$

In the limit $\alpha \to 0$, we obtain

$$\lim_{\alpha\to 0} x_+(y) = \frac{k(d-1)y}{2}, \qquad \lim_{\alpha\to 0} x_-(y) = \frac{k(d-1)y}{6}. \quad (6.70)$$

Among these two, only the former satisfies Eq. (6.28) with $\alpha = 0$. For this reason, we will focus only on $x_+(y)$ hereafter because $x_-(y)$ does not admit the general relativistic limit.

Physical domain of solutions

Solutions of Eq. (6.29) are realized as intersections of $h(x, y) = 0$ with $y = m/x^{(d-5)/2}$ in the (x, y) plane. In addition, they must be located in the physical domain where all the constraints on the solutions are satisfied.

The inequality $(\mathcal{A})$ gives a constraint between x and y for physical solutions:

$$x > \frac{(d-1)k}{4}y - 2\tilde{\alpha}k =: x_{\min}(y). \quad (6.71)$$

Also, the inequality $(\mathcal{B})$ gives another constraint:

$$-2k\tilde{\alpha} < x < \frac{(d-1)k}{2}y - 2k\tilde{\alpha} =: x_{\max}(y), \quad (6.72)$$

where the left inequality comes from $a_0^2 + 2k\tilde{\alpha} > 0$. In summary, physical solutions must be located in the domain of $x_{\min}(y) < x < x_{\max}(y)$ and $y < 0$. Since a static solution is realized as an intersection of the hyperbola with $y = m/x^{(d-5)/2}$ in this domain, the number of static solutions depend on the value of m. (See Fig. 6.2 as an example.)

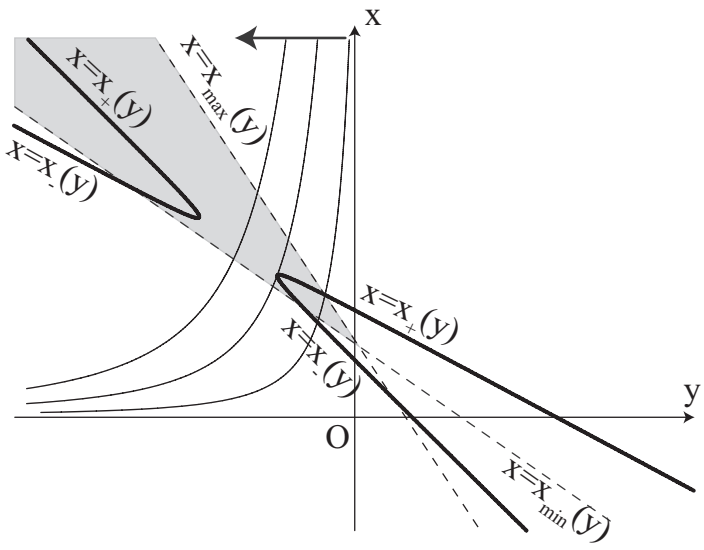

Figure 6.2: The (x, y) plane for $-1 < 4\tilde{\alpha}\tilde{\Lambda} < -(2d-5)/(2d-1)$ with $k = -1$, $\alpha > 0$, and $d = 6$. The thick hyperbola consists of $x = x_+(y)$ and $x = x_-(y)$, while dashed lines consist of $x = x_{\rm max}(y)$ and $x = x_{\rm min}(y)$. Thin curves correspond to $y = m/x^{(d-5)/2}$ with three different values of negative m. It moves to the left as $m(< 0)$ decreases. Since a static solution is realized as an intersection of the hyperbola with $y = m/x^{(d-5)/2}$ in the shadowed region, the number of static solutions depend on the value of m.

Stable domain of solutions

Substituting Eq. (6.30) into Eq. (6.61), we write $P(a_0)$ as a function of x and y as

$$\begin{aligned} P(x,y) =& k\left\{(d-1)(d-3)y - 16\tilde{\alpha}\right\}x \\ & - \frac{1}{4}\left\{(d-3)(d-1)^2y^2 - 8d(d-1)\tilde{\alpha}y + 128\tilde{\alpha}^2\right\}. \end{aligned} \tag{6.73}$$

The stable domain of solutions are given by $P(x, y) > 0$ in the (x, y) plane. The curve $P(x, y) = 0$ representing marginal stability is given by

$$x = \frac{(d-3)(d-1)^2y^2 - 8d(d-1)\tilde{\alpha}y + 128\tilde{\alpha}^2}{4k\{(d-1)(d-3)y - 16\tilde{\alpha}\}} =: x_{\rm P}(y). \tag{6.74}$$

We have $x_{\rm P}(0) = -2k\tilde{\alpha}$ and

$$\lim_{y\to-\infty} x_{\rm P}(y) \simeq \frac{d-1}{4k}y - \frac{2d\tilde{\alpha}}{k(d-3)}. \tag{6.75}$$

Since $P(x, y)$ is an increasing function of x in the negative domain of y and we have

$$P(x_{\rm min}(y), y) = 2(d-1)\tilde{\alpha}y < 0, \tag{6.76}$$

$$P(x_{\rm max}(y), y) = -\frac{(d-1)y\left\{8\tilde{\alpha} - (d-1)(d-3)y\right\}}{4} > 0, \tag{6.77}$$

$x_{\rm P}(y)$ satisfies $x_{\rm min}(y) < x_{\rm P}(y) < x_{\rm max}(y)$. (See Fig. 6.3 as an example.)

Now we are ready to perform the stability analysis. We will treat the cases of $\Lambda \geq 0$ and $-1 < 4\tilde{\alpha}\tilde{\Lambda} < 0$, separately.

6.11.2 Non-existence for $\Lambda \geq 0$

In this subsection, we treat the case of $\Lambda \geq 0$. Similar to the general relativistic case, Einstein-Gauss-Bonnet gravity also does not admit static thin-shell wormholes in this parameter region.

For $4\tilde{\alpha}\tilde{\Lambda} > 3$, Eq. (6.68) shows that $x_+ < 0 < x_-$ holds in the domain of $y < 0$ with $k = -1$. Since $x = x_+(y)$ does not satisfy the necessary condition $x > 0$, there is no static solution in this case.

In the special case of $4\tilde{\alpha}\tilde{\Lambda} = 3$, $h(x, y) = 0$ is solved to give

$$x(y) = \frac{(d-1)^2y^2 - 16d\tilde{\alpha}y + 64\tilde{\alpha}^2}{8k\{(d-1)y - 8\tilde{\alpha}\}} (> 0), \tag{6.78}$$

which satisfies

$$x_{\rm min}(y) - x(y) = \frac{(d-1)^2y^2 - 16(d-2)\tilde{\alpha}y + 64\tilde{\alpha}^2}{8k\{(d-1)y - 8\tilde{\alpha}\}} > 0, \tag{6.79}$$

where $x_{\rm min}(y)$ is defined in Eq. (6.71). Because the necessary condition $x > x_{\rm min}$ is not satisfied, there is no static solution for $4\tilde{\alpha}\tilde{\Lambda} = 3$.

Lastly, in order to show the non-existence for $0 \leq 4\tilde{\alpha}\tilde{\Lambda} < 3$, we will use the following fact: The sign of $x_{\rm max}(y) - x_+(y)$ is definite in some domain of y if the curves $x_+(y)$ and $x_{\rm max}(y)$ do not intersect and $x_+(y)$ is continuous there. Actually, $x_+(y)$ is continuous in the negative domain of y for $4\tilde{\alpha}\tilde{\Lambda} \geq -(2d-5)/(2d-1)$ because Eq. (6.69) shows that $Z(y)$ is non-negative then.

It is also possible to show that $x_+(y)$ and $x_{\rm max}(y)$ do not intersect in the negative domain of y. For $\Lambda = 0$, $x_+(y) = x_{\rm max}(y)$ is solved to give

$$y = \frac{2\tilde{\alpha}}{d-3}, \tag{6.80}$$

which is positive. For $0 < 4\tilde{\alpha}\tilde{\Lambda} < 3$, the solution is

$$\begin{aligned} y =& \frac{4(d-1)\tilde{\alpha}\tilde{\Lambda} + d - 3 \pm \sqrt{\left\{4(d-1)\tilde{\alpha}\tilde{\Lambda} + d - 3\right\}^2 - 4(d-1)^2\tilde{\alpha}\tilde{\Lambda}(1 + 4\tilde{\alpha}\tilde{\Lambda})}}{(d-1)^2\tilde{\Lambda}} \\ =& \frac{4(d-1)\tilde{\alpha}\tilde{\Lambda} + d - 3 \pm \sqrt{4(d-1)(d-5)\tilde{\alpha}\tilde{\Lambda} + (d-3)^2}}{(d-1)^2\tilde{\Lambda}} =: y_{\rm c(\pm)}, \end{aligned} \tag{6.81}$$

where inside the square-root is positive for $4\tilde{\alpha}\tilde{\Lambda} > -1$. By direct calculations, both $y_{\rm c(+)}$ and $y_{\rm c(-)}$ are shown to be positive for $\Lambda > 0$. (We note that $y_{\rm c(+)} < 0$ and $y_{\rm c(-)} > 0$ are satisfied for $\Lambda < 0$.)

We have shown that the sign of $x_+(y) - x_{\rm max}(y)$ is definite in the domain of negative y for $\Lambda > 0$. This sign is actually negative, as shown below. From the following

expression;

$$x_{\max}(y) - x_+(y) = \frac{k(d-1)(1-4\tilde{\alpha}\tilde{\Lambda})y + 4k\tilde{\alpha}(1+4\tilde{\alpha}\tilde{\Lambda}) - \sqrt{Z(y)}}{2(3-4\tilde{\alpha}\tilde{\Lambda})}$$
$$= \frac{-4k\tilde{\alpha}\{(d-1)y - 4\tilde{\alpha}\}\tilde{\Lambda} + k(d-1)y + 4k\tilde{\alpha} - \sqrt{Z(y)}}{2(3-4\tilde{\alpha}\tilde{\Lambda})}, \tag{6.82}$$

we obtain

$$x_{\max}(0) - x_+(0) = \frac{2k\tilde{\alpha}(1+4\tilde{\alpha}\tilde{\Lambda}) - 4\tilde{\alpha}\sqrt{1+4\tilde{\alpha}\tilde{\Lambda}}}{3-4\tilde{\alpha}\tilde{\Lambda}}, \tag{6.83}$$

which is negative for $-1 < 4\tilde{\alpha}\tilde{\Lambda} < 3$. Because $x_+(y) - x_{\max}(y)$ is continuous, it is concluded that $x_+(y) > x_{\max}(y)$ is satisfied in the negative domain of y for $0 < 4\tilde{\alpha}\tilde{\Lambda} < 3$.

6.11.3 Pictorial analysis for $-1 < 4\tilde{\alpha}\tilde{\Lambda} < 0$

Now we focus on the case of $-1 < 4\tilde{\alpha}\tilde{\Lambda} < 0$. In this case, there exit static solutions but their existence and stability depend on the parameters in a complicated manner. We will clarify them by a pictorial analysis.

Geometric shape of $h(x, y) = 0$

In the case of $-1 < 4\tilde{\alpha}\tilde{\Lambda} < 0$, $h(x, y) = 0$, where $h(x, y)$ is defined by Eq. (6.67), is a hyperbola in the (x, y) plane in general. In order to understand the shape of the hyperbola, we present

$$h(0, y) = \frac{1}{4}(d-1)^2 y^2 - 4d\tilde{\alpha}y + 16\tilde{\alpha}^2, \tag{6.84}$$
$$h(x, 0) = (3-4\tilde{\alpha}\tilde{\Lambda})x^2 + 16\tilde{\alpha}kx + 16\tilde{\alpha}^2. \tag{6.85}$$

$h(0, y) = 0$ has two positive solutions $y = y_1(> 0)$ and $y = y_2(> y_1)$, where

$$y_1 := \frac{8\tilde{\alpha}(d - \sqrt{2d-1})}{(d-1)^2}, \qquad y_2 := \frac{8\tilde{\alpha}(d + \sqrt{2d-1})}{(d-1)^2}. \tag{6.86}$$

$h(x, 0) = 0$ also has two positive solutions $x = x_1(> 0)$ and $x = x_2(> x_1)$, where

$$x_1 := \frac{-8\tilde{\alpha}k - 4\tilde{\alpha}\sqrt{1+4\tilde{\alpha}\tilde{\Lambda}}}{3-4\tilde{\alpha}\tilde{\Lambda}}, \qquad x_2 := \frac{-8\tilde{\alpha}k + 4\tilde{\alpha}\sqrt{1+4\tilde{\alpha}\tilde{\Lambda}}}{3-4\tilde{\alpha}\tilde{\Lambda}}. \tag{6.87}$$

The shape of the hyperbola drastically changes at the following critical value;

$$4\tilde{\alpha}\tilde{\Lambda} = -\frac{2d-5}{2d-1}, \tag{6.88}$$

which is located in the domain $-1 < 4\tilde{\alpha}\tilde{\Lambda} < 0$. With this critical value of Λ, $h(x, y)$ becomes factored;

$$h(x, y) = \frac{1}{4}(d-1)^2\left(y - \frac{64k\tilde{\alpha}x}{(d-1)\{8\tilde{\alpha} - (d-1)w\}} + \frac{64\tilde{\alpha}^2}{(d-1)^2 w}\right)$$
$$\times \left(y + \frac{8kwx}{8\tilde{\alpha} - (d-1)w} + w\right), \tag{6.89}$$

where a constant w satisfies $(d-1)^2w^2+16d\tilde{\alpha}w+64\tilde{\alpha}^2=0$, and therefore $h(x,y)=0$ consists of two straight lines.

$x=x_+(y)$ and $x=x_-(y)$ coincide when $Z(y)$ vanishes. These points are located on $x=x_{\rm P}(y)$ only for $d=5$ or $4\tilde{\alpha}\tilde{\Lambda}=-(2d-5)/(2d-1)$. For $4\tilde{\alpha}\tilde{\Lambda}=-(2d-5)/(2d-1)$, $Z(y)$ vanishes at

$$y=-\frac{8\tilde{\alpha}}{d-1}=:y_0. \tag{6.90}$$

For $d=5$, it vanishes at

$$y=\frac{\tilde{\alpha}\left\{20\tilde{\alpha}\tilde{\Lambda}+1\pm\sqrt{(4\tilde{\alpha}\tilde{\Lambda}-3)(36\tilde{\alpha}\tilde{\Lambda}+5)}\right\}}{2(1+4\tilde{\alpha}\tilde{\Lambda})}=:y_{5(\pm)}. \tag{6.91}$$

The (x,y)-planes for $-1<4\tilde{\alpha}\tilde{\Lambda}<0$ are drawn in Figs. 6.4–6.6.

Existence of solutions

In the present case, existence of static solutions depends on the value of the mass parameter m. First of all, as in Einstein gravity, it is shown that there is no static solution for sufficiently small $|m|$. For $-1<4\tilde{\alpha}\tilde{\Lambda}<0$, Eq. (6.81) shows that $x_+(y)<x_{\rm max}(y)$ holds in the domain $y<y_{{\rm c}(+)}$. As seen in Fig. 6.2, the curve $y=m/x^{(d-5)/2}$ moves to the right as $m(<0)$ increases approaching the x-axis in the limit of $m\to-0$. Therefore, there exists a critical value $m_{\rm c}$ such that, for $m_{\rm c}<m(<0)$, the intersection of $x=x_+(y)$ with $y=m/x^{(d-5)/2}$ is located outside the physical domain in the (x,y) plane and hence there is no static solution. This critical value $m_{\rm c}$ is obtained by solving the following algebraic equations:

$$\begin{cases}2x=(d-1)ky(m_{\rm c})-4k\tilde{\alpha},\\ (d-1)^2\tilde{\Lambda}y(m_{\rm c})=4(d-1)\tilde{\alpha}\tilde{\Lambda}+d-3+\sqrt{4(d-1)(d-5)\tilde{\alpha}\tilde{\Lambda}+(d-3)^2},\end{cases} \tag{6.92}$$

where $y(m_{\rm c}):=m_{\rm c}/x^{(d-5)/2}$.

In the case of $-(2d-5)/(2d-1)\le 4\tilde{\alpha}\tilde{\Lambda}<0$, $Z(y)$ is non-negative and hence $x=x_+(y)$ is continuous. Therefore, as seen in Figs. 6.4 and 6.5, there is a static solution for each value of m satisfying $m\le m_{\rm c}$.

In the case of $-1<4\tilde{\alpha}\tilde{\Lambda}<-(2d-5)/(2d-1)$, in contrast, $Z(y)$ is negative in the domain of $y_-<y<y_+$, where

$$y_\pm:=\frac{8\tilde{\alpha}\left\{4d\tilde{\alpha}\tilde{\Lambda}+(d-4)\pm\sqrt{(4\tilde{\alpha}\tilde{\Lambda}-3)[4(2d-1)\tilde{\alpha}\tilde{\Lambda}+2d-5]}\right\}}{(d-1)^2(1+4\tilde{\alpha}\tilde{\Lambda})}(<0). \tag{6.93}$$

As seen in Fig. 6.6, the curve $x=x_+(y)$ is no more continuous and does not exist in the domain of $y_-<y<y_+$. Since the curve $y=m/x^{(d-5)/2}$ moves to the left as m decreases, there exists a range of negative $m\in(m_-,m_+)$ such that the curve $y=m/x^{(d-5)/2}$ does not intersect with the hyperbola $h(x,y)=0$ and hence there is no static solution. This shows a sharp difference from the general relativistic case.

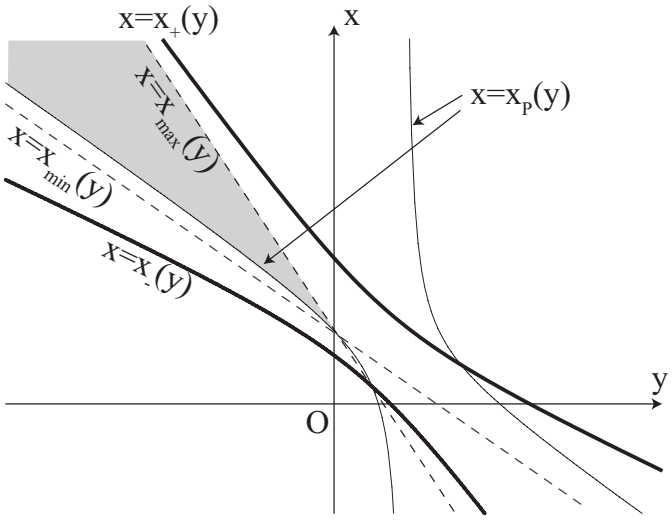

Figure 6.3: The (x, y) plane with $\Lambda = 0$, $\tilde{\alpha} = 1$, and $d = 6$. Thick solid curves consists of $x = x_+(y)$ and $x = x_-(y)$, while thin solid curves are $x = x_{\rm P}(y)$ corresponding to $P = 0$. The dashed lines consist of $x = x_{\rm max}(y)$ and $x = x_{\rm min}(y)$. The shadowed region corresponds to $P > 0$ in the physical region in the domain of $x > 0$, $y < 0$.

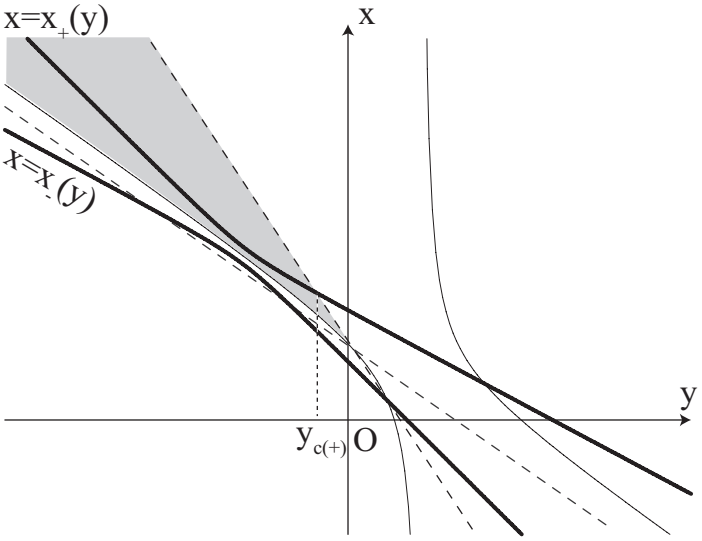

Figure 6.4: The (x, y) plane for $-(2d-5)/(2d-1) < 4\tilde{\alpha}\tilde{\Lambda} < 0$. If $4\tilde{\alpha}\tilde{\Lambda}$ is close to $-(2d-5)/(2d-1)$, a part of $x = x_-(y)$ enters the physical region but the corresponding solutions are unstable.

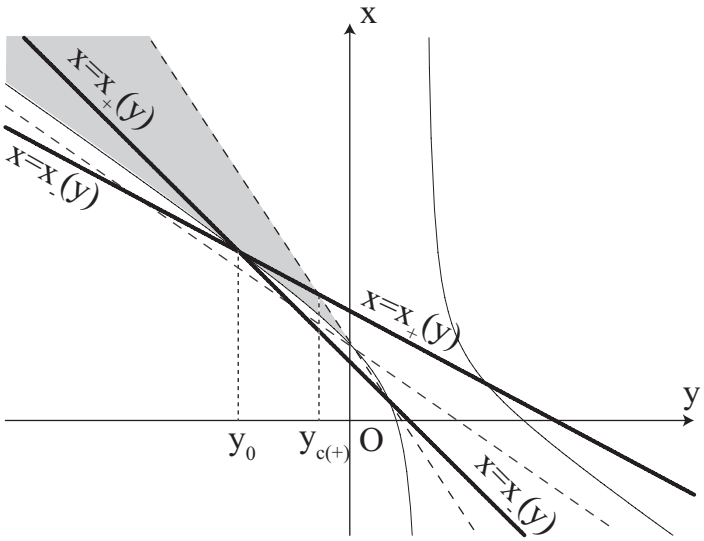

Figure 6.5: The (x, y) plane for $4\tilde{\alpha}\tilde{\Lambda} = -(2d-5)/(2d-1)$. The intersection between $x = x_+(y)$ and $x = x_-(y)$ is located on $x = x_{\rm P}(y)$ (thin solid curve) for any d.

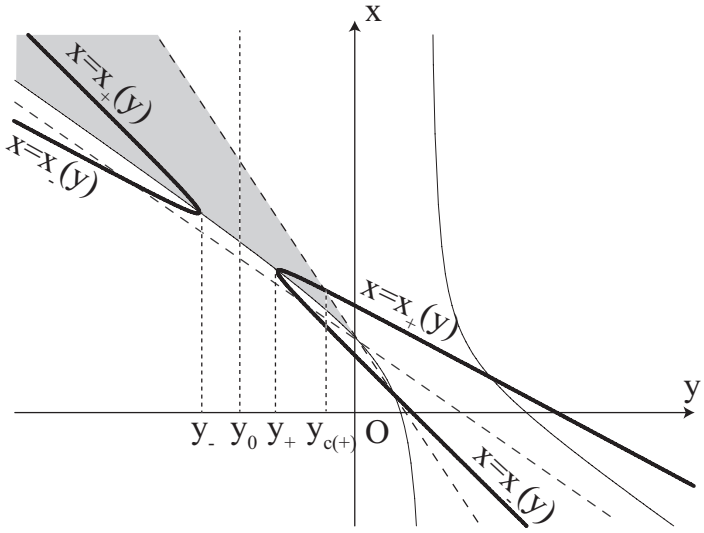

Figure 6.6: The (x, y) plane for $-1 < 4\tilde{\alpha}\tilde{\Lambda} < -(2d-5)/(2d-1)$. At $y = y_\pm$, $Z = 0$ (and hence $x_+ = x_-$) are satisfied. It is noted that the points (x_+, y_+) and (x_+, y_-) are located on $x = x_{\rm P}(y)$ (thin solid curve) only for $d = 5$.

Stability of solutions for $d = 5$

Now let us study the stability of solutions. For this purpose, we use the following quantity:

$$x_+(y) - x_{\rm P}(y) = \frac{S(y) + 2k\left\{(d-1)(d-3)y - 16\tilde{\alpha}\right\}\sqrt{Z(y)}}{4k(3-4\tilde{\alpha}\tilde{\Lambda})\left\{(d-1)(d-3)y - 16\tilde{\alpha}\right\}}, \tag{6.94}$$

where

$$\begin{aligned} S(y) :=& (d-3)(d-1)^2(1+4\tilde{\alpha}\tilde{\Lambda})y^2 - 8(d-1)\tilde{\alpha}(4d\tilde{\alpha}\tilde{\Lambda} + d - 4)y + 128\tilde{\alpha}^2(1+4\tilde{\alpha}\tilde{\Lambda}) \\ =& 4\tilde{\alpha}\tilde{\Lambda}\{(d-3)(d-1)^2y^2 - 8\tilde{\alpha}(d-1)dy + 128\tilde{\alpha}^2\} \\ & + (d-3)(d-1)^2y^2 - 8\tilde{\alpha}(d-1)(d-4)y + 128\tilde{\alpha}^2. \end{aligned} \tag{6.95}$$

If $S(y)$ is positive in some negative domain of y, then $x_+(y) > x_{\rm P}(y)$ holds there, which means that $P > 0$ is satisfied at $x = x_+(y)$. Therefore, if there are intersections of $x = x_+(y)$ with $y = m/x^{(d-5)/2}$ in the physical domain with $S(y) > 0$, the corresponding static solutions are stable. Since the stability of static solutions is different between $d = 5$ and $d \geq 6$, we treat the case of $d = 5$ here and the case of $d \geq 6$ will be treated separately.

In the case of $d = 5$, the solution cannot be unstable, shown as follows. For $d = 5$, $S(y) = 2Z(y)$ is satisfied and so Eq. (6.94) becomes quite simple. Since $Z(y) \geq 0$ is satisfied on the curve $x = x_+(y)$, we have $x_+(y) \geq x_{\rm P}(y)$ there and the corresponding static solutions are stable or marginally stable.

Marginally stable static solutions are realized at $y = y_{5(\pm)}$ satisfying $Z(y_{5(\pm)}) = 0$, where $y_{5(\pm)}$ is given by Eq. (6.91). Because the reality of $y_{5(\pm)}$ requires $4\tilde{\alpha}\tilde{\Lambda} \leq -5/9$, static solutions for $-5/9 < 4\tilde{\alpha}\tilde{\Lambda} < 0$ are all stable. (See Fig. 6.4.)

On the other hand, for $-1 < 4\tilde{\alpha}\tilde{\Lambda} \leq -5/9$, the static solutions with $m = y_{5(\pm)}$ are marginally stable, while the solutions with $m < y_{5(-)}$ or $y_{5(+)} < m$ are stable. For $y_{5(-)} < m < y_{5(+)}$, there is no solution. Figure 6.5 shows the case of $4\tilde{\alpha}\tilde{\Lambda} = -5/9$, in which y_0 becomes $y_{5(+)} = y_{5(-)}$ for $d = 5$. Figure 6.6 shows the case of $-1 < 4\tilde{\alpha}\tilde{\Lambda} < -5/9$, in which y_+ and y_- become $y_{5(+)}$ and $y_{5(-)}$ for $d = 5$, respectively.

Stability of solutions for $d \geq 6$

In order to discuss the stability for $d \geq 6$, we evaluate the function $h(x, y)$ on the marginally stable curve $x = x_{\rm P}(y)$:

$$h(x_{\rm P}(y), y) = -\frac{W(y)}{16\{(d-1)(d-3)y - 16\tilde{\alpha}\}^2}, \tag{6.96}$$

where

$$\begin{aligned} W(y) :=& 4\tilde{\alpha}\tilde{\Lambda}\left\{(d-3)(d-1)^2y^2 - 8d(d-1)\tilde{\alpha}y + 128\tilde{\alpha}^2\right\}^2 \\ & + (d-3)^2(d-1)^4y^4 - 16(d-3)(d^2-5d+12)(d-1)^2\tilde{\alpha}y^3 \\ & + 64(d-1)(d^3+3d^2-52d+112)\tilde{\alpha}^2y^2 \\ & - 2048(d^2-d-8)\tilde{\alpha}^3y + 16384\tilde{\alpha}^4. \end{aligned} \tag{6.97}$$

We will show that the sign of $h(x_{\rm P}(y), y)$ is definite in the domain of negative y for $-(2d-5)/(2d-1) < 4\tilde{\alpha}\tilde{\Lambda} < 0$, which means that $x = x_+(y)$ does not intersect with $x = x_{\rm P}(y)$. Then, by continuity of the curves $x = x_+(y)$ and $x = x_{\rm P}(y)$ for $y \leq 0$, the sign of $x_+(y) - x_{\rm P}(y)$ is the same as $x_+(0) - x_{\rm P}(0)$ and it is actually positive;

$$x_+(0) - x_{\rm P}(0) = \frac{-2k\tilde{\alpha}(1+4\tilde{\alpha}\tilde{\Lambda}) + 4\tilde{\alpha}\sqrt{(1+4\tilde{\alpha}\tilde{\Lambda})}}{3-4\tilde{\alpha}\tilde{\Lambda}} > 0. \tag{6.98}$$

Therefore, $x_+(y) > x_{\rm P}(y)$ is satisfied for $y < 0$ and hence the corresponding static solutions are stable. (See Fig. 6.4.)

In order to prove the definiteness of the sign of $h(x_{\rm P}(y), y)$ for $-(2d-5)/(2d-1) < 4\tilde{\alpha}\tilde{\Lambda} < 0$, we use the fact that $W(y)$ is an increasing function of Λ. From the following two expressions;

$$\begin{aligned} W(y)|_{\tilde{\Lambda}=0} =& (d-3)^2(d-1)^4y^4 - 16(d-3)(d^2-5d+12)(d-1)^2\tilde{\alpha}y^3 \\ &+ 64(d-1)(d^3+3d^2-52d+112)\tilde{\alpha}^2y^2 \\ &- 2048(d^2-d-8)\tilde{\alpha}^3y + 16384\tilde{\alpha}^4 > 0, \end{aligned} \tag{6.99}$$

$$W(y)|_{4\tilde{\alpha}\tilde{\Lambda}=-\frac{2d-5}{2d-1}} = \frac{4\left\{(d-1)y+8\tilde{\alpha}\right\}^2\left\{(d-1)^2(d-3)^2y^2 - 32d(d-3)\tilde{\alpha}y + 256\tilde{\alpha}^2\right\}}{2d-1} \geq 0, \tag{6.100}$$

it is concluded that the sign of $W(y)$ and hence the sign of $h(x_{\rm P}(y), y)$ is definite in the negative domain of y.

In the case of $4\tilde{\alpha}\tilde{\Lambda} = -(2d-5)/(2d-1)$, the solution can be marginally stable. Because the equality in Eq. (6.100) holds only at $y = -8\tilde{\alpha}/(d-1)$, $h(x_{\rm P}(y), y) = 0$ is satisfied only at $y = -8\tilde{\alpha}/(d-1)$ and the sign of $h(x_{\rm P}(y), y)$ is definite elsewhere. Therefore, $x_+(y) > x_{\rm P}(y)$ and $x_+(y) = x_{\rm P}(y)$ are satisfied at $y \neq -8\tilde{\alpha}/(d-1)$ and $y = -8\tilde{\alpha}/(d-1)$, respectively. Namely, the static solution with a critical value of m corresponding to $y = -8\tilde{\alpha}/(d-1)$ is marginally stable and solutions with other values of negative m are stable. (See Fig. 6.5.)

The situation is complicated for $-1 < 4\tilde{\alpha}\tilde{\Lambda} < -(2d-5)/(2d-1)$. In this parameter region, the solution may be dynamically unstable which shows a sharp difference from the general relativistic case.

Figure 6.6 shows the (x, y)-plane in this case. $x = x_+(y)$ exists only in the domains of $y \leq y_-$ and $y_+ \leq y (< 0)$ because $Z(y)$ is negative in the domain of $y_- < y < y_+$, where $y_\pm$ are defined by Eq. (6.93) and satisfy $Z(y_\pm) = 0$. From the following expression;

$$Z(y_0) = \frac{128\tilde{\alpha}^2\left\{4(2d-1)\tilde{\alpha}\tilde{\Lambda} + (2d-5)\right\}}{d-1} (< 0), \tag{6.101}$$

where $y_0 := -8\tilde{\alpha}/(d-1)$, we obtain an inequality $y_- < -8\tilde{\alpha}/(d-1) < y_+$.

For our purpose, we use the fact that $S(y)$ is an increasing function of Λ. Non-negativity of Z gives the following inequality:

$$4\tilde{\alpha}\tilde{\Lambda} \geq 3 - \frac{4\{(d-1)y - 8\tilde{\alpha}\}^2}{\{(d-1)^2y^2 - 16d\tilde{\alpha}y + 64\tilde{\alpha}^2\}}. \tag{6.102}$$

This lower bound gives a lower bound of S:

$$S(y) \geq \frac{32(d-5)\tilde{\alpha}y\left\{64\tilde{\alpha}^2-(d-1)^2y^2\right\}}{(d-1)^2y^2-16d\tilde{\alpha}y+64\tilde{\alpha}^2}. \tag{6.103}$$

If the right-hand side is positive in some domain of y, $x_+(y) > x_{\rm P}(y)$ is satisfied there and hence the corresponding static solutions are stable.

Because of the inequality $y_- < -8\tilde{\alpha}/(d-1) < y_+$, static solutions corresponding to $y \leq y_-$ are dynamically stable. In contrast, the static solution with $y = y_+$ is dynamically unstable since we have

$$x_+(y_+) - x_{\rm P}(y_+) = \frac{8(d-5)\tilde{\alpha}y_+\left\{64\tilde{\alpha}^2-(d-1)^2y_+^2\right\}}{k(3-4\tilde{\alpha}\tilde{\Lambda})\left\{(d-1)(d-3)y_+-16\tilde{\alpha}\right\}\left\{(d-1)^2y_+^2-16d\tilde{\alpha}y_++64\tilde{\alpha}^2\right\}} < 0. \tag{6.104}$$

Figure 6.6 shows that the dynamically unstable solutions are realized only very close to $y = y_+$ and the solutions with $y_+ \ll y(< 0)$ become stable. All the results obtained in the present analysis are summarized in Table 6.2.

Table 6.2: The existence and stability of Z_2 symmetric static thin-shell wormholes made of pure negative tension in the GR branch with $\tilde{\alpha} > 0$ and $1 + 4\tilde{\alpha}\tilde{\Lambda} > 0$. "S", "M", "U" stand for "Stable", "Marginally stable", and "Unstable", respectively

		Static solutions exist?	Stability
$k=1$	$m>0$	Yes	U
	$m\leq 0$	No	–
$k=0$	$m=0$	$\Lambda \geq 0$: No	–
		$\Lambda < 0$: Yes	M
	$m\neq 0$	No	–
$k=-1$	$m\geq 0$	No	–
	$m<0$	$\Lambda \geq 0$: No	–
		$-(2d-5)/(2d-1) < 4\tilde{\alpha}\tilde{\Lambda} < 0$: Yes	S
		$4\tilde{\alpha}\tilde{\Lambda} = -(2d-5)/(2d-1)$: Yes	S or M
		$-1 < 4\tilde{\alpha}\tilde{\Lambda} < -(2d-5)/(2d-1)$ with $d=5$: Yes	S or M
		$-1 < 4\tilde{\alpha}\tilde{\Lambda} < -(2d-5)/(2d-1)$ with $d\geq 6$: Yes	S, M, or U

7 Discussions and conclusions

7.1 In Einstein gravity

We developed the thin shell formalism for d dimensional spacetimes which is more general than Dias and Lemos formalism [30]. We investigated spherically, planar (cylindrically) and hyperbolically symmetric wormholes with a pure negative tension brane and found and classified Z_2 symmetric static solutions which are stable against radial perturbations. We found that in most cases charge is needed to keep the static throat radius positive and that a negative cosmological constant tends to decrease the radius of the black hole horizon and then to achieve the horizon avoidance. So the combination of an electric charge and a negative cosmological constant makes it easier to construct stable wormholes. However, a negative cosmological constant is unnecessary in a certain situation of $k = +1$ and $M > 0$ and charge is unnecessary in a certain situation of $k = -1$ and $M < 0$. We summarize the results in Tables 7.1, 7.2, 7.3 and 7.4.

In three dimensions, there is only possibility to have a marginally stable wormhole. The ingredients of this wormhole are a couple of AdS space-times.

Then, we restrict the spacetime dimensions to be higher than or equal to four. For $k = +1$, spherically symmetric thin shell wormholes which are made with a negative tension brane are investigated. It turns out that the mass must be positive, i.e., $M > 0$. The obtained wormholes can be interpreted as the higher dimensional counterpart of Barceló-Visser wormholes [32]. As a special case, if $1/2 < q < q_c$, one can obtain a stable wormhole without a cosmological constant. This wormhole consists of a negative tension brane and a couple of over-charged Reissner-Nordström space-times.

For $k = -1$, though it is hard to imagine how such symmetry is physically realized, they are interesting from the viewpoint of stability analyses. It turns out that M can be positive, zero and negative for stable wormholes. In this geometry, there is no upper limit for $|Q|$ for stable wormholes. There is possibility for a stable wormhole without charge if $M < 0$ and $\lambda < N(d, 0)$ is satisfied.

For $k = 0$, the geometry is planar symmetric or cylindrically symmetric. In this case, since the generalized Birkhoff's theorem does not apply [31], we should regard the Reissner-Nordström-(anti) de Sitter spacetime as a special solution to the electrovacuum Einstein equations. This means that the present analysis only covers a part of possible static thin shell wormholes and the stability only against a part of possible radial perturbations. Under such a restriction, we find that we need $Q \neq 0$ and $\Lambda < 0$ to have stable wormholes. There is no upper limit for $|Q|$. In the zero mass case, the wormhole is marginally stable.

We would note that the existence and stability of negative tension branes as thin shell wormholes crucially depend on the curvature of the maximally symmetric $(d-2)$ dimensional manifolds. On the other hand, they do not qualitatively but only quantitatively depend on the number of space time dimensions.

We considered only radial stability for TSWs here. In a realistic situation, a wormhole in the universe would be suffered by gravitational waves that are produced by a particle falling into the wormhole, or, incidental waves produced from gravitational collapses of nearby stars, etc. In such situations we must consider non-radial gravitational perturbations for wormholes. So far, there is no stability analysis for gravitational perturbations for TSWs. A linear stability analysis on a specific-perturbation mode (so

called axial perturbations) for a wormhole that corresponds to Morris-Thorne type has been investigated [43]. In [43], the matter distribution is continuous not as a shell. Since matters of TSWs are localized on their throat as a shell, the perturbation analysis for TSWs is not like that of Morris-Thorne type. To treat the non-spherically perturbed shell, we can employ the perturbed junction condition developed by Gerlach and Sengupta [44]. By using the perturbed junction condition, Kodama *et al.* investigated whether a domain wall emits gravitational waves or not. In their work, a domain wall is constructed by pasting a couple of Minkowski space times with a negative tension brane localized at their boundary [45]. Since their situation is similar to that of a TSW, we expect their study can be extended to the case of shell wormholes.

Looking back on studies for black holes (BHs) may give us a suggestion about stabilities of TSWs. Linearized gravitational perturbations for BHs can be decomposed into three types, scalar, vector and tensor modes in terms of their tensorial behavior on a rotation of a unit sphere [46]. The Schwarzschild BH is stable for all modes [46, 47]. Higher dimensional extension of the Schwarzschild BH, so called the Tangherlini space time [48], is also stable even for any maximally symmetric Tangherlini BHs ($k = 1, 0, -1$) [49, 50]. Schwarzschild BH including a cosmological constant system (Schwarzschild-(anti) de Sitter solution) and their topological extension ($k = 0, -1$) is stable in four dimension [50]. Higher dimensional counterpart of them are stable for vector and tensor modes, but uncertain for the scalar mode. According to numerical calculation, Tangherlini-de Sitter BH is stable for scalar mode for $d = 5, 6, ..., 11$ [51].

A charged BH with a cosmological constant is our interest. The Reissner-Nordström BHs ($k = 1, 0, -1$) in four dimension are stable for all modes even if any value of a cosmological constant is included [52, 50]. However, it is not known for arbitrary dimensions. Numerically, spherically symmetric Reissner-Nordström BH in anti de-Sitter space time (RNAdS BH) is stable for $d = 5, 6, ..., 11$ [53]. Surprisingly, spherically symmetric Reissner-Nordström BH with de-Sitter solution (RNdS BH) shows a peculiar aspect for higher dimensions. It is also numerically proved that though the five and the six dimensional RNdS BHs are stable, it becomes unstable for large values of the electric charge and the cosmological constant for $d \geq 7$ [54].

In this view, since the ingredient space times of TSWs that are radially stable are, in most cases, the non-extremal RNAdS BH which is stable against non-spherical gravitational perturbations as mentioned above, we perhaps expect the existence of TSWs which are stable against all kinds of perturbations. This is a problem to be solved and would be reported in our future work.

Table 7.1: The existence and stability of Z2 symmetric static wormholes in three dimensions. $k = 1$, 0 and -1 correspond to spherical, planar (cylindrical) and hyperbolic symmetries, respectively.

	Static solution	Horizon avoidance	Stability
$k - M + Q^2 = 0$	$\forall a_0 > 0$	Satisfied	Marginally stable
$k - M + Q^2 \neq 0$	None	–	–

Table 7.2: The existence and stability of Z2 symmetric static wormholes in spherical symmetry in four and higher dimensions. q, λ and q_c are defined as $q := |Q/M|$, $\lambda := (\Lambda/3)|M|^{\frac{2}{d-3}}$ and $q_c := (d-1)/(4\sqrt{d-2})$, respectively. The expressions for the static solutions $a_{0\pm}$ ($0 < a_{0-} < a_{0+}$) are given by Eqs. (5.15) and (5.16) with $k = 1$. $H_\pm(d, q)$ are given by Eq. (5.24) and plotted in Fig. 5.3. $R(d)$ is positive and given by Eq. (5.20). Note that $H_+ > 0$ for $0 \leq q \leq q_c$, while $H_- > 0$ only for $1/2 < q \leq q_c$. Therefore, if $\Lambda = 0$, the horizon-avoidance condition holds for a_{0+} for $0 \leq q \leq q_c$, while it does for a_{0-} only for $1/2 < q \leq q_c$. For $M > 0$ and $q = q_c$, the double root solution $a = a_{0\pm}$ is linearly marginally stable but nonlinearly unstable.

		Static solution	Horizon avoidance	Stability
$M > 0$	$q = 0$	$[(d-1)M/2]^{1/(d-3)}$	$\lambda < H_+(d, 0)$	Unstable
	$0 < q < q_c$	$a_{0\pm}$	$\lambda < H_\pm(d, q)$ for $a_{0\pm}$	a_{0-}: Stable a_{0+}: Unstable
	$q = q_c$	$[(d-1)M/4]^{1/(d-3)}$	$\lambda < R(d)$	Unstable
	$q_c < q$	None	–	–
$M < 0$		None	–	–
$M = 0$		None	–	–

Table 7.3: The existence and stability of Z2 symmetric static wormholes in hyperbolic symmetry in four and higher dimensions. The definitions for q and λ are same as in Table 7.2. The expressions for the static solutions $a_{0\pm}$ are given by Eqs. (5.15) and (5.16) with $k = -1$. $I(d, q)$ and $N(d, q)$ are given by Eqs. (5.30) and (5.33) and plotted in Figs. 5.4 and 5.5, respectively. $S(d, q)$ is given by Eq. (5.36). Since all of I, N and S are negative, the horizon-avoidance condition cannot be satisfied with $\Lambda = 0$ for any cases in hyperbolic symmetry.

		Static solution	Horizon avoidance	Stability
$M > 0$	$q = 0$	None	–	–
	$q > 0$	a_{0-}	$\lambda < I(d, q)$	Stable
$M < 0$	$q = 0$	$[(d-1)\lvert M\rvert/2]^{1/(d-3)}$	$\lambda < N(d, 0)$	Stable
	$q > 0$	a_{0+}	$\lambda < N(d, q)$	Stable
$M = 0$	$Q = 0$	None	–	–
	$\lvert Q\rvert > 0$	$[\sqrt{d-2}\lvert Q\rvert]^{1/(d-3)}$	$\Lambda/3 < S(d, q)$	Stable

Table 7.4: The existence and stability of Z2 symmetric static wormholes in planar or cylindrical symmetry in four and higher dimensions. The definitions for q and λ are same as in Table 7.2. Note that we assume that the bulk spacetime is described by the Reissner-Nordström-(anti) de Sitter metric or its higher dimensional counterpart. $J(d, q)$ is given by Eq. (5.39) and plotted in Fig. 5.6. Since J is negative, the horizon-avoidance condition cannot be satisfied with $\Lambda = 0$ for $M > 0$ and $q > 0$ in planar or cylindrical symmetry.

		Static solution	Horizon avoidance	Stability
$M > 0$	$q = 0$	None	–	–
	$q > 0$	$[2(d-2)q^2M/(d-1)]^{1/(d-3)}$	$\lambda < J(d, q)$	Stable
$M < 0$	$q = 0$	None	–	–
	$q > 0$	None	–	–
$M = 0$	$Q = 0$	$\forall a_0 > 0$	Satisfied	Marginally stable
	$\lvert Q\rvert > 0$	None	–	–

7.2 In Einstein-Gauss-Bonnet gravity

In this thesis , $d(\geq 5)$-dimensional static thin-shell wormholes with the Z_2 symmetry have been investigated in the spherically ($k = 1$), planar ($k = 0$), or hyperbolically ($k = -1$) symmetric spacetime in Einstein-Gauss-Bonnet gravity. For our primary motivation to reveal the effect of the Gauss-Bonnet term on the static configuration and dynamical stability of a wormhole, we have studied the stability against linear perturbations preserving symmetries in the simplest set up where the thin shell is made of pure negative tension, which satisfies the null energy condition.

In this system, the dynamics of the shell can be treated as a one-dimensional potential problem characterized by a mass parameter m in the vacuum bulk spacetime for a given value of d, k, the cosmological constant Λ, and the Gauss-Bonnet coupling constant α. We have studied solutions which admit the general relativistic limit $\alpha \to 0$ and considered a very conservative region in the parameter space. The shape of the effective potential for the shell dynamics clarifies possible static configurations of a wormhole and their dynamical stability.

As seen in Tables 6.1 and 6.2, the results with and without the Gauss-Bonnet term are similar in many cases. For $k = 1$, static wormholes require $m > 0$ and they are dynamically unstable. For $k = 0$, static wormholes require $m = 0$ and $\Lambda < 0$ and they are marginally stable. For $k = -1$, $m < 0$ and $\Lambda < 0$ are required for static wormholes.

We have clarified the effect of the Gauss-Bonnet term on the stability in a perturbative method by expanding the equation in a power series of $\tilde{\alpha}$. We have shown that, for $\tilde{\alpha}/a_E^2 \ll 1$, the Gauss-Bonnet term tends to destabilize spherically symmetric thin-shell wormholes ($k = 1$), while it stabilizes hyperbolically symmetric wormholes ($k = -1$). For planar symmetric wormholes ($k = 0$), the Gauss-Bonnet term does not affect their stability and they are marginally stable, same as in Einstein gravity. However, we have observed that the non-perturbative effect is quite non-trivial.

Notable difference between Einstein gravity and Einstein-Gauss-Bonnet gravity appears in the case of $k = -1$. In Einstein gravity, static wormholes exist when the mass parameter m is less than a critical negative value and they are dynamically stable. This is also the case in Einstein-Gauss-Bonnet gravity for $-(2d-5)/(2d-1) < 4\tilde{\alpha}\tilde{\Lambda} < 0$. However, for $4\tilde{\alpha}\tilde{\Lambda} = -(2d-5)/(2d-1)$, a static wormhole becomes marginally stable if m is fine-tuned. For $-1 < 4\tilde{\alpha}\tilde{\Lambda} < -(2d-5)/(2d-1)$, in contrast, static wormholes cease to exist for a finite range of m and furthermore, dynamical property of the wormhole is different for $d = 5$ and $d \geq 6$. For $d = 5$, static wormholes are generically stable but become marginally stable if m is fine-tuned. For $d \geq 6$, in addition to them, wormholes are dynamically unstable in a finite range of m. In summary for $k = -1$, the Gauss-Bonnet term shrinks the parameter region admitting static wormholes and tends to destabilize them non-perturbatively.

As the effect of the Gauss-Bonnet term on the existence and stability of static wormholes has been revealed in the thesis, the effect of its dilaton coupling is now of great interest. Unfortunately in the presence of a dilaton, exact bulk solutions are not available to construct thin-shell wormholes. Nevertheless, this is a promising direction of research leading to understand the result in [36]. We hope that the result will be reported elsewhere.

Appendix

A The condition for right solutions

We obtained the equation of motion (3.22) by twice squaring Eq. (3.17). Eq. (3.17) is equivalent to

$$\begin{cases} C^2\sigma^2 = (A_+ + A_-)^2, \\ \sigma < 0. \end{cases} \tag{A.1}$$

The above is also equivalent to

$$\begin{cases} \left(C^2\sigma^2 - A_+^2 - A_-^2\right)^2 = (2A_+A_-)^2, \\ C^2\sigma^2 - A_+^2 - A_-^2 > 0, \\ \sigma < 0. \end{cases} \tag{A.2}$$

The first equation of Eqs. (A.2) is obtained by squaring the first equation of Eqs. (A.1). By recasting the first equation of Eqs. (A.2), we obtain the equation of motion Eq. (3.22). However, the solution of Eq. (3.22) is valid if and only if the second and third inequalities of Eqs. (A.2) are satisfied. The second inequalities of Eqs. (A.2) is represented explicitly as

$$A_0^2 > 0, \tag{A.3}$$

where Eq. (5.4) is used. Since $A_0^2 = f(a_0) > 0$ is guaranteed by the horizon-avoidance condition, our analysis does not contain wrong solutions of Eq. (3.22).

B Derivation of the equation of motion for a thin shell

In this appendix, we present the details how to derive the equation of motion for the shell (6.8) and (6.9) from the junction conditions (6.4).

For the following vacuum bulk metric (6.1);

$$\mathrm{d}s_d^2 = g_{\mu\nu}\mathrm{d}x^\mu \mathrm{d}x^\nu = -f(r)\mathrm{d}t^2 + f(r)^{-1}\mathrm{d}r^2 + r^2\gamma_{AB}\mathrm{d}z^A\mathrm{d}z^B, \tag{B.1}$$

$$f(r) := k + \frac{r^2}{2\tilde{\alpha}}\left(1 \mp \sqrt{1 + \frac{4\tilde{\alpha}m}{r^{d-1}} + 4\tilde{\alpha}\tilde{\Lambda}}\right), \tag{B.2}$$

the non-vanishing components of the Levi-Civitá connection are given by

$$\begin{aligned} &\Gamma^r{}_{tt} = \frac{1}{2}f\frac{\mathrm{d}f}{\mathrm{d}r}, \quad \Gamma^t{}_{tr} = \frac{1}{2f}\frac{\mathrm{d}f}{\mathrm{d}r}, \quad \Gamma^r{}_{rr} = -\frac{1}{2f}\frac{\mathrm{d}f}{\mathrm{d}r}, \\ &\Gamma^r{}_{AB} = -rf\gamma_{AB}, \quad \Gamma^A{}_{Br} = \frac{1}{r}\delta^A{}_B, \quad \Gamma^A{}_{BC} = \hat{\Gamma}^A{}_{BC}(z), \end{aligned} \tag{B.3}$$

where $\hat{\Gamma}^A{}_{BC}$ is the Levi-Civitá connection on the maximally symmetric base manifold.

In this spacetime, the position of the thin shell is described by $r = a(\tau)$ and $t = T(\tau)$, where τ is the proper time on the shell. The future directed unit tangent vector to the shell is

$$u^\mu\frac{\partial}{\partial x^\mu} = \dot{T}\frac{\partial}{\partial t} + \dot{a}\frac{\partial}{\partial r}\,, \tag{B.4}$$

of which normalization condition $u_\mu u^\mu = -1$ is written as

$$1 = f(a)\dot{T}^2 - \frac{\dot{a}^2}{f(a)}\,, \tag{B.5}$$

where a dot denotes the differentiation with respect to τ. The unit normal one-form n_μ to the shell is given by

$$n_\mu \mathrm{d}x^\mu = -\dot{a}\mathrm{d}t + \dot{T}\mathrm{d}r\,, \tag{B.6}$$

which satisfies $n_\mu u^\mu = 0$ and $n_\mu n^\mu = 1$. The vector $n^\mu(\partial/\partial x^\mu)$ is pointing increasing direction of r.

The $(d-1)$-dimensional induced metric h_{ij} on the shell is given by

$$\mathrm{d}s_{d-1}^2 = h_{ij}(\xi)\mathrm{d}\xi^i\mathrm{d}\xi^j = -\mathrm{d}\tau^2 + a(\tau)^2\gamma_{AB}\mathrm{d}z^A\mathrm{d}z^B\,. \tag{B.7}$$

where $\xi^0 = \tau$. Non-zero components of the Levi-Civitá connection ${}^{(d-1)}\Gamma^i_{jk}$ in this spacetime are

$${}^{(d-1)}\Gamma^\tau_{AB} = a\dot{a}\gamma_{AB}, \quad {}^{(d-1)}\Gamma^A_{\tau B} = \frac{\dot{a}}{a}\delta^A_B, \quad {}^{(d-1)}\Gamma^A_{BC} = \hat{\Gamma}^A_{BC}. \tag{B.8}$$

From our definition of the Riemann tensor;

$$R^\mu{}_{\nu\rho\sigma} = \partial_\rho\Gamma^\mu{}_{\nu\sigma} - \partial_\sigma\Gamma^\mu{}_{\nu\rho} + \Gamma^\mu{}_{\kappa\rho}\Gamma^\kappa{}_{\nu\sigma} - \Gamma^\mu{}_{\kappa\sigma}\Gamma^\kappa{}_{\nu\rho}, \tag{B.9}$$

the non-zero components of the Riemann tensor $\mathcal{R}^{i}{}_{ijk}$, Ricci tensor $\mathcal{R}_{ij}$, and Ricci scalar $\mathcal{R}$ are computed to give

$$\mathcal{R}^{\tau}{}_{B\tau D} = a\ddot{a}\gamma_{BD}, \qquad \mathcal{R}^{A}{}_{BCD} = (k+\dot{a}^2)(\delta^{A}{}_{C}\gamma_{BD} - \delta^{A}{}_{D}\gamma_{BC}), \tag{B.10}$$

$$\mathcal{R}_{\tau\tau} = -(d-2)\frac{\ddot{a}}{a}, \qquad \mathcal{R}_{AB} = \left\{a\ddot{a} + (d-3)(k+\dot{a}^2)\right\}\gamma_{AB}, \tag{B.11}$$

$$\mathcal{R} = 2(d-2)\frac{\ddot{a}}{a} + (d-2)(d-3)\left(\frac{k}{a^2} + \frac{\dot{a}^2}{a^2}\right). \tag{B.12}$$

From these expressions, we obtain the non-zero components of $P^{i}{}_{jkl}$:

$$P^{\tau}{}_{B\tau D} = \frac{1}{2}(d-3)(d-4)(k+\dot{a}^2)\gamma_{BD}, \tag{B.13}$$

$$P^{A}{}_{BCD} = (d-4)\left\{a\ddot{a} + \frac{1}{2}(d-5)(k+\dot{a}^2)\right\}(\delta^{A}{}_{C}\gamma_{BD} - \delta^{A}{}_{D}\gamma_{BC}). \tag{B.14}$$

The extrinsic curvature of the shell is computed from the following definition:

$$\begin{aligned} K_{ij} :=& (\nabla_\mu n_\nu) e^{\mu}_{i} e^{\nu}_{j} \\ =& -n_\mu e^{\mu}_{i,j} - \Gamma^{\kappa}_{\mu\nu} n_\kappa e^{\mu}_{i} e^{\nu}_{j}\,, \end{aligned} \tag{B.15}$$

where $e^{\mu}_{i} := \partial x^\mu / \partial \xi^i$. Using

$$e^{0}_{i}\mathrm{d}\xi^i = \dot{T}\mathrm{d}\tau\,, \qquad e^{1}_{i}\mathrm{d}\xi^i = \dot{a}\mathrm{d}\tau\,, \qquad e^{A}_{i}\mathrm{d}\xi^i = \delta^{A}_{B}\mathrm{d}z^B\,, \tag{B.16}$$

and Eq. (B.5) together with its derivative with respect to τ, we obtain the non-zero components of $K^{i}{}_{j}$:

$$K^{\tau}{}_{\tau} = \frac{1}{f\dot{T}}\left(\ddot{a} + \frac{f'}{2}\right), \qquad K^{A}{}_{B} = \frac{f\dot{T}}{a}\delta^{A}{}_{B}\,, \tag{B.17}$$

where a prime denotes the derivative with respect to a. From the above expressions, we compute

$$K = \frac{1}{f\dot{T}}\left(\ddot{a} + \frac{f'}{2}\right) + \frac{(d-2)f\dot{T}}{a}, \tag{B.18}$$

$$K_{ij}K^{ij} = \frac{1}{f^2\dot{T}^2}\left(\ddot{a} + \frac{f'}{2}\right)^2 + (d-2)\left(\frac{f\dot{T}}{a}\right)^2, \tag{B.19}$$

$$J^{\tau}{}_{\tau} = -\frac{(d-2)(d-3)}{3}\frac{f\dot{T}}{a^2}\left(\ddot{a} + \frac{f'}{2}\right), \tag{B.20}$$

$$J^{A}{}_{B} = -\frac{(d-3)f\dot{T}}{3a}\left\{\frac{2}{a}\left(\ddot{a} + \frac{f'}{2}\right) + (d-4)\left(\frac{f\dot{T}}{a}\right)^2\right\}\delta^{A}{}_{B}\,, \tag{B.21}$$

$$J = -\frac{(d-2)(d-3)f\dot{T}}{3a}\left\{\frac{3}{a}\left(\ddot{a} + \frac{f'}{2}\right) + (d-4)\left(\frac{f\dot{T}}{a}\right)^2\right\}. \tag{B.22}$$

Now we are ready to write down the equation of motion for the shell. Under the assumptions of the Z_2 symmetry and the form of $S^{i}{}_{j}$ as

$$S^{i}{}_{j} = \mathrm{diag}(-\rho, p, p, \cdots, p) + \mathrm{diag}(-\sigma, -\sigma, -\sigma, \cdots, -\sigma,)\,, \tag{B.23}$$

the junction conditions (6.4) give (6.8) and (6.9), where we used Eq. (B.5) in the following form:

$$\left(\frac{f\dot{T}}{a}\right)^2 = \frac{f}{a^2} + \frac{\dot{a}^2}{a^2}. \tag{B.24}$$

C Static thin-shell wormholes made of a perfect fluid

In this Appendix, we present a stability criterion for thin-shell wormholes made of a perfect fluid. Since we have studied a negative tension brane, we set $\sigma = 0$ in Eq. (6.7) and Eq. (6.14). In this case, Ω is no more constant in general.

C.1 Expressions of $V''(a_0)$

C.1.1 Einstein gravity

To derive a stability criterion, we adopt the same method in section 6.8. From Eq. (6.40) and the relation $\dot{a}^2 + V(a) = 0$, we get the following relations at $a = a_0$, defined by $V(a_0) = V'(a_0) = 0$;

$$\Omega_0^2 = \frac{f_0}{a_0^2}, \tag{C.1}$$

$$2\Omega_0\Omega_0' = \frac{(d-3)\,(k-f_0) - a_0^2(d-1)\tilde{\Lambda} - 2f_0}{a_0^3}, \tag{C.2}$$

$$2\left(\Omega_0\Omega_0'' + (\Omega_0')^2\right) = \frac{(d-1)d(a_0^2\tilde{\Lambda} + f_0) - a_0^2 V''(a_0) - (d-2)(d-3)k}{a_0^4}. \tag{C.3}$$

Eliminating Ω_0 from Eqs. (C.1) and (C.2), we obtain an algebraic equation to determine a_0:

$$(d-1)ma_0^{-(d-3)} - 2k + 2a_0^2\sqrt{f_0}\Omega_0' = 0, \tag{C.4}$$

where we have eliminated $\tilde{\Lambda}$ by using Eq. (6.44). If ρ =const., Eq. (C.4) yields Eq. (6.48). Solving Eq. (C.3) for $V''(a_0)$ and eliminating $\tilde{\Lambda}$ by using Eq. (C.2), we obtain $V''(a_0)$ in a compact form:

$$V''(a_0) = -\frac{2(d-3)k}{a_0^2} - 2\frac{I(a_0)}{a_0^{d-2}}, \tag{C.5}$$

$$I(a_0) := (a^d\Omega\Omega')_0'. \tag{C.6}$$

C.1.2 Einstein-Gauss-Bonnet gravity

We also play the same game in Einstein-Gauss-Bonnet gravity. Equation (6.53) is evaluated at $a = a_0$ to give

$$\Omega_0^2 = \frac{f_0\left\{\tilde{\alpha}(6k - 2f_0) + 3a_0^2\right\}^2}{9a_0^6}. \tag{C.7}$$

Differentiating Eq. (6.53) and evaluating at $a = a_0$, we obtain

$$6a_0^7\Omega_0\Omega_0' = \left\{\tilde{\alpha}(6k - 2f_0) + 3a_0^2\right\}\Big[a_0^2\left\{-(d-1)(a_0^2\tilde{\Lambda} + f_0) + (d-3)k\right\} + \tilde{\alpha}\left\{-2(d+1)f_0k + (d-1)f_0^2 + (d-5)k^2\right\}\Big], \tag{C.8}$$

where we used Eq. (6.55). Equation (C.8) is a cubic equation for f_0 and will be used to replace f_0^p $(p = 3, 4, \cdots)$ by f_0^2 and f_0.

An algebraic equation to determine a_0 is obtained by eliminating Ω_0 from Eqs. (C.7) and (C.8) as

$$(d-1)ma_0^{5-d} - 2k\left\{a_0^2 + 2\tilde{\alpha}(k+f_0)\right\} + 2a_0^4\sqrt{f_0}\Omega_0' = 0, \tag{C.9}$$

where we have eliminated $\tilde{\Lambda}$ by using Eq. (6.54). Differentiating Eq. (6.53) twice and using Eqs. (6.55) and (6.56), we finally obtain $V''(a_0)$ as

$$V''(a_0) = -\frac{P_3(a_0)}{a_0^2(3w_- + 4\tilde{\alpha}f_0)^3 w_+ w_-}, \tag{C.10}$$

$$w_\pm := a_0^2 + 2k\tilde{\alpha} \pm 2\tilde{\alpha}f_0 (> 0), \tag{C.11}$$

$$P_3(a_0) := 2k(3w_- + 4\tilde{\alpha}f_0)^3 P(a_0) + 6a_0^7 P_2(a_0), \tag{C.12}$$

where we have eliminated $\tilde{\Lambda}$ by using Eq. (C.8). In the above, $P(a_0)$ is defined by Eq. (6.61) and

$$P_2(a_0) := (3w_- + 4\tilde{\alpha}f_0)^2\left\{w_- a_0^{-(d-1)} I(a_0) + 8\tilde{\alpha}k\Omega_0\Omega_0'\right\} + 12\tilde{\alpha}a_0^7(\Omega_0\Omega_0')^2. \tag{C.13}$$

The expression (C.10) reduces to Eq. (C.5) for $\alpha \to 0$. Equation (C.10) shows that the signs of k, $P(a_0)$ and $P_2(a_0)$ determine the stability of the shell.

C.2 Sufficient condition for instability

In the previous subsection, we have derived the expressions of $V''(a_0)$ in the presence of a perfect fluid. They are more complicated than the pure-tension case, in which Ω_0' and $I(a_0)$ are vanishing. Nevertheless, both in Einstein and Einstein-Gauss-Bonnet gravity, it is not difficult to prove the instability for $k = 1, 0$ if $I(a_0) > 0$ holds. In other words, $I(a_0) > 0$ is the sufficient condition for instability for $k = 1, 0$. A dust fluid $(p = 0)$ is actually an example of such a matter field. In this case, the energy density ρ is given by Eq. (6.12) with $\gamma = 1$ and the expression of $I(a_0)$ is given by

$$I(a_0) = \frac{(d-3)\kappa_d^4 a_0^{d-2}\rho(a_0)^2}{4(d-2)} (> 0). \tag{C.14}$$

In Einstein gravity, Eq. (C.5) clearly shows that wormholes are unstable for $k = 1, 0$ if $I(a_0) > 0$. This is consistent with the result of the chapter 15.2.6 in [22]. In Einstein-Gauss-Bonnet gravity, on the other hand, stability is determined by Eq. (C.10). In the pure tension case, $P_2(a_0)$ vanishes and $P(a_0) > 0$ holds, and hence wormholes are dynamically unstable and marginally stable for $k = 1$ and $k = 0$, respectively. In the case of a perfect fluid satisfying $I(a_0) > 0$, we will treat the case with different k separately.

C.2.1 $k = 1, 0$

In the case of $k = 1$, $P_3(a_0)$ is shown to be positive as

$$\begin{aligned}
P_3(a_0) :=& 2(3w_- + 4\tilde{\alpha}f_0)^3 P(a_0) \\
&+ 6a_0^7\left\{(3w_- + 4\tilde{\alpha}f_0)^2\left(w_- a_0^{-(d-1)} I(a_0) + 8\tilde{\alpha}\Omega_0\Omega_0'\right) + 12\tilde{\alpha}a_0^7(\Omega_0\Omega_0')^2\right\} \\
>& 2(4\tilde{\alpha}f_0)^3 P(a_0) + 6a_0^7\left\{(4\tilde{\alpha}f_0)^2(8\tilde{\alpha}\Omega_0\Omega_0') + 12\tilde{\alpha}a_0^7(\Omega_0\Omega_0')^2\right\} \\
>& 2(4\tilde{\alpha}f_0)^3 16\tilde{\alpha}^2 f_0 + 6a_0^7\left\{(4\tilde{\alpha}f_0)^2(8\tilde{\alpha}\Omega_0\Omega_0') + 12\tilde{\alpha}a_0^7(\Omega_0\Omega_0')^2\right\} \\
=& 8\tilde{\alpha}\left\{(4\tilde{\alpha}f_0)^4 + 6(4\tilde{\alpha}f_0)^2 a_0^7\Omega_0\Omega_0' + 9(a_0^7\Omega_0\Omega_0')^2\right\} \\
=& 8\tilde{\alpha}\left\{(4\tilde{\alpha}f_0)^2 + 3a_0^7\Omega_0\Omega_0'\right\}^2 > 0,
\end{aligned} \tag{C.15}$$

where we used $w_\pm > 0$ and $I(a_0) > 0$ at the first inequality and $P(a_0) > 16\tilde{\alpha}^2 f_0$ (see Eq. (6.66)) at the second inequality.

In the case of $k = 0$, positivity of $P_3(a_0)$ is directly shown by the following expression:

$$P_3(a_0) = 6a_0^7\left\{(3w_- + 4\tilde{\alpha}f_0)^2 w_- a_0^{-(d-1)} I(a_0) + 12\tilde{\alpha}a_0^7(\Omega_0\Omega_0')^2\right\} > 0. \tag{C.16}$$

Therefore, thin-shell wormholes made of a perfect fluid satisfying $I(a_0) > 0$ are unstable for $k = 1, 0$ also in Einstein-Gauss-Bonnet gravity.

C.2.2 $k = -1$

In the case of $k = -1$, a simple stability criterion is not available as in the pure-tension case. The expression of $P_2(a_0)$ for a dust fluid is given by

$$P_2(a_0) = \frac{\rho(a_0)^2\kappa_d^4}{4a_0(d-2)^2}\left\{3a_0^6\tilde{\alpha}\rho(a_0)^2\kappa_d^4 + (d-2)(3w_- + 4\tilde{\alpha}f_0)^2\left((d-3)w_- + 8\tilde{\alpha}\right)\right\}. \tag{C.17}$$

Although $P_2(a_0)$ is positive, the sign of $P(a_0)$ depends on values of m, Λ and d in a complicated manner, as seen in Section 6.11. We leave this stability analysis for future investigations.

References

[1] E. Poisson, *A Relativist's Toolkit*, Cambridge University Press (2007) chap 3.

[2] C. Barrabés and G. F. Bressange, Class. Quant. Grav. **14**, 805 (1997) [gr-qc/9701026].

[3] C. Barrabés and P. A. Hogan, *Singular Null Hypersurface in General Relativity*, World Scientific (2003).

[4] T. Kokubu and T. Harada, Class. Quant. Grav. **32**, 20, 205001 (2015)

[5] T. Kokubu, H. Maeda and T. Harada, Class. Quant. Grav. **32**, 23, 235021 (2015)

[6] M.S. Morris, K.S. Thorne, and U. Yurtsever, Phys. Rev. Lett. **61**, 1446 (1988).

[7] L.Flamm, Physikalische Zeitschrift. **17**, 448 (1916). Note: This article is unavailable online. As an alternative, a commentary for Flamm's article can be available online: Gen Relativ Gravit **47**, 71 (2015).

[8] A.Einstein and N.Rosen, Phys. Rev. **48**,73 (1935).

[9] R.Fuller and J.Wheeler, Phys. Rev. **128**,2,919 (1962).

[10] M.S.Morris and K.S.Thorne, Am. J. Phys. **56**, 395(1988).

[11] H.G.Ellis, J. Math. Phys. **14**, 104 (1973);
K.A.Bronnikov, Acta Phys. Polon. B **4**, 251 (1973);
T.Kodama, Phys. Rev. D **18**, 3529 (1978).

[12] C. Armendariz-Picon, Phys. Rev. D **65**, 104010 (2002).

[13] H. Shinkai and S. A. Hayward, Phys. Rev. D **66**, 044005 (2002).

[14] J. A. González, F. S. Guzman and O. Sarbach, Class. Quantum Grav. **26**, 015010 (2009).

[15] J. A. González, F. S. Guzman and O. Sarbach, Class. Quantum Grav. **26**, 015011 (2009).

[16] J. A. Gonzalez, F. S. Guzman and O. Sarbach, Phys. Rev. D **80**, 024023 (2009).

[17] T. Torii and H. Shinkai, Phys. Rev. D **88**, 064027 (2013).

[18] T. Kaluza, Sitzungsber. Preussische Akad. Wiss. **96**, 69 (1921);
O. Klein, Eur. Phys. J. A **37**, 895 (1926).

[19] J. Maldacena, Adv. Theor. Math. Phys. **2**, 231 (1998).

[20] L. Randall and R. Sundrum, Phys. Rev. Lett. **83**, 3370 (1999).

[21] D. J. Gross and E. Witten, Nucl. Phys. **B277**, 1 (1986);
D. J. Gross and J. H. Sloan, Nucl. Phys. **B291**, 41 (1987);
R. R. Metsaev and A. A. Tseytlin, Phys. Lett. B **191**, 354 (1987);
B. Zwiebach, Phys. Lett. B **156**, 315 (1985);
R. R. Metsaev and A. A. Tseytlin, Nucl. Phys. **B293**, 385 (1987).

[22] M.Visser, *Lorentzian Wormholes*, AIP Press, New York(1996);
M.Visser, Phys. Rev. D **39**, 3182 (1989);
M.Visser, Nucl. Phys. B**328**, 203 (1989).

[23] E. Poisson and M. Visser, Phys. Rev. D **52**, 7318(1995).

[24] E. F. Eiroa and G. E. Romero, Gen Relativ. Gravit. **36**, 651 (2004);
E. F. Eiroa, Phys. Rev. D **78**, 024018 (2008).

[25] M.Ishak and K.Lake, Phys. Rev. D **65**,044011(2002).

[26] F.S.N.Lobo and P.Crawford, Class. Quantum Grav. **21**, (2004).391-404

[27] E. F. Eiroa and C. Simeone, Phys. Rev. D **70**, 044008 (2004);
C. Bejarano, E. F. Eiroa and C. Simeone, Phys. Rev. D **75**, 027501 (2007);
E. F. Eiroa and C. Simeone, Phys. Rev. D **81**, 084022 (2010);
S. H. Mazharimousavi, M. Halilsoy and Z. Amirabi, Phys. Rev. D **89**, 084003 (2014).

[28] E. F. Eiroa and C. Simeone, Phys. Rev. D **82**, 084039 (2010);
M. G. Richarte, Phys. Rev. D **87**, 067503 (2013).

[29] N. M. Garcia, F. S. N. Lobo and M. Visser, Phys. Rev. D **86**, 044026(2012).

[30] G. A. S. Dias and J. P. S. Lemos, Phys. Rev. D **82**,084023(2010).

[31] V. Ruban, Gen. Relat. Grav. GR 8 Waterloo, 303 (1977);
K. Bronnikov and M. Kovalchuk, J. Phys. A. Math. Gen. **13**, 187 (1980);
K. Bronnikov and V. Melnikov, Gen. Relat. Grav. **27**, 465 (1995);
H. Goenner, Commun. Math. Phys. **16**, 34-47 (1970);
H. Sato and H. Kodama, *Ippan sotaisei riron*, Iwanami Shoten (1992) Chap. 5.

[32] C. Barceló and M. Visser, Nucl. Phys. B **584**, 415-435 (2000).

[33] K. Bronnikov and S. G. Rubin, *Black holes, Cosmology and Extra dimensions*, World Scientific (2013) chap6, p.184.

[34] E. F. Eiroa and C. Simeone, Phys. Rev. D **71**,127501 (2005);
F. Rahaman, S. Chakraborty and M. Kalam, Int. J. Mod. Phys. D **16**, 1669 (2007);
M. G. Richarte and C. Simeone, Phys. Rev. D **80**,104033 (2009);
M. G. Richarte, Phys. Rev. D **82**, 044021 (2010);
A. A. Usmani, Z. Hasan, F. Rahaman, S. A. Rakib, S. Ray and P. K. F. Kuhfittig, Gen Relativ Grav. **42**, 2901 (2010);
F. Rahaman, P. K. F. Kuhfittig, M. Kalam, A. A. Usmani and S. Ray, Class.

Quantum Grav. **28**, 155021 (2011);
S. Habib Mazharimousavi, M. Halilsoy, and Z. Amirabi, Phys. Lett. A **375**, 231-236 (2011);
M. H. Dehghani and M. R. Mehdizadeh, Phys. Rev. D **85**, 024024 (2012);
S. M. Kozyrev, 1401.6662v1[gr-qc] (2014).

[35] L. Randall and R. Sundrum, Phys. Rev. Lett. **83**, 4690 (1999).

[36] P. Kanti, B. Kleihaus, and J. Kunz, Phys. Rev. Lett. **107**, 271101 (2011);
P. Kanti, B. Kleihaus, and J. Kunz, Phys. Rev. D **85**, 044007 (2012).

[37] M. Thibeault, C. Simeone, and E.F. Eiroa, Gen. Rel. Grav. **38**, 1593 (2006);
M.G. Richarte and C. Simeone, Phys. Rev. D **76,** 087502 (2007); [Erratum-ibid. D **77**, 089903 (2008)];
C. Garraffo, G. Giribet, E. Gravanis, and S. Willison, J. Math. Phys. **49**, 042502 (2008);
T. Bandyopadhyay and S. Chakraborty, Class. Quant. Grav. **26**, 085005 (2009);
S.H. Mazharimousavi, M. Halilsoy, and Z. Amirabi, Phys. Rev. D **81**, 104002 (2010);
C. Simeone, Phys. Rev. D **83**, 087503 (2011);
M.H. Dehghani and M.R. Mehdizadeh, Phys. Rev. D **85**, 024024 (2012);
Z. Amirabi, M. Halilsoy, and S.H. Mazharimousavi, Phys. Rev. D **88**, 124023 (2013).

[38] D. G. Boulware, and S. Deser, Phys. Rev. Lett. **55**, 2656 (1985);
J. T. Wheeler, Nucl. Phys. **B268**, 737 (1986);
D. Lorenz-Petzold, Mod. Phys. Lett. **A3**, 827 (1988);
R.-G. Cai, Phys. Rev. D **65**, 084014 (2002);
R.-G. Cai and Qi Guo, Phys. Rev. D **69**, 104025 (2004).

[39] T. Torii and H. Maeda, Phys. Rev. D **71**, 124002 (2005).

[40] R. C. Myers, Phys. Rev. D **36**, 392 (1987).

[41] S.C. Davis, Phys. Rev. D **67**, 024030 (2003).

[42] E. Gravanis and S. Willison, Phys. Lett. **B562**, 118 (2003).

[43] K.Bronnikov, L.N.Lipatova, I.D.Novikov and A.A.Shatskiy, Gravit. Cosmol. **19** ,4 , 269 (2013).

[44] U.H. Gerlach and U.K. Sengupta, Phys. Rev. D **19**, 2268 (1979);
U.H. Gerlach and U.K. Seugupta, Phys. Rev. D **20**, 3009 (1979);
U.H. Gerlach and U.K. Sengupta, J. Math. Phys. **20**, 2540 (1979);
U.H. Gerlach and U.K. Sengupta, Phys. Rev. D **22**, 1300 (1980).

[45] H. Kodama, H. Ishihara and Y. Fujiwata Phys. Rev. D. **50**, 7292 (1994).

[46] T. Regge and J. A. Wheeler, Phys. Rev. **108**, 1063 (1957).

[47] L. A. Edelstein and C. V. Vishveshwara, Phys. Rev. D, **1**, 3514 (1970);
C.V.Vishveshwara, Phys. Rev. D, **1**, 2870 (1970);
F. J. Zerilli, Phys.Rev.Lett, **24**, 737(1970).

[48] F. R. Tangherlini, Nuovo Cimento **27**, 636 (1963).

[49] H. Kodama and A. Ishibashi. Prog. Theor. Phys. **110**, 701 (2003) (arXiv: [hep-th] 0305147v3);
H. Kodama and A. Ishibashi, Prog. Theor. Phys. **111**, 29 (2004) (arXiv:[gr-qc]0312012v1).

[50] A. Ishibashi and H. Kodama, Prog. Theor. Phys. Supplement. **189**, 165 (2011).

[51] R. Konoplya and A. Zhidenko, Nucl. Phys B **777**, 182 (2007).

[52] V. Moncrief, Phys. Rev. D **9**, 2707 (1974);
V. Moncrief, Phys. Rev. D **10**,1057 (1974).

[53] R. Konoplya and A. Zhidenko Phys. Rev. D **78**,104017 (2008).

[54] R. Konoplya and A. Zhidenko, Phys. Rev. Lett. **103**, 161101 (2009).